Metabolite Transporters in the Chloroplast Envelope

Dissertation der Fakultät für Biologie

der

Ludwig-Maximilians-Universität München

vorgelegt von

Ingrid Karin Jeshen

München, den 16. Mai 2012

Erstgutachter: Prof. Dr. J. Soll

Zweitgutachter: PD Dr. Bolle

Tag der mündlichen Prüfung: 26. Juni 2012

Summary

In the plant cell, the chloroplast is the organelle where photosynthesis as well as biosynthesis of many other important metabolites takes place. Therefore, a permanent and regulated exchange of inorganic cations, anions and a variety of organic biosynthetic pathway intermediates is needed between plastids and the cytosol. Due to the nature of the double membrane of the chloroplast an efficient transport across the inner and outer envelope is necessary. At the inner envelope carriers and at the outer envelope OEPs (*outer envelope proteins*) mediate this transport. In this work, the physiological function of OEP24 and OEP21 using the model plant *Arabidopsis thaliana* was studied. For AtOEP24.1 several mutant lines were characterised showing that this isoform is not essential for plant development. A complete OEP24 loss of function could not be studied due to the limited availability of mutant lines for the second isoform AtOEP24.2. For OEP21, single mutants for both *Arabidopsis* isoforms where characterised and a double mutant knock-out was generated. No phenotype was detected for the double mutant. However, for an overexpression line of AtOEP21.1 amino acid accumulation was found at the end of the night period suggesting a possible relation between OEP21 and amino acid homeostasis.

The second part of the work was focused on the discovery of new transporters located in the chloroplast envelope. For this purpose, protein sequencing of outer envelope membranes of pea chloroplasts and subsequent *in silico* analysis led to the identification of three unknown proteins: NOEP23, NOEP40 and NIEP57. The complete cDNA sequences in pea were obtained. Further, NOEP40 could be located at the outer envelope and NIEP57 at the inner envelope of the chloroplast using *in vivo* GFP-targeting and immunoblot. Subcellular localisation of NOEP23 is still unclear. NOEP40 showed all characteristics of typical OEPs and a knock-down mutant line in *Arabidopsis* has an early growth and flowering phenotype under cold stress when compared to the wild-type. NIEP57 is an integral membrane protein composed of four α-helical membrane domains with N- and C-termini facing the intermembrane space. For AtNIEP57 several mutant lines were characterised, demonstrating that AtNIEP57 corresponds to a novel inner envelope protein essential for embryo development. Mature plants with a knock-down of AtNIEP57 showed a chlorotic phenotype suggesting an important function of the protein during the vegetative plant life as well.

Zusammenfassung

In der pflanzlichen Zelle ist der Chloroplast das Organell, in dem die Photosynthese sowie die Biosynthese vieler wichtiger Metabolite stattfinden. Dafür ist ein dauerhafter und regulierter Austausch von anorganischen Kationen, Anionen und organischen Stoffwechselprodukten zwischen Plastid und Zytosol notwendig. Durch die Anwesenheit einer doppelten Hüllmembran der Chlorpolasten ist die Existenz von mehreren Transporter-Proteinen nötig. Der Austausch zwischen Plastiden und Zytosol wird in der inneren Hüllmembran von Carrier-Proteinen und in der äußeren Hüllmembran von den OEPs (für engl. *outer envelope proteins*) vermittelt. In dieser Arbeit wurde die physiologische Bedeutung von OEP24 und von OEP21 mittels der Modellpflanze *Arabidopsis thaliana* untersucht. Für AtOEP24.1 wurden verschiedene Mutantenlinien charakterisiert, und es konnte gezeigt werden, dass diese Isoform für das Leben der Pflanze nicht essentiell ist. Ein kompletter OEP24 *knock-out* konnte durch die limitierte Verfügbarkeit von Mutanten der zweiten Isoform AtOEP24.2 nicht untersucht werden. Mutantenlinien für beide vorkommende OEP21-Isoformen wurden in Rahmen dieser Arbeit charakterisiert und eine Doppelmutante wurde hergestellt. Für die Doppelmutante wurde kein Phänotyp detektiert. Eine Überexpressionslinie für OEP21.1 zeigte jedoch eine Änderung im Aminosäurengehalt die eine Beteiligung von OEP21 in der Aminosäure Homöostase nahe liegen könnte.

Im zweiten Teil meiner Arbeit wurden neue Metabolit-Transporter in der Hüllmembran von Chloroplasten entdeckt. Für diesen Zweck wurden Proteine von der äußeren Hüllmembran aus Erbsenchloroplasten sequenziert und *in silico* charakterisiert. Hierbei wurden drei neue, bisher unbekannte Proteine identifiziert: NOEP23, NOEP40 und NIEP57. Die komplette cDNA aus Erbse wurde für diese Proteine isoliert. Über *in vivo* GFP-targeting und Immunoblots wurden NOEP40 in der äußeren Hüllmembran und NIEP57 in der inneren Hüllmembran des Chloroplasten lokalisiert. Die subzelluläre Lokalisierung für NOEP23 konnte nicht eindeutig geklärt werden. NOEP40 weist alle typischen Eigenschaften der OEPs auf, und eine *knock-down* Mutante in *Arabidopsis* zeigte, unter Kälte, ein früheres Wachstum und Blühen als der Wildtyp. NIEP57 ist ein integrales Membranprotein, das aus vier α-helicalen transmembranen Domänen besteht. N- und C-Terminus des Proteins sind in den Intermembranraum orientiert. Durch die Analyse mehrerer Mutantenlinien Analyse für NIEP57 konnte gezeigt werden, dass AtNIEP57 ein neues Protein mit essentieller Funktion für die Embryonalentwicklung darstellt. *Knock-down* Linien für NOEP57 zeigten einen

chlorotisches Phänotyp in maturen Pflanzen, der auch auf eine wichtige Funktion des Proteins im späteren Leben der Pflanze hinweist.

Table of contents

Abbreviations

2D	two dimensional
aa	amino acids
AGI	*Arabidopsis* Genome Initiative
AP	alkaline phosphatase
At	*Arabidopsis thaliana*
AtD-LDH	*Arabidopsis thaliana* D-lactate dehydrogenase
ATP	adenosine triphosphate
BCA	bicinchoninic acid
bp	base pair
BSA	bovine serum albumin
CD	circular dichroism
cDNA	complementary DNA
CNBr	cyanogen bromide
Col-0	Columbia 0 ecotype
Col-er	Columbia erecta ecotype
CpHsc70-1	chloroplast heat shock protein 70-1
DNA	deoxyribonucleic acid
dNTP	deoxynucleotide triphosphates
DTT	dithiothreitol
DUF	domain of unknown function
E. coli	*Escherichia coli*
ECL	enhanced chemiluminescence
EDTA	ethylenediaminetetraacetic acid
EST	expressed sequence tag
GAPDH	glyceraldehyde-3-phosphate dehydrogenase
GFP	green fluorescent protein
GPT1	glucose 6-phophate/phosphate translocator
GTP	guanosine-5'-triphosphate
he	heterozygous
Hepes	(4-(2-hydroxyethyl)-1-piperazineethanesulfonic acid)
ho	homozygous
IEF	isoelectric focusing
IP	isoelectric point
kDa	kilo Dalton
LB	lysogeny broth
MOPS	3-(N-morpholino) propanesulfonic acid
mRNA	messenger RNA
MS	Murashige and Skoog
MVA	mevalonate
MW	molecular weight
NAPP	sodium pyrophosphate
OEPs	outer envelope proteins

PAGE	polyacrylamide gel electrophoresis
PCR	polymerase chain reaction
PEG-Mal	metoxypolyethylenglycol-maleimide
Pi	inorganic phosphate
PMSF	phenylmethylsulfonyl fluoride
Ps	*Pisum sativum*
PVDF	polyvinylidene fluoride
rec	recombinant
RER1	reticulata-related
RNA	ribonucleic acid
RNAi	RNA interference
rpm	revolutions per minute
RT PCR	reverse-transcription polymerase chain reaction
RT	room temp
RuBisCo	ribulose-1,5-bisphosphate carboxylase/oxygenase
SD	standard deviation
SDS	sodium dodecyl sulphate
T-DNA	Transfer-DNA
Tic	translocon at the inner envelope of chloroplasts
TILLING	targeting induced local lesions in genomes
Toc	translocon at the outer envelope of chloroplasts
TP	triosephosphate
Trafo	transformation
Tris	tris(hydroxymethyl) aminomethane
UTR	untranslated region
v/v	volume per volume
VDAC	voltage dependent anion channel
w/v	weight per volume
wt	wild-type
x g	times the force of gravity

I. Introduction

A characteristic feature of metabolism in eukaryotic cells is the spatial compartmentation into membrane-delimited organelles. The most important organelles in the plant cell are the plastids and mitochondria. Among the plastid family the chloroplast is the organelle where photosynthesis – conversion of CO_2 into carbohydrate with the release of O_2 – takes place. However, besides this essential chemical process, biosynthesis of many other important metabolites such as fatty acids, isoprenoids, tetrapyrroles, nucleic acids, aromatic and non aromatic amino acids, poliphenols and lignins, and reduction of NO_2^- and SO_4^{2-} is carried out in the plastids as well. To fulfil all these biosynthetic functions, a permanent and regulated exchange of inorganic cations, anions and a variety of organic biosynthetic pathway intermediates is necessary between plastids and the cytosol. The plastid, as well as the mitochondrion, is surrounded by two envelope membranes and this feature is related to the origin of both organelles. Chloroplast arose from an endosymbiotic event in which an ancestor of nowadays living cyanobacteria was engulfed by a mitochondria-containing eukaryotic host cell. The mitochondrion, on the other hand, originated from an earlier independent endosymbiosis where an α-proteobacteria was engulfed (for overview see Gould *et al*., 2008; Gross and Bhattacharya, 2009a; Figure 1). Therefore, both organelles show similarities to the Gram-negative ancestors that gave them origin. Due to the presence of two membranes delimiting the organelles – in the chloroplast these two membranes are named outer and inner envelope, and are separated by an intermembrane space – the existence of ion channels and metabolite transporters regulating the exchange with the cytosol are necessary. The exchange across the inner chloroplast envelope membrane is carried out by characterised carrier proteins (for overview see Philippar and Soll 2007; Linka and Weber 2010). These transporters located in the inner envelope usually contain α-helical transmembrane domains, mediating the passage of hydrophilic solutes (for overview see Facchinelli and Weber 2011). The transport across the outer chloroplast envelope was however long time assumed to occur via an unselective diffusion pore like the porin VDAC (*voltage dependent anion channel*) located in the outer membrane of mitochondria (Figure 1). VDAC, a β-barrel pore, transports ions and metabolites in an unselective way, acting rather as a size-exclusion filter. The hypothesis of such a simplification in the transport across the outer envelope in the chloroplast could be refused by the identification of several abundant channel proteins that

regulate the transport of small solutes and are called OEPs, for *outer envelope proteins* (Figure 1; for overview see Philippar and Soll 2007; Duy *et al*., 2007; Pudelski *et al*., 2010).

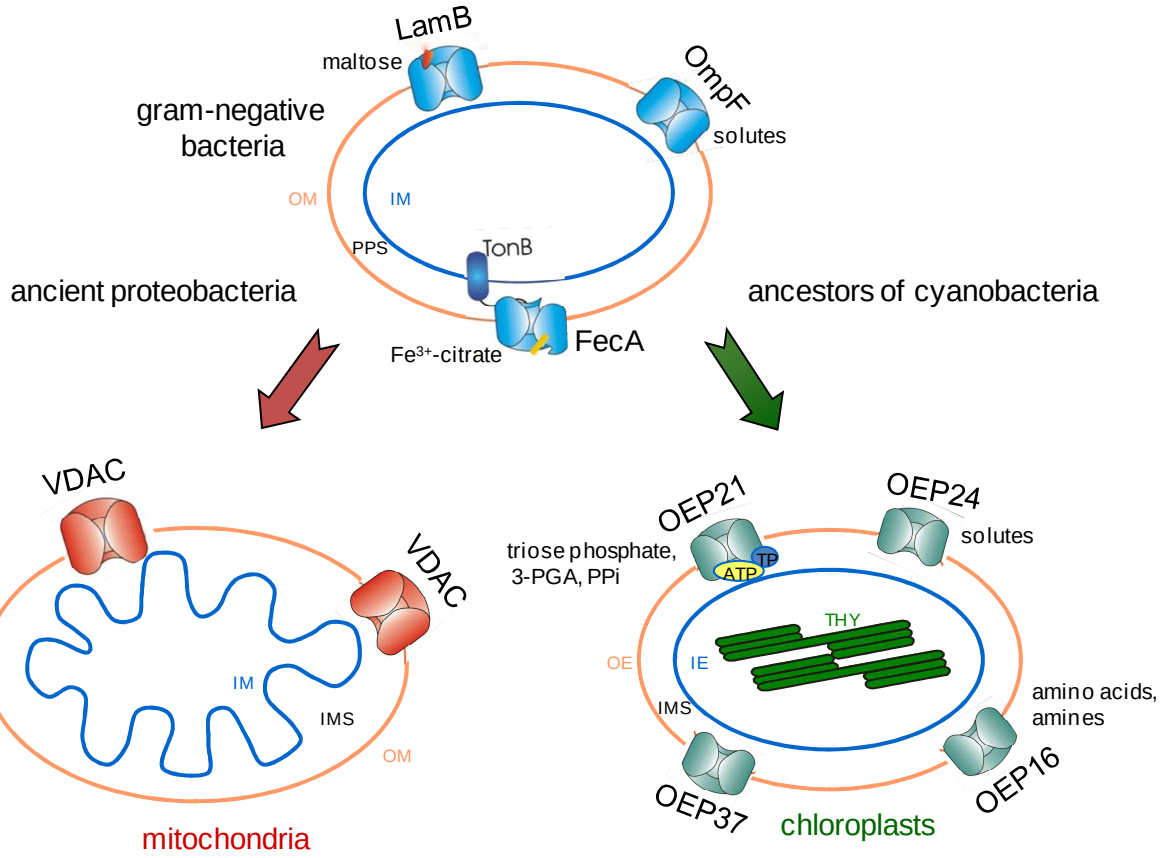

Figure 1: Metabolite channels in the outer envelope membrane of mitochondria and chloroplasts; Evolution from bacteria to organelles (adapted from Bölter and Soll, 2001)
Different types of porins in the outer envelope of Gram-negative bacteria. OmpF as a representative of classical solute porins, LamB as a specific maltose porin, and FecA depicting the TonB-dependent receptor-gated channels for Fe^{3+}-chelates. The Gram-negative bacteria represent the evolutionary ancestor that gave origin to mitochondria and chloroplasts. In the outer membrane of mitochondria VDAC is an unspecific porin. In the outer envelope of the chloroplasts the different OEPs characterised as well as the solutes that they transport *in vitro* are depicted. OM: outer membrane, IM: inner membrane, PPS: periplasmic space, OE: outer envelope, IE: inner envelope, IMS intermembrane space, THY: thylakoids, 3-PGA: 3-phosphoglycerate, PPi: inorganic pyrophosphate.

The existence of the selective OEPs in chloroplasts in contrast to mitochondria can evolutionary be explained by the necessity of a regulated and selective transport due to the origin of newly formed metabolic networks during the transformation of the endosymbiont into the plastid organelle. The OEPs characterised in the last years were all isolated from the outer chloroplast envelope membrane of pea where they represent abundant proteins (for overview see Duy *et al*., 2007). As other channel pores (VDAC, TOC75), they are deeply embedded in the membrane, and have a neutral or alkaline isoelectric point (Bölter *et al*., 1999). All discovered OEPs were named according to the molecular weight in kilo Daltons. The majority of them, resembling the porins present in the outer membrane of the Gram-

negative ancestor's, have a β-barrel structure (OEP21, OEP24 and OEP37). In contrast, OEP16 proteins are α-helical. Thus, for OEP16 an evolution from the plasma membrane of either the bacterial endosymbiont or the eukaryotic host can be proposed (for overview see Duy *et al*., 2007). The β-barrel porins in the outer membrane of Gram-negative bacteria are composed by an even number of amphiphilic β-sheets and are water-filled. Usually 14, 16 or 18 strands are connected by hydrophilic loops forming the bacterial porin barrel, most of them being functionally as homo-oligomers (for overview see Zeth and Thein, 2010). Porins can be subdivided into classical (allowing diffusion of small solutes), slow (slower diffusion of larger solutes), specific channels (specifically binding the solutes to be transported) and TonB-dependent receptor-gated channels (where a specific binding of iron chelates induces a TonB-mediated conformational change of the channel; for overview see Duy *et al*., 2007). Another characteristic of the OEPs is the way of insertion into the outer envelope membrane of the chloroplast. The majority of the plastid localised proteins are encoded in the nucleus and post-translationally imported into the plastid from the cytoplasm. This is a consequence of the loss of more than 90% of their genetic information to the host nucleus during evolution (see Benz *et al*., 2009 and references therein). To achieve the correct localisation, the encoded preproteins are translated with an N-terminal extension called transit peptide which allows targeting, specific recognition and subsequent regulated translocation via the Toc (translocon at the outer envelope of chloroplasts) and Tic (translocon at the inner envelope of chloroplasts) complexes (for overview see Benz *et al*., 2009, Andrès *et al*., 2010). In contrast to this well understood mechanism, specific signals for targeting of most β-barrel proteins and all OEPs to the chloroplast outer envelope as well as insertion pathways in the membrane are still unknown (for overview see Walther *et al.*, 2009). The OEPs are present in the genome of all land plants (mono and dicotyledons as well as in *Physcomitrella patents*), but no sequence homologues could be identified in cyanobacteria or in other Gram-negative bacteria (for overview see Duy *et al*., 2007).

1 OEP24

In 1998, OEP24 was discovered in pea and characterised as an integral membrane protein (Pohlmeyer *et al*., 1998). PsOEP24 has an isoelectric point of 9.1 and was found to be present in different plastid types of shoots, roots and leaves. Hydropathy analysis as well as circular dichroism (CD) from recombinant OEP24 protein reconstituted into liposomes suggested twelve putative amphiphilic β-strands, proposing a pore-forming protein built by homodimers (Schleiff *et al*., 2003). *In vitro*, electrophysiological measurements of PsOEP24 liposomes showed that the OEP24 channel has a slight preference for cations. A high conductance with a

diameter of 3 nm for the simple water-filled pore could be calculated. Osmotically induced fusion of PsOEP24 liposomes with the planar lipid bilayer as well as light scattering of PsOEP24 (rec) liposomes experiments demonstrated that OEP24 is permeable to sugars (manitol and glucose), glucose 6-phosphate, gluconate, phosphoglyceric acid, dihydroxyacetone, ATP, acetate, malate, α-ketoglutarate, Pi and charged amino acids suggesting a large rather not selective pore (Pohlmeyer *et al*., 1998). Although the primary sequence of OEP24 shows no homology to mitochondrial or bacterial porins, it could be demonstrated that pea OEP24 can functionally replace the mitochondrial VDAC in yeast, suggesting that OEP24 forms a general solute channel also *in vivo* (Röhl *et al*., 1999).

2 OEP21

OEP21 was isolated only a year later than OEP24 also corresponding to an abundant protein in the outer envelope of pea chloroplast (Bölter *et al*., 1999). PsOEP21 has an isoelectric point of 9.6 and was shown to be an integral membrane protein present in different types of plastids. CD analysis as well as *in silico* analysis proposed an eight β-strand formed pore with N- and C-termini facing the cytosol that mostly forms homodimers (Hemmler *et al*., 2006). Electrophysiological studies described OEP21 as an intrinsically rectifying anion channel permeable to HPO_4^{2-} and phosphorylated carbohydrates (triosephosphate, 3-phosphoglycerate, Gluc-6-phosphate). The rectification and ion selectivity of the channel was further shown to be regulated by ATP and triosephosphate (Bölter *et al*., 1999). Moreover, a fine tuning of PsOEP21 was proposed due to the existence of two ATP-binding sites: one high affinity site at the centre and a second at the vestibule facing the intermembrane space, harbouring an FX_4K motif (Hemmler *et al*., 2006). This motif had been previously described in ATP sensitive K^+ channels and in P-type ATPases (McIntosh *et al*., 1996; Drain *et al*., 1998; Seino, 1999; Kühlbrandt, 2004; Bryan *et al*., 2004). Binding of ATP to the inner site blocks the channel current whereas binding to both sites decreased the anion selectivity of OEP21. Triosephosphate (TP) can bind to both sites with the same affinity and thus compete with ATP. In consequence, increasing the TP:ATP ratio at the intermembrane space releases the current block and increases anion selectivity, resulting in net efflux of TPs (Hemmler *et al*., 2006). This feature described for the first time a regulatory step in the transport of metabolites across the outer envelope of the chloroplast.

3 Other OEPs

OEP37 from pea was described as a cation selective channel (Götze *et al*., 2006). It forms also a β-barrel pore with 12 β-strands (Schleiff *et al*., 2003), being the substrate specificity of this

channel still unclear. In the model plant *Arabidopsis thaliana* OEP37 represents a single copy gene; however knock-out mutants show no obvious phenotype under standard conditions although the expression is high in early germinating seedlings as well as in late embryogenesis (Götze *et al*., 2006).

From all OEPs the α-helical OEP16 is the best characterised. This protein is part of the PRAT – preprotein and amino acid transporter – superfamily (Murcha *et al*., 2007; Pudelski *et al*., 2010), and capable to transport amino acids *in vitro* (Pohlmeyer *et al*., 1997). *In vivo*, it could be shown that the loss of OEP16 causes metabolic imbalance, in particular that of amino acids during seed development and early germination, corroborating the function in shuttling amino acids across the outer envelope of seed plastids (Pudelski *et al*., 2011).

OEP7 is a very short protein composed of only one α-helix, was the first OEP identified and corresponds to the most abundant OEP (Joyard *et al*., 1982, Salomon *et al*., 1990, Li *et al*., 1991, Li and Chen, 1996). The function of OEP7 as a channel pore is still unclear and knock-out *Arabidopsis* plants show no obvious phenotype although OEP7 again present an OEP-typical differential expression pattern during seed development (Li, Philippar and Soll, unpublished).

The abundance of the known OEPs in pea chloroplast, as well as the different expression pattern during plant development of the orthologs found in *Arabidopsis* strongly support the theory of a regulated and selective transport across the outer envelope of the chloroplast. Moreover, new plastid proteome analysis (Froehlich *et al*., 2003; Kleffmann *et al*., 2004; Baginsky *et al*., 2004; von Zychlinski *et al*., 2005; Zybailov *et al*., 2008; Bräutigam *et al*., 2008a; Bräutigam *et al*., 2008b; Bräutigam and Weber, 2009; Ferro *et al*., 2010) reveals the existence of many unknown transporters confirming a selective and regulated transport across the outer envelope of the chloroplast by more than only one unselective porin-like protein.

4 Aim of the work

The objective of my PhD research project was to describe the physiological meaning of the metabolite channels OEP24 and OEP21 in their respective organ specific forms (e.g. plastids of pollen, embryos or mature leaves) using the model plant *Arabidopsis thaliana*.

Further, a screening assay on purified outer envelope membranes of pea chloroplast should lead to the identification and characterisation of new and up to now unknown metabolite and ion channels.

As a whole, basic findings on the connection of plastid biosynthesis ways with the metabolic competence and function of the plant cell during development and differentiation of the respective organs are expected. The regulation of solute fluxes between plastids and the surrounding cell can lead to significant changes in the content of the most important plant substances (proteins/lipids/carbohydrates) and in the long term can be of general importance for plant productivity.

II. Materials

1 Chemicals

All chemicals used in this work were purchased from Applichem (Darmstadt, Germany), Fluka (Buchs, Switzerland), Biomol (Hamburg, Germany), Difco (Detroit, USA), Sigma-Aldrich (Steinheim, Germany), GibcoBRL (Paisley, UK), Merck (Darmstadt, Germany), Roth (Karlsruhe, Germany), Roche (Penzberg, Germany) und Serva (Heidelberg, Germany).

2 Enzymes

Restriction enzymes were obtained from MBI Fermentas (St. Leon-Rot, Germany), New England Biolabs GmbH (Frankfurt am Main, Germany). T4-ligase was purchased from MBI Fermentas (St. Leon-Rot, Germany) and Invitrogen (Karlsruhe, Germany). Taq Polymerase was obtained from Diagonal (Münster, Germany), Eppendorf, MBI Fermentas, Clontech (Saint-Germainen-Laye, France), Finnzymes (Espoo, Finland) and Bioron (Ludwigshafen am Rhein, Germany). Reverse transcriptase was obtained from Promega (Madison, USA), RNase free DNase I from Roche (Mannheim, Germany) and RNase from Amersham Biosciences (Uppsala, Sweden). Cellulase R10 and Macerozyme R10 for digestion of the plant cell wall were from Yakult (Tokyo, Japan) and Serva (Heidelberg, Germany).

3 Oligonucleotides

Oligonucleotides were ordered from Qiagen/Operon (Köln, Germany) and from Metabion (Martinsried, Germany) in standard desalted quality. They were used for cloning, real time RT PCR and for genotyping mutant lines.

Table 1: Oligonucleotides used in this work

Name	Sequence (5'-3'orientation)	Application
oligo-dT-Primer Reverse T	T25V[NQ]	Reverse transcription
Act2/8fw	GGTGATGGTGTGTCT	Real time RT PCR
Act2/8rev	ACTGAGCACAATGTTAC	"
AtOEP24.1LCfw	GGGACTTTGCGATTTCT	"
AtOEP24.1LCrev	CTTTTACTACTAATTGGACTCACTAATA	"
AtOEP24.2LCfw	TGGTGATAATGTGAGGGC	Real time RT PCR / genotyping
AtOEP24.2LCfw	ACGAAACTGCTAGTAATAATAATG	*oep24.2-1*
AtOEP21.1LCfw	GTGTCTTGTACGCGGA	Real time RT PCR
AtOEP21.1LCrev	TGTGTTCATCAGCAGTGG	"
21.1LC_komp_fw	AAAAAAGCAGGCTCCG	Characterisation of OEP21.1
21.1LC_komp_rev	ACACGCTTATCAGCTCT	overexpression line
AtOEP21.2LCfw	AGGATTTACGCCTCAGAA	Real time RT PCR
AtOEP21.2LCfw	AATTTGCTCTCAACTGGT	"
At_noep40_LC_fw	CGTTAGGGTTCCTACGG	"
At_noep40_LC_rev	CTCAGCTACATTGCCCTC	"
At_noep57_LC_fw	AGGGATTATCGAGGGC	"
At_noep57_LC_rev	AGATGGGACCGTCACA	"
LB1SAIL	GCCTTTTCAGAAATGGATAAATAGCCTTGCTTCC	Genotyping SAIL mutant lines
LB2SAIL	GCTTCCTATTATATCTTCCCAAATTACCAATACA	"
LB1SAILTAIL	CAAAAGTGTACCAAACAACGCTTTACAGCA	"
LBa1	TGGTTCACGTAGTGGGCCATCG	Genotyping SALK mutant lines
RBKp1SALK	AGCTCATTAAACTCCAGAAACCCGCG	"

GABI RBI GABILB2	CCAAAGATGGACCCCCACCCAC ATATTGACCATCATACTCATTGC	Genotyping GABI mutant lines "
SAIL1225fw	CGTCAACAATCGTCCGGTTAT	Genotyping *oep24.1-1 and 24.1-3*
SAIL1225rev	TCGTCGCCGGTCCTAGCTT	Genotyping *oep24.1-1 and 24.1-3*
OEP24.1i1fw	TGAAATTGTATGGAGTCTCTGAG	"
OEP24.1i2rev	TATAAGAGTATCTAGTGTCAACTGTTGG	Genotyping *oep24.1-1*
24.1-2-GABI086fw 24.1-2-GABI086rev.1 24.1-2-GABI086rev.2	GGGAAGAAATAAGACAAAAAGCAAGTTGGC GCTTCTCAACGGCGAGAGAGAGACC CTTTTTAGGGACGTTGTAGTCGATG	Genotyping *oep24.1-2* " "
24.1-1RB_rev.1	CAGACAACTTGTTTGCTGGATCAATCAC	T-DNA right border characterisation
21.1A-fw 21.1A-rev oep21-C-TDNA Oep21.1_LC_F	CCCAAAGGAGCAGCAGAATTTG CCCTTCATGTTCGCGTTGAGA AAATGCAGTTACAGGTCATACCGCAAGTT GGACTTAAATCAGAAGAACC	Genotyping *oep21.1-1* " " "
21.1B-fw 21.1B-rev OEP21N-TDNA oep21E2R	TTAAAGGAGCTCTTGGAGTTATGAAAC CATCGCACAGAAGTAACTCGGAGC TTGAGGAAAATGGAGACTTCTATGAGGTA CAGTATCTAACTCTCCATGAAG	Genotyping *oep21.1-2* " " "
TILL21.2fw TILL21.2rev	TTTTCATCACTTGTGTTTCTTTGATGG GGTTTAAGACCACGCATAAAGTCAAAC	Genotyping *oep21.2-1* "
23-1fw 23-1rev	TCGTGTTTTAGTCGGTTCTGG CAAGTCCTTGGGAGATAAGGC	Genotyping *noep23-1* "
40-1fw 40-1rev	GGGATAAACAAACAACCAGGC TATCCACCACCTCAATCGAAG	Genotyping *noep40-1* "
SAIL 57 fw SAIL 57 rev RPnoep57SAIL	TATAAACTTCTTTTGGACAAGCTGCC ATGCACCATAACCAAGAGCATTTGTG CTTCCTCAGGGATTATCGAGG	Genotyping *noep57 -1* " "
57-2fw LPnoep57SAIL	TTCCTATGGAAACACATTCCG ATCTTCTTGCTTCTTCCCGAG	Genotyping *noep57 -2* "
LPnoep57SALK	TTTCCTCGTCTACTTGTGGG	Genotyping *noep57 -3, noep57-4*
RPnoep57SALK	TTCCATAGGAACGACATGGAG	"
24.1-gene_fw.1 24.1-gene_rev.1	ACTTCTTTGTCTGGTTGCATTTCGATG GGAGTTAACCAACAACAAATACCTCATG	Cloning of AtOEP24.1 for complementation "
oep24.1komp attB2 oep24.1komprev LC 24.1_3'fw LC 24.1_3'fw komp mut fw1 komp mut rev1	TAGAGCTGGTTCCTCTGTTGATGG ACCACTTTGTACAAGAAAGCTGGG TTTGAAGCTAGAAAGCTGAGAG TTCGGTTGTTTGATGTGG GCAAATTCTTCATGTATTTGTG AATCAAGCAACCTATAACAATCCACATAGC ATTTGGTTTGTGTGCTTTGCTTTCG	Genotyping of AtOEP24.1 complementation " " " " " "
oep21.1promo_ fw_n0 oep21.1gene rev	CAGGATAAATCAGGAACAGATAAAGCCAAG GCTCTGAGTTAGTTTGTTTTTCGATGG	Cloning of AtOEP21.1 for complementation "
oep21.1-Ncofw oep21.1cDNA+stop	CACCATGGAGACTTCTATGAGGTATAC TTACAGGTCATACCGCAAGTTCCAT	Cloning of AtOEP21.1 for overexpression "
noep23fw noep23rev	ATGGTTTTCTTGAGCTGGGTTCGCCCC TTATGATTTTGATGAATTAATGTGTTTCAGCA	Cloning of psNOEP23 "
noep23ps_NcoI(B) noep23ps_XhoI	CACCATGGTTTTCTTGAGCTGGGTTCG AACTCGAGTGATTTTCATCAATTAATGTGTTTCAG	Cloning of psNOEP23 for overexpression in *E. coli*
noep23At_fw(cacc) noep23At_rev_ohne stop	CACCAGGTGTTCTTGAGTTGGGGCCG CGAAGCATTGACATGTTTCAGCACAG	Cloning of AtNOEP23 for GFP
noep40fw noep40revB	ATGAAGCTCTCCCTCAAATTCCACAAC AAACTTGTTCTCCCCTTATTGCTTGC	Cloning of psNOEP40 "
noep40ps_NcoI noep40ps_XhoI	GGCCATGGCCATGAAGCTCTCCCTCAAATTCCAC TGCTCGAGGGAAGAAGAAGCAGCAGTGGCA	Cloning of psNOEP40 for overexpression in *E.coli* "
noep40at_fw(cacc) noep40at_rev_ohne stop	CACCATGAAGGCATCGATGAAGTTTCGTG AGCAGCTCCTTTCAAAGCTTTCTTCAG	Cloning of AtNOEP40 for GFP "
noep57fw noep57rev	CTTTCCTCTCTTCAGTTCTCTTATCTC GTCGACATAGAATCCCTACAAAAAA	Cloning of psNIEP57 "
NcoI_Ctb noep57ps_XhoI	CCATGGCTCCTTGTCGTTCATATGGAAACA TCCTCGAGAGCAGATCCTGCAACAACCTTCTTC	Cloning of psNIEP57 for overexpression in *E.*coli "
noep57at_fw(cacc) noep57at_rev_ohne stop	CACCATGTCACATATGGTGTTTCAGAGCG AGAGGCAGATGCAGCCACCTTC	Cloning of AtNIEP57 for GFP "
At_noep57_RNAi	TTTCCAATGTTTCCACCCCCTCC	Cloning of AtNIEP57 for const. and inducible RNAi lines in *At.*
At_noep57_stop	TTAAGAGGCAGATGCAGCCACCTTC	Cloning of AtNIEP57 for const.

		and inducible overexpression lines in *At.*
35Spromotor	GATGTGATATCTCCACTGACGTAAGG	Genotyping of overexpression lines in *At.*

4 Vectors and constructs

All plasmid vectors used in this work are enumerated in table 2.

Table 2: Plasmid vectors used in this work

Plasmid vector	Application	Origin
pCRblunt	Subcloning, sequencing	Invitrogen
pCR-XL-TOPO	Subcloning, sequencing	"
pCR/8/GW-TOPO TA	Entry vector for GATEWAY recombination	"
pENTR/D/TOPO	Entry vector for GATEWAY recombination	"
pJET1.2	Subcloning, sequencing	Fermentas
pET21d	Expression vector for *E. coli*	Novagene/Merck (Darmstadt, Germany)
pHGW	Single fragment recombination vector	Plant System Biology (University of Ghent, Belgium)
pH2GW7	Overexpression vector	"
pH7GWIWG2(II)	RNAi vector	"
p2GWF7	GFP fusion vector	"
pOpOffII	Inducible RNAi vector	Wielopolska *et al*., 2005
pOpOn	Inducible overexpression vector	

All constructs created in this work are enumerated in table 3.

Table 3: Constructs created in this work.

Protein	Plasmid-vector	Application
AtOEP24.1	pCR-XL-TOPO	Subcloning
AtOEP24.1	pCR/8/GW-TOPO TA	Gateway recombination
AtOEP24.1	pHGW	AtOEP 24.1 complementation
AtOEP21.1(c-DNA)	pENTR/D/TOPO	Gateway recombination
AtOEP21.1(c-DNA)	pH2GW7	AtOEP 21.1 overexpression
AtOEP21.1	pENTR/D/TOPO	Gateway recombination
AtOEP21.1	pHGW	AtOEP 21.1 complementation
PsNOEP23	pCRblunt	Sequencing, subcloning
PsNOEP23	pET21d	*E.coli* overexpression
AtNOEP23-stop codon	pENTR/D/TOPO	Gateway recombination (GFP)
AtNOEP23-stop codon	p2GWF7	GFP fusion
PsNOEP40	pCRblunt	Sequencing, subcloning
PsNOEP40	pET21d	*E.coli* overexpression
AtNOEP40-stop codon	pENTR/D/TOPO	Gateway recombination (GFP)
AtNOEP40-stop codon	p2GWF7	GFP fusion
PsNIEP57	pCRblunt	Sequencing, subcloning
PsNIEP57 (C_terminal)	pET21d	*E.coli* overexpression
AtNIEP57-stop codon	pENTR/D/TOPO	Gateway recombination (GFP)
AtNIEP57-stop codon	p2GWF7	GFP fusion
AtNIEP57(c-DNA)	pENTR/D/TOPO	Gateway recombination
AtNIEP57(c-DNA)	pH2GW7	AtNIEP57 overexpression
AtNIEP57 (RNAi)	pENTR/D/TOPO	Gateway recombination
AtNIEP57(RNAi)	pH7GWIWG2(II)	AtNIEP57 RNAi
AtNIEP57(c-DNA)	pOpOn	Inducible AtNIEP57 overexpression
AtNIEP57 (RNAi)	pOpOffII	Inducible AtNIEP57 RNAi

5 Molecular weight markers and DNA standards

*Pst*I digested Phage DNA (MBI Fermentas) was used as a molecular size marker for agarose-gel electrophoresis. For SDS-PAGE the Low Molecular Weight Marker composed of Lactalbumin (14 kDa), Trypsin-Inhibitor (20 kDa), Trypsinogen (24 kDa), Carboanhydrase (29 kDa), Glyceraldehyd-3-Dehydrogenase (36 kDa), Ovalbumin (45 kDa) and Bovine Serum Albumin (66 kDa) from Sigma-Aldrich was used. The peqGOLD Protein Marker II from Peqlab was also used.

6 Antisera

The following primary antibodies were generated in this work: psNOEP23 (mature protein form from pea), psNOEP40 (mature protein form from pea), psNIEP57 (C-terminal part, amino acid 301-526 of the protein from pea). Production and purification of the respective antigens are described under biochemical methods, section 4.6. All peptides/proteins were sent to Pineda, (Berlin, Germany) for immunization of rabbits. Primary antibodies directed against AtOEP24.1, AtOEP21.1, AtOEP37, AtPIC1, PsLSU, PsLHCP, PsOEP16.1, PsTic62, RuBisCo, GAPDH, CpHsc70-1 were already available in the lab. Antiserum recognizing AtOEP21.1 was purchased from Uniplastomic (France) and antiserum recognizing RuBisCo activase (from *Gossipium hirsutum*) was purchased from Agrisera (Sweden).

7 Strains

Cloning in *E. coli* was performed using the following strains: DH5-α (Invitrogen, Karlsruhe, Germany), TOP10 (Invitrogen), and MACH1 (Invitrogen). The strain BL21 (DE3) (Novagen/Merck, Darmstadt, Germany) were used for heterologous expression of proteins. The *Agrobacterium tumefaciens* GV3101::pMK90RK (Koncz and Schell, 1986), strain used in the stabile transformation of *Arabidopsis thaliana* was a kind gift of Dr. J. Meurer (Dept. Biologie I, Botany, LMU München).

8 Plant material

All experiments were performed on *Arabidopsis thaliana* plants, ecotype Col-0 (Columbia 0 Lehle seeds, Round Rock, USA) and ecotype Col-erecta (Col-er).

The T-DNA lines (Alonso *et al*., 2003; Rosso *et al*., 2003) SAIL_1225_B03, SAIL_548_C05, SALK_058578, SALK_122968, SAIL_266_D10, SAIL_64_A05, SAIL_1156_E1, SALK_033007 and SALK_089076 were purchased from NASC (University of Nottingham, GB). The lines GABI_086_H07 and GABI_279G09 were purchased from GABI-Kat (MPI for Plant Breeding Research, Köln, Germany). The TILLING mutant lines CS91501,

CS92311, and CS86516, were ordered at the Seattle TILLING Service (http://tilling.fhcrc.org; Till *et al*., 2003) and purchased from NASC (Scholl *et al*., 2000). Peas (*Pisum sativum*) var. "Arvica" were ordered from Bayerische Futtersaatbau (Ismaning, Germany).

III. Methods

1 Plant methods

1.1 Growth of *Arabidopsis thaliana*

Seeds of *Arabidopsis* were sown on MS media (0.215% MS, 0.05% (2-(N-morpholino) ethanesulfonic acid) MES, 0.3% gelrite (pH 5.8 with KOH), (Murashige and Skoog, 1962), in some cases supplemented with 1% (w/v) sucrose, or directly on soil. Before sowing on sterile media, the seeds were surface sterilised in 70% ethanol (1-2 min), 6% NaClO plus 0.05% tween 20 (3-5 min) followed by washing tree times in sterile H_20. For bigger amounts of seeds an alternative dry sterilization was performed in which the seeds were put in a close recipient (desiccator) in the presence of the sterilising gas originated by the mixture of 12% NaClO (20 ml) supplied with 1 ml of HCl for 16 h. To synchronize germination, the seeds were vernalized for 24 h at +4°C in the dark. To select the transformed plants and T-DNA insertion lines, the seeds were grown on MS media containing the adequate antibiotic or herbicide (25 µg/ml hygromycin, 100 µg/ml kanamycin or 50 µg/ml ammonium glufosinate, BASTA). After 2 to 3 weeks the plants were transferred to soil. Unless stated otherwise, plants were grown in a 16 h light (+21°C; 100 µmol photons $m^{-2}s^{-1}$) and 8 h dark (+16°C) cycle (long-day). For short day conditions an 8 h light (+21°C; 100 µmol photons $m^{-2}s^{-1}$) and 16 h dark (+16°C) cycle was used. For continuous light 100 µmol photons $m^{-2}s^{-1}$(21°C), and for continuous low light 10 µmol photons $m^{-2}s^{-1}$(21°C) were applied. The *noep40-1* phenotype was detected in long day conditions at 10°C.

1.2 Cross fertilization of *Arabidopsis thaliana*

Two mutant lines for *OEP21.1*: *oep21.1-1* (SAIL_548_C05) (F4) and *oep21.1-2* (SALK_058578) (F6) were crossed with the mutant line *21.2-1* CS86516 (F4). Double mutant as well as double wild-type lines were characterised by PCR (T-DNA insertion lines) and sequencing (TILLING lines). To perform the cross, flowers from the female parents were used before the anthers began to shed pollen onto the stigma. For each flower the sepals, petals and each anther was removed leaving the carpel intact. For the male parent, flowers were chosen that visibly were shedding pollen. These flowers were removed and squeezed near the bases with forceps to separate the anthers from the other organs. The convex surface of the anthers was brushed against the stigmatic surface of the exposed carpels on the female parent. The elongated siliques resulting from the cross were harvested after 2-3 weeks and dried at room temperature for 2 weeks before planting (Detlef and Glazebrook, 2002).

1.3 Stable transformation of *Arabidopsis thaliana*

The stable transformation of *Arabidopsis* plants was performed as referred by Bechtold *et al*., (1993). 3 days before plant transformation, a 10 ml *Agrobacterium* strain harbouring the right vector with the construct for the transformation was incubated in LB media and incubated at +28°C and 180 rpm. After two days, 500 ml of LB media were inoculated with 5 ml *Agrobacterium* culture and allowed to grow for one day under continuous shaking at +28°C. On the day of the transformation, the bacteria were harvested (6,000 x g, 10 min) and the pellet was reconstituted in 400 ml infiltration media (5% (w/v) sucrose, 0.215% MS, 0.05% (v/v) Silwet L-77). The plants to be transformed were prepared the night before as following: already formed siliques were cut and the plants were covered with a plastic bag to allow a maximum opening of the stomata cells. The plants were transformed under vacuum in a desiccator for 5 min in which they were immersed upside down in the infiltration media. After the transformation, the plants were allowed to recover lying on a humid paper and covered again until the next day when they were rinsed with water and erected. The T1 seeds from the transformed plants were harvested and selected on MS media supplied with the corresponding antibiotic or herbicide.

1.4 Preparation and transient transfection of *Arabidopsis thaliana* protoplasts

Arabidopsis mesophyll protoplasts were isolated from leaves of four-week-old plants and transiently transfected according to the protocol of Jen Sheen (available at http://genetics.mgh.harvard.edu/sheenweb/protocols_reg.html). GFP fluorescence was observed with a Leica TCS SP5 confocal laser-scanning microscope (Leica Microsystems, Wetzlar, Germany).

2 Microbiology methods

2.1 Media and growth

E. coli was cultivated in LB media (1% tryptone, 0.5% yeast extract, 1% NaCl and if necessary 1.5% agar) at +37°C in either liquid culture or on agar plates supplemented with the appropriate antibiotics (ampicillin 100 μg/ml, kanamycin 50 μg/ml, streptomycin 50 μg/ml and spectinomycin 100 μg/ml).

Agrobacterium was cultivated in LB media (liquid as well as on plates), at +28°C, supplemented with the appropriate antibiotics according to the resistance (50 μg/ml kanamycin (resistance strain GV3101), 100 μg/ml rifampicin (resistance Ti-plasmid), and the resistance of the transformed vector.

2.2 Bacteria transformation

The preparation of chemical competent cells for transformation was done according to the protocol of Hanahan (1983). The transformation of the bacteria was performed using the heat shock method (Sambrook *et al*., 1989).

For the preparation of competent *Agrobacterium* cells, 10 ml of liquid media supplied with the necessary antibiotic were inoculated with a single colony and incubated over night under continuous shaking at +28°C. The cells were harvested in 1 ml aliquots by centrifugation (5 min, 6,000 x g, +4°C). The pellet was resuspended in 100 µl, $CaCl_2$ (10 mM) at +4°C and centrifuged again (5 min, 6,000 x g at +4°C). The pellet was resuspended in 50 µl $CaCl_2$ (10 mM) at +4°C, and snap frozen in liquid nitrogen. The competent cells were stored at –80°C. For transformation of the cells, 0.5 µg of DNA plasmid was given to 50 µl of competent cells and snap frozen for 1 min in liquid nitrogen. After that, the cells were incubated at +37°C for 5 min and chilled down on ice. After the addition of 400 µl LB media or SOC media (2% trypton, 0.5% yeast extract, 10 mM NaCl, 2.5 mM KCl, 10 mM $MgCl_2$, 10 mM $MgSO_4$, 20 mM glucose) a 2-4 h incubation under continuous shaking at +28°C was achieved. After centrifugation for 10 s at 16,000 x g, the pellet was resuspended in a minimal amount of media and spread on LB plates supplied with the corresponding antibiotic and incubated for 2 to 3 days at +28°C. The colonies were tested by colony PCR.

3 Molecular biology methods

3.1 Polymerase Chain Reaction (PCR)

DNA fragments for cloning into vectors and genotyping of plant mutant lines were amplified using Polymerase Chain Reaction (PCR) (Saiki *et al*., 1988). The protocol applied was according to the manufacturer's recommendations. The BioTherm *Taq*-Polymerase (Diagonal), (Bioron) and the Tripel Master *Taq*-polymerase (Eppendorf) were used for PCR-genotyping. The *Pfu*-Polymerase (MBI Fermentas), *Phusion*-Polymerase (Finnzymes) and Advantage®2 Polymerase Mix (Clontech Laboratories) were used for subcloning from PCR amplified fragments.

3.2 Cloning strategies

General molecular biological methods like restriction digestion of vectors, DNA ligation, determination of DNA concentrations and agarose gel electrophoresis were performed as described in Sambrook *et al*., (1989) as well as according to the manufacture's recommendations. For purification of DNA fragments from agarose gels or directly after PCR

amplification the “Nucleospin Extract II Kit” from Macherey and Nagel (Düren, Germany) and QIAEXII Agarose Gel Extraction Kit or the QIAquick Gel Extraction Kit both from Qiagen (Hilden, Germany), were used. LR-recombination using the GATEWAY system (Invitrogen) was performed according to the manufacturer’s recommendations. The LR recombination reaction for the inducible pOpOn and pOpOffII vectors was incubated over night at 25°C.

3.3 Isolation of DNA plasmids from *Escherichia coli*

DNA plasmid preparation from transformed *E. coli* cells was performed by alkaline lysis with SDS and NaOH from 3-5 ml overnight cultures according to the protocol from Zhou *et al*., (1990). For high yield DNA purification, the Nucleobond AX Plasmid Purification Midi („AX 100“) und Maxi („AX 500“) kits from Macherey and Nagel (Düren, Germany) according to the manufacture’s recommendations were used.

3.4 Preparation of genomic DNA from *Arabidopsis thaliana*

For genotyping of T-DNA insertion lines the following protocol was used: 2-3 *Arabidopsis* rosette leaves were supplied with 450 µl of extraction buffer (0.2 M Tris-HCl (pH 7.5), 0.25 M NaCl, 25 mM EDTA, 0.5% SDS, 100 µg/ml RNase) and disrupted using the Tissue Lyser from Retsch/Qiagen for 3 min. Afterwards the samples were incubated at +37°C for 10 min and centrifuged for 10 min at 16,000 x g. The DNA present in the clear supernatant was precipitated with 300 µl of isopropanol for 5 min. After 5 min centrifugation at 16,000 x g at +4°C, the pellet was washed with 70% ethanol and after drying, 50 µl 10 mM Tris-HCl (pH 8) buffer was added to the DNA. For one PCR reaction (25 µl), 5 µl of DNA were used.

For the preparation of big genomic fragments of DNA (amplification of genes for complementation) 200 mg of leaves were placed immediately in liquid nitrogen and ground thoroughly with a mortar and a pestle. The powder was recovered in 750 µl extraction buffer (1.4 M NaCl, 20 mM EDTA, 0.1 M Tris-HCl (pH 8), 3% (w/v) cetrimonium bromide (CTAB) plus 8 µl 10% dithiothreitol (DTT)) and incubated for 30 min at +65°C. The sample was supplied with 1 sample volume of chloroform/isoamylalcohol (24:1) and centrifuged at 16,000 x g for 15 min at +4°C. The upper phase containing the DNA was precipitated with 1 sample volume of isopropanol and centrifuged again at 16,000 x g for 15 min at +4°C. The pellet was washed in 70% ethanol, dried and resuspended in 400 µl TE-buffer (pH 8). Rest RNA was digested incubating the samples with 100 µg/ml RNase for 30 min at +37°C. After this step, a second extraction of the DNA was performed adding 1 sample volume of chloroform/isoamylalcohol and centrifugation for 5 min at maximum speed. The DNA

presented in the upper phase was precipitated using 1/10 sample volume 3 M NaOAc (pH 5.6) and 2.5 sample volume of ethanol for 2 h at -20°C. After this step the samples were centrifuged for 10 min (16,000 x g at +4°C). The pellet was washed with 70% ethanol, dried and resuspended in 50 µl mM Tris-HCl (pH 8). The DNA concentration was measured and the corresponding amount according to the manufacture's recommendations for each polymerase was used for PCR amplification.

3.5 Determination of DNA and RNA concentrations

The concentration of DNA and RNA was measured photometrically according to the Lambert-Beer principle. The absorption of a diluted sample at 260 nm and 320 nm was determined and the concentration in µg/µl was calculated according to the following calculation:

DNA: $c\ [\mu g/\mu l] = (E_{260} - E_{320}) \times 0{,}05 \times f_{dil}$

RNA: $c\ [\mu g/\mu l] = (E_{260} - E_{320}) \times 0{,}04 \times f_{dil}$

E denotes absorption of the sample at the given wavelength and f_{dil} denotes the dilution factor of the sample. Additionally, the absorption at 280 nm was measured as an indication of protein contamination. In pure nucleic acids the relation E260/E280 corresponds to 1.8-2.

3.6 Characterisation of plant T-DNA insertion lines

T-DNA insertion lines were genotyped by PCR. To identify mutants with the T-DNA insertion in both alleles (homozygous) a combination of gene-specific primers flanking the predicted T-DNA insertion sites and T-DNA-specific primers were used. Amplification using T-DNA specific primer (LB or RB) in combination with a specific gene primer will only generate an amplification product in heterozygous and homozygous plants. Amplification using only gene specific primers flanking the T-DNA insertion site will only generate an amplification product in wild-type and heterozygous plants. The combination of these two PCR results allows a clear discrimination between wild-type, heterozygous and homozygous plants for the T-DNA insertion.

Table 4: PCR primer combination for genotyping mutant lines in *Arabidopsis*
The most used combination of primers is shown. For primer sequence please refer to table 1.

Allele	Line	PCR for…	Primer
oep24.1-1	SAIL_1225_B03	wt	SAIL1225rev
			SAIL1225fw
		T-DNA	LB1SAIL
			SAIL1225rev
oep24.1-2	GABI_086_H07	wt	24.1-2-GABI086fw
			24.1-2-GABI086rev.1
		T-DNA	24.1-2-GABI086rev.1
			GABI RBI
oep24.1-3	CS91501	TILLING	SAIL1225rev
			SAIL1225fw (sequencing: OEP24.1i1fw)
oep24.2	CS92311	TILLING	AtOEP24.2LCfw
			AtOEP24.2LCrev (sequencing: AtOEP24.2LCfw)
oep21.1-1	SAIL_548-C05	wt	21.1A-fw
			21.1A-rev
		T-DNA	21.1A-rev
			LB1SAIL
oep21.1-2	SALK_058578	wt	21.1B-fw
			21.1B-rev
		T-DNA	21.1B-fw
			LBa1
oep21.2-1	CS86516	TILLING	TILL21.2fw
			TILL21.2rev (sequencing: TILL21.2fw)
noep23-1	GABI_279G09	wt	23-1fw
			23-1rev
		T-DNA	23-1fw
			GABILB2
noep40-1	SAIL_266_D10	wt	40-1fw
			40-1rev
		T-DNA	40-1fw
			LB1SAIL
niep57-1	SAIL_64_A05	wt	SAIL 57 fw
			SAIL 57 rev
		T-DNA	SAIL 57 fw
			LB1SAIL
niep57-2	SAIL_1156_E1	wt	57-2fw
			LPnoep57SAIL
		T-DNA	57-2fw
			Lb2SAIL
niep57-3 *niep57-4*	SALK_033007 SALK_089076	wt	LPnoep57SALK
			RPnoep57SALK
		T-DNA	LPnoep57SALK
			LBa1
AtOEP24.1	Complementation	Trafo detection	oep24.1komp
			attB2
		Homozygous plants	oep24.1komprev
			OEP24.1i1fw
AtOEP21.1	Overexpression of *AtOEP21.1* in the double mutant 21dmA#35	Trafo detection	35S
			oep21.1cDNA+stop
	Complementation of the double mutant 21dmA#35 with *AtOEP21.1*	Trafo detection	21.1A-fw
			attB2
AtNIEP57	RNAi lines, overexpression lines	Trafo detection	35S
			At_noep57_RNAi

For the determination of the specific insertion site and analysis of the unknown borders of the T-DNAs, amplified DNA fragments with several primer combinations (T-DNA specific and gene specific primers, Table 4 and 5) were cloned and subsequently sequenced.

The base pare number of the T-DNA insertion sites depicted in the figures of this work, were placed in relation to the +1 of the genes proposed by TAIR. In the TILLING lines, however, the site of the point mutation corresponds to the position given by TILLING.

Table 5: PCR primer combination for T-DNA right border (RB) characterisation in the mutant lines in *Arabidopsis.* Primer combination used to sequence and analyse the unknown borders of the T-DNA insertions. For primer sequence please refer to table 1.

Allele	Line	Primer
oep24.1-1	SAIL_1225_B03	LB1SAIL
		24.1-1RB_rev.1
oep21.1-2	SALK_058578	LBa1
		21.1B-rev
niep57-1	SAIL_64_A05	LB1SAIL
		SAIL 57 rev
niep57-3	SALK_033007	RBKp1SALK
		RPnoep57SALK

3.7 Characterisation of plant TILLING lines

To screen the TILLING mutant plants, amplification of the DNA fragment harbouring the point mutation was performed. The PCR amplified bands were purified directly from the PCR using the Kits enumerated in section 3.2 Cloning strategies and sent to sequence.

3.8 DNA sequencing

DNA sequencing was performed by the sequencing service of the Faculty of Biology, Genetics, Ludwig-Maximilians-Universität München.

3.9 RNA extraction and real time RT-PCR

Total RNA from *Arabidopsis* and pea plants was isolated using the Plant RNeasy Extraction kit (Qiagen, Hilden, Germany). The DNA was digested with RNase-free DNase I (Qiagen) and transcribed into cDNA using MMLV Reverse transcriptase (Promega, Mannheim). For that purpose a final volume of 10 µl composed of 0.5-1.0 µg RNA, 4 µM oligo-dT-Primer, 0.5 mM dNTP and 2 units of MMLV was incubated at +42°C for 1.5 h (adaptation Clausen *et al*., 2004). The cDNA was diluted 1:20 and the PCR was performed using the FastStart DNA Master SYBR-Green Plus Kit (Roche, Penzberg) according to the manufacture's recommendations. The detection and quantification of transcripts were performed using the LightCycler system (Roche, Penzberg). A total of 45 cycles composed of 1 s at +95°C (denaturation), 7 s at 49+ (annealing), 19 s at +72°C (elongation) and 5 s at +79°C (detection)

were realised (Philippar *et al.*, 2004). The gene specific mRNA content was normalised to 10,000 actin molecules. For that purpose, real time RT PCR using oligonucleotides amplifying AtAct2 (At3g18780) and AtAct8 (At1g49240) was performed. The relative amount of RNA was calculated using the following calculation:

Relative amount of cDNA = $2^{[n(Aktin)-n(Gen)]}$

with n=threshold cycle of the respective PCR product.

4 Biochemical methods

4.1 Determination of protein concentration

The protein concentration of the samples was determined using the Bradford (Bradford, 1976) (Bio-Rad Protein Assay, Bio-Rad, München, Germany) or BCA (bicinchoninic acid) method (Pierce BCA Protein Assay Kit, Thermo Scientific, Rockford, USA).

4.2 Protein extraction from *Arabidopsis thaliana*

For the protein extraction plant leaves were placed immediately in liquid nitrogen and ground thoroughly with a mortar and a pestle. The powder was mixed with one sample volume extraction buffer (50 mM Tris-HCl, (pH 8), 50 mM EDTA, 2% LDS (Lithium dodecyl sulphate), 10 mM DTT, 0.1 mM PMSF) and incubated on ice for 30 min. A centrifugation step followed (15 min at 16,000 x g at +4°C) to get rid of insoluble components. The protein concentration was determined using the BCA method.

4.3 SDS-Polyacrylamide –gel electrophoresis (SDS-PAGE)

The separation of proteins was performed according to Laemmli (1970) with an acrylamid concentration (relation of acrylamid to N,N'-methylenebisacrylamide 30:0.8) from 12.5 to 15% in the separating gel. For the stacking gel 0.5 M Tris-HCl (pH 6.8) and for the separating gel 1.5 M Tris-HCl (pH 8.8) was used. To achieve a better resolution gels according to Shägger and Jagow (1987) were performed. For the stacking and separating gel 3 M Tris-HCl (pH 8.45) and 0.3% SDS was used. 13% of glycerine was added to the separating gel. The buffer used for these gels contained 0.2 M Tris-HCl (pH 8.9) in the anode buffer and 0.1 M Tris-HCl (pH 8.25), 0.1 M Tricine and 0.1% SDS in the cathode Buffer. Prior to loading the samples on the gels, they were solubilised in the Laemmli buffer (250 mM Tris-HCl (pH 6.8), 40% glycerine, 9% SDS, 20% ß-mercaptoethanol, 0.1% bromophenol blue).

4.4 Staining of acrylamide gels

SDS gels were stained using 0.18% Coomassie Brilliant Blue R250 dissolved in 50% methanol and 7% acetic acid for 15 min. Destaining was performed using 40% methanol, 7% acetic acid and 3% glycerine. Afterwards the gels were incubated in water and dried under vacuum.

IEF gels were stained using colloidal coomassie. Therefore the gels were incubated in staining solution (Coomassie Blue G-250, 10% (1 mg dye/ml) 10% ammonium sulfate, 2% phosphoric acid (85%) and 20% methanol, added freshly) on a shaker at RT overnight. The gels were then washed three times for 20 min in H_2O (or longer) and were then ready for scanning and analysis.

4.5 Immunodetection

4.5.1 Electrotransfer of proteins

The proteins separated by SDS-PAGE were transferred to a nitrocellulose (PROTRAN BA83, 0.2 µm, Whatman/Schleicher & Schüll) or to a PVDF membrane (Zefa Transfermembran Immobilon-P, 0.45 µm, Zefa-Laborservice GmbH, Harthausen, Germany) by a semi-dry-blot equipment (Amersham Biosciences) (Kyhse-Andersen, 1984). For this purpose 3 whatman papers were soaked in anode buffer I (300 mM Tris, 20% methanol, (pH 10,4), and placed in the blotting equipment (anode). 2 whatman papers, the membrane (PVDF membrane was activated in methanol before) and the gel, all of them soaked in the anode buffer II (25 mM Tris, 20% methanol (pH 10.4)) were placed on top. 3 more whatman papers soaked in cathode buffer (25 mM Tris, 40 mM aminocapron acid, 20% methanol (pH 7.6)) were placed on the stack and the blotting equipment was closed with the cathode. The transfer was conducted for 1.5 h at 0.8 mA per cm^2 membrane surface. After the transfer the marker proteins were cut from the membrane and visualized by staining with amido black (0.1% in ddH_2O, Moser/Roth).

4.5.2 Detection of proteins

Labelling with protein-specific primary antibodies was carried out with polyclonal antibodies, and bound antibodies were visualized either with alkaline phosphatase (AP)-conjugated secondary antibodies (goat anti-rabbit IgG (whole molecule)-AP conjugated, Sigma-Aldrich Chemie GmbH, Taufkirchen) or using a chemiluminescence detection system (ECL, see below) in combination with a horseradish peroxidase-conjugated secondary antibody (goat anti-rabbit (whole molecule)-peroxidase conjugated, Sigma). The membrane was blocked 3 times with skimmed-milk buffer and incubated with a dilution of the primary antibody (1:250-

1:2,000) in TTBS (100 mM Tris-HCl (pH 7.5), 0.2% tween 20, 0.1% BSA, 150 mM NaCl) at room temperature for two hours or overnight at +4°C. The membrane was blocked again in skimmed-milk buffer and incubated for 1 hour with the secondary antibody (1:10,000-1:8,000). The membrane was washed twice in skimmed-milk and afterwards two times in water. Detection of AP signals was performed in a buffer containing 66 µl/10 ml NBT (nitro blue tetrazolium chloride, 50 mg/ml in 70% N,N-dimethylformamide) and 132 µl/10 ml BCIP (5-bromo-4-chloro-3-indolyl phosphate, 12.5 mg/ml in 100% N,N-dimethylformamide) in 100 mM Tris-HCl (pH 9.5), 100 mM NaCl, 5 mM $MgCl_2$ buffer. To stop the reaction the membrane was incubated in 50 mM EDTA.

To detect signals with the Enhanced Chemiluminescence (ECL) method, the Pierce ECL Western Blotting Substrate Kit (Thermo Fisher Scientific Inc., Rockford, USA) was used after manufacture's recommendations. The following protocol was also used: solution 1 (100 mM Tris-HCl (pH 8.5), 1% (w/v) luminol, 0.44% (w/v) coomaric acid) and solution 2 (100 mM Tris-HCl (pH 8.5), 0.018% (v/v) H_2O_2) were mixed in a 1:1 ratio and added to the blot membrane (1-2 ml per small gel). After incubation for 1 min at RT (in the dark) the solution was removed and the luminescence detected with a film (Kodak Biomax MR, PerkinElmer, Rodgau, Germany).

4.6 Generation of antisera

For the generation of antisera against the new envelope proteins the pea sequence of NOEP23 (full length), NOEP40 (full length) and NIEP57 (C-terminal: amino acid 301-526) were subcloned into the vector pET21d (Novagen/Merck). For heterologous expression, constructs were transformed in *E. coli* BL21 (DE3) cells (Novagen/Merck) and grown at +37°C in LB or M9ZB media in the presence of 100 µg/ml ampicillin to an OD_{600} of 0.4-0.6. Expression was induced by addition of 1 mM IPTG (isopropyl β-D-1-thiogalactopyranoside). Cells were grown for 3 h at +37°C and harvested at 6,000 x g for 15 minutes, at +4°C. The bacteria were resuspended in resuspension buffer (50 mM Tris-HCl (pH 8.0), 200 mM NaCl, 5 mM ß-mercaptoethanol) and cells were broken using the Microfluidizer-Processor from Microfludics (Newton, USA). Afterwards the samples were sonified to break the DNA, and centrifuged at 20,000 x g for 30 min at +4°C. The hard inclusion bodies were resuspended in the detergent buffer (20 mM Tris-HCl (pH 7.5), 200 mM NaCl, 1% deoxycholic acid, 1% nonidet P-40, 10 mM ß-mercaptoethanol) and centrifuged again at 12,000 x g for 10 min at +4°C). The pellet was resuspended in triton buffer (20 mM Tris-HCl (pH 7.5) 0.5% triton X-100, 5mM ß-mercaptoethanol) and centrifuged (12,000 x g, 10 min, +4°C). This step was performed twice. The inclusion bodies were washed twice in Tris-buffer (20 mM Tris-HCl (pH 8.0), 10 mM

DTT) and dissolved in buffer G (50 mM NAPP (pH 8), 100 mM NaCl, 2 mM ß-mercaptoethanol and 6 M guanidinium chloride). All proteins were purified via their C-terminal polyhistidine tags using Ni-NTA-Sepharose (GE Healthcare, Munich, Germany) and eluted with 50-500 mM imidazole in buffer A (50 mM NaPP (pH 8.0), 100 mM NaCl, 2 mM ß-mercaptoethanol, 8 M urea). To electroelute recombinant psNIEP57 acrylamid gel slices containing the recombinant protein were electroeluted at 24 mA overnight in a dialyse tubing (14 kDa) in an SDS running buffer containing 4 M urea. All peptides/proteins were sent to Pineda (Berlin, Germany) for the immunization of rabbits.

4.7 Purification of PsNOEP40 antiserum

Due to the high background of the antiserum raised against PsNOEP40, a purification using CNBr-activated Sepharose ™ 4B (GE, Healthcare) was performed according to the manufacturer's recommendations with slight deviations. For that, the recombinant expressed PsNOEP40 (7 mg protein in 6 ml after purification from Ni-NTA-Sepharose columns) was dialysed over night against coupling buffer (0.1 M NaHCO3 (pH 8.3), 0.5 M NaCl, 1% triton X-100). The next day, lyophilized sepharose (0.23 gr of sepharose = 1 ml gel) was swollen in 5 ml 1 mM HCl (15 min on shaker at RT) and washed afterwards 10 times (10 ml) with 1 mM HCl. The recombinant protein was added to the sepharose beads and rotated for 1 h at RT. The excess of ligand was washed with at least 5 ml of the coupling buffer and the beads were blocked with 5 ml of blocking buffer (100 mM Tris-HCl (pH 8), 0.2 M glycine and 0.5 M NaCl, 1% triton X-100) for 2 h at RT. Afterwards an alternating washing (3-5 cycles) with 5 ml of acetat buffer (0.1 M sodium acetate (pH 4), 0.5 M NaCl, 1% triton X-100) and blocking buffer was performed. The beads were equilibrated with 5 ml of equilibration buffer (100 mM Tris (pH 7.5) and 150 mM NaCl, 0.1% triton X-100). The antiserum (1 ml, diluted in 2 ml of TN buffer (100 mM Tris-HCl (pH 8.0), 150 mM NaCl) was added to the beads and rotated 1 h at RT. The beads where then washed with 5 ml of TN buffer and the elution was performed adding 0.2 M glycine (pH 2.6). For this step 1 ml eluted antiserum was neutralized quickly in 100 µl 1 M Tris (pH 8). All washing steps were performed in batch (15 ml falcon tube and the centrifugation steps were performed at no more than 1,000 x g). The antiserum was dialysed over night against ddH_20, concentrated and stabilised adding 1% of BSA. Aliquots of the antiserum were snap frozen in liquid nitrogen and stored at –80°C and used as normal.

4.8 Isoelectric focusing (IEF)

4.8.1 Preparation of stroma samples

Rehydration buffer (7 M urea, 2 M thiourea, 0.2% biolytes 3-10 (Bio-Rad, München), 2% 3-[(3-cholamidopropyl) dimethylammonio]-1-propanesulfonate (CHAPS), 100 mM (DTT), bromophenol blue) was supplemented just before use with protease inhibitors 25X complete (in H_2O). 100 to 200 µg soluble proteins (with a concentration of at least 6 mg/ml) was filled up with this buffer to a total volume of 200 µl and incubated at RT for 1 h. The samples were centrifuged for 10 min at 20,000 x g at RT and the supernatant was loaded into an IEF-tray (for 11 cm strips).

4.8.2 First dimension IEF

The samples (200 µl) were loaded into the IEF-tray, the protection foil was removed from the strips (ReadyStrip IPG strips, pH range 5-8, Bio-Rad, München) and gel strips were put on top of the sample avoiding air bubbles between the strip and the sample (gel side on bottom, writing on the left hand side). After incubation for 1 h at RT, the strips were covered with mineral oil and the run was started (Protean IEF Cell; Bio-Rad; settings: preset method; rapid; rehydration: yes, active; gel length 11 cm; pause after rehydration: yes; hold at 500V: yes). After 12 h of rehydration, the run pauses and wet wicks (use 10 µl H2O per wick) were inserted between strips and electrodes. Then the program was continued for ~ 9.5 h (35000 Vh, end voltage: 8000 V). After the run finished, the strips were drained on a tissue to remove oil and transferred into a clean tray (with gel side facing up). They could either be applied directly to the second dimension or stored at -80°C for several weeks.

4.8.3 Second dimension SDS-PAGE

The strips were transferred to a clean tray and equilibrated for 20 min in equilibration buffer I (6 M urea, 2% SDS, 50 mM Tris (pH 8.8), 20% glycerol, 2% DTT). After incubation in equilibration buffer II (6 M urea, 2% SDS, 50 mM Tris (pH 8.8), 20% glycerol, 2.5% iodoacetamide) for 10 min, the strips were covered with running buffer. Normal SDS gels were performed. The IEF strip was placed to the top of the separating gel and overlaid with the stacking gel. Electrophoresis was performed at 35 mA per gel.

4.9 Protein identification by mass spectrometry (MS)

Colloidal coomassie *Arabidopsis* stained protein spots were cut from SDS-PAGE gels and sent for identification to the “Zentrallabor für Proteinanalytik” (ZfP, Adolf-Butenandt-Institut, LMU München). There, tryptic peptides were detected by Peptide Mass Fingerprint (MALDI, Matrix Assisted Laser Desorption/Ionization) and protein identification was then

accomplished with a Mascot software assisted database search (Perkins *et al*., 1999). To identify new envelope proteins of the chloroplast LC-MS/MS (Liquid Chromatography with MS runs) was used and the results were compared with a pea EST database (Franssen *et al*., 2011).

4.10 Hydrophobicity test

Fractions of isolated inner envelope from pea chloroplasts were ultracentrifuged at 256,000 x g for 10 min at +4°C. The inner envelopes were resuspended in different treatment buffers: NaCl (1 M), Na_2CO_3 0.1 M (pH 11.3), urea (6 M) and triton 1%. After incubation on ice (urea at RT) for 20 min the membranes were ultracentrifuged at 100,000 x g for 10 min and supernatant and pellet were supplied with solubilisation buffer. The proteins were separated on SDS-PAGE and analysed by immunoblot.

4.11 Proteolysis of inner envelope vesicles from *Pisum sativum*

Proteolysis of chloroplasts inner envelopes to identify the orientation of PsNIEP57 was performed using the proteases thermolysin and trypsin. The envelopes were incubated in 330 mM sorbitol, 50 mM Hepes (pH 7.6) and 0.5 mM $CaCl_2$ with 1 µg thermolysin or 0.1 µg trypsin pro 1 µg protein and incubated for 15 min for the protease thermolysin or 5 min for trypsin on ice. For envelope solubilisation 1% triton was added. The thermolysin proteolysis was stopped by the addition of 5 mM EDTA and the trypsin proteolisis by the addition of 1 µg α-Macroglobulin per 1 µg protease, 1 mM PMSF and 5 µg trypsin inhibitor per 1 µg protease. The proteins were separated on SDS-PAGE and analysed by immunoblot.

4.12 PEGylation assay

Inner envelope vesicles were treated with 7.5 mM metoxypolyethylenglycol-maleimide 5,000 Da (PEGMAL, Laysan Bio, Arab, AL) in a buffer containing 100 mM Tris/HCl (pH 7.0), 1 mM EDTA, for 0, 5, 10, and 30 min, at 4° C in the dark in absence or presence of 1% SDS. The PEGylation reaction was stopped by addition of 100 mM DTT and SDS-PAGE sample buffer. Bis-Tris gels (0.36 M Bis-Tris-HCl (pH 6.5-6.8), 7.5% acrylamide), were employed using a MOPS running buffer (50 mM MOPS, 50 mM Tris, 1 mM EDTA, 1 mM, 0.1% SDS). The protein was detected by immunoblotting.

5 Cell biology methods

5.1 Preparation of inner and outer envelope vesicles from *Pisum sativum*

For isolation of IE and OE vesicles from chloroplasts, pea seedlings grown for 9-11 days on sand under a 12/12 h dark/light regime were used. All procedures were carried out at +4°C.

Pea leaves cut from ~ 20 trays were ground in a kitchen blender in 10-15 l isolation media (330 mM sorbitol, 20 mM MOPS, 13 mM Tris, 0.1 mM $MgCl_2$, 0.02% (w/v) BSA) and filtered through four layers of mull and one layer of gauze (30 µm pore size). The filtrate was centrifuged for 5 min at 1,500 x g, the pellet gently resuspended with a brush and intact chloroplasts reisolated via a discontinuous Percoll gradient (40% and 80%). Intact chloroplasts were washed twice with wash media (330 mM sorbitol, Tris-base (~ pH 7.6)), homogenized and further treated according to the modification (Waegemann *et al*., 1992) of the previously described method (Keegstra and Youssif, 1986).

5.2 Isolation and fractionation of *Arabidopsis thaliana* chloroplasts

Intact *Arabidopsis* chloroplasts were prepared from ~ 150 g fresh weight leaf material of four week old plants grown on soil essentially as described in Seigneurin-Berny *et al*., 2008. Chloroplasts were subsequently taken up in 15 ml of 10 mM Hepes KOH (pH 7.6), 5 mM $MgCl_2$ and lysed using 50 strokes in a small (15 ml) Dounce-homogenizer (Wheaton, Millville, NJ, USA). Further separation in envelopes was done according to Li *et al*., 1991. For only stroma preparation a shorter protocol was used. After disruption of the chloroplast with the Dounce-homogenizer the samples were centrifuged for 10 min at 3,800 x g followed by an ultracentrifugation at 195,000 x g, 15 min to remove the membrane fraction. The samples were concentrated using Amicon Ultra-15 Centrifugal Filter Units (Millipore, Schwalbach, Germany).

5.3 Isolation of *Arabidopsis thaliana* chloroplasts

Chloroplasts were isolated according to Aronsson and Jarvis (2002) with the following modifications: 21-day-old plants grown on soil were homogenized in 25 ml of isolation buffer (0.3 M sorbitol, 5 mM $MgCl_2$, 5 mM EGTA, 5 mM EDTA, 20 mM Hepes/KOH (pH 8.0), 10 mM $NaHCO_3$, 50 mM ascorbic acid). After three homogenisation and filtration steps, the combined homogenate was pelleted at 1,000 x g for 5 min and resuspended in isolation buffer. Resuspended chloroplasts were separated on a two-step Percoll gradient (30/82% (w/v) Percoll) in a swing-out rotor at 1,500 x g for 10 min. The lower band comprising intact chloroplasts was washed in 50 mM Hepes/KOH (pH 8.0), 3 mM $MgSO_4$, 0.3 M sorbitol, 50 mM ascorbic acid. After a final wash, the chloroplasts were pelleted at 1,000 x g for 5 min and resuspended in 1 ml of wash buffer.

5.4 Preparation of microsomal fraction from *Pisum sativum*

Microsomal fractionation was performed according to Masatoshi (1974) with slight modifications: 100-140 mg of 8-day old pea leaves were ground in a kitchen blender in 200

ml buffer (0.05 M Tris-HCl (pH 7.5), 0.5 M sucrose, 1 mM EDTA) and filtered through four layers of mull and centrifuged first at 4,200 x g for 10 min at +4°C. The supernatant was afterwards centrifuged again at 10,000 x g, for 10 min at +4°C. To pellet the membranes, an ultracentrifuge step at 100,000 x g for 60 min at +4°C was performed. The membranes were resuspended in 0.01 M Tris-HCl (pH 7.5), 0.25 M sucrose and 0.5 mM EDTA.

6 Metabolite analysis

For OEP21 metabolite analysis ~ 50 mg of leaves of 4-week-old 21dmA2#35 (F4), 21dwA2#38 (F4), K4.3 (T3) and K2.4 (T3) grown on soil, under a light/dark cycle of 12 h/12 h, a day/night temperature 21°C/18°C were harvest. Extraction and analysis was performed in the group of Prof. Sonnewald, Universität Erlangen-Nürnberg under the supervision of Dr. Hofmann as described previously (Kogel *et al*., 2010).

7 Microscopy

To analyse the embryo lethality of AtNIEP57, heterozygous mutant plants (*niep57-1*) were grown under standard conditions (long day 16 h light, +21°C, 8 h dark +16°C). Siliques were prepared and destained using Hoyers-Solution (Liu and Meinke, 1998). After 1-2 days of incubation at dark, the seeds were analysed and photographed using a Differential Interference contrast microscopy (DIC), Zeiss Axiophot.

To perform crosses, general phenotype analysis of mutants and to prepare the siliques for the embryo analysis, a stereo microscope, Stemi 2000-C (Zeiss, Göttingen, Germany) and a light microscope, Leica DM 1000, (Leica, Wetzlar, Germany) were used.

8 Computational methods

Table 6: Software, databases and algorithms used in the present study

Name	**Reference**	**URL**
BLAST (Databank GenBank)	Altschul *et al.,* 1997	http://www.ncbi.nlm.nih.gov/BLAST
Genedoc	Nicholas and Nicholas, 1997	http://www.psc.edu/biomed/genedoc
ClustalX	Thompson *et al*., 1997	
Vector NTI	Invitrogen	
ExPASy	Gasteiger *et al*., 2003	http://www.expasy.org/
TopPred	Heijne 1992; Claros and Heijne 1994	http://mobyle.pasteur.fr/cgi-bin/portal.py?#forms::toppred
ARAMEMNON version 3.2	Schwacke *et al*., 2003	http://aramemnon.botanik.uni-koeln.de
ChloroP 1.1	Emmanuelsson *et al*., 1999	http://www.cbs.dtu.dk/services/ChloroP/
TargetP 1.1	Emmanuelsson *et al*., 2000	http://www.cbs.dtu.dk/services/TargetP/
Microarray-Data, AtGenExpress Consortium	Schmid *et al*., 2005	http://bar.utoronto.ca/efp/cgi-bin/efpWeb.cgi
TAIR (The *Arabidopsis* Information Resource)	Lamesch *et al*., 2011	http://www.arabidopsis.org
Gene Networks in Seed Development Website		http://seedgenenetwork.net/
ATTEDII Co-expression analysis	Obayashi *et al*., (2011)	http://atted.jp/top_search.shtml#CoExSearch

IV. Results

1 OEP24 in *Arabidopsis*

OEP24 was initially identified as an integral protein located in the outer envelope membrane of the chloroplast in pea. It was described to function *in vitro* as a weak cation selective channel with a large conductivity, transporting small hydrophilic solutes and metabolites (Pohlmeyer *et al*., 1998). *In silico* topology analysis of AtOEP24.1 suggested a β-barrel channel-forming protein composed of 12 β-sheets with the N- and C-termini of the protein facing the cytosol (Schleiff *et al*., 2003).

In *Arabidopsis* two different isoforms of OEP24 are present: OEP24.1 (At1g45170) and OEP24.2 (At5g42960). Both isoforms share an amino acid identity of 75% (213 amino acids), leading to a molecular weight of 23.6 kDa for OEP24.1 and 23.4 kDa for OEP24.2 respectively. Both proteins have an isoelectric point of 9.6. Further, *OEP24.1* is also present as a splice variant with 167 amino acids and a molecular weight of 18.4 kDa (The *Arabidopsis* Information Resource (TAIR), Lamesh *et al*., 2011). The transcript content of *OEP24.1* and *OEP24.2* is comparatively low in all developmental stages of the plant life (AtGenExpress Consortium, Schmid *et al*., 2005). However, a differential expression of both genes can be observed when the pollen and seed development is analysed in detail. AtOEP24.1 is mostly expressed in the immature pollen stadium (uni and bicellular pollen, Honys *et al*., 2003), whereas AtOEP24.2 transcripts are highest in the late stage of embryo development (torpedo and mature embryo (Schmid *et al*., 2005). Immunoblot analysis of *Arabidopsis* chloroplast sub-fractions showed the localisation of OEP24 at the envelope membrane (Figure 2).

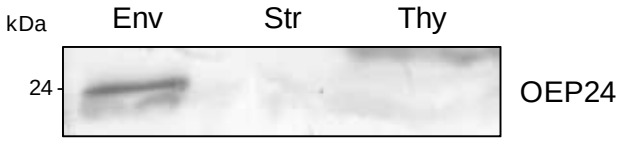

Figure 2: Localisation of OEP24 at the envelope of *Arabidopsis* chloroplasts Immunoblot analysis of the *Arabidopsis* chloroplast sub-fractions envelope (Env, 4 µg protein), stroma (Str, 10 µg protein) and thylakoids (Thy, 5 µg protein) using an antiserum raised against AtOEP24.1.

1.1 Characterisation of OEP24.1 mutants in *Arabidopsis*

In order to investigate the physiological function of OEP24.1, a T-DNA insertion line in *Arabidopsis thaliana*, *oep24.1-1* (SAIL_1225_B03) was analysed. In this line, the T-DNA insertion is located in the first intron of the *OEP24.1* gene (Figure 3). Previous work on this line showed that after PCR-genotyping of 418 plants from five different generations no homozygous mutant progeny was found, leading to a segregation of 52.2% heterozygous

mutant and 47.8% wild-type plants. During my thesis work, further genotyping of 319 *oep24.1-1* F3 plants showed a segregation of 46.5% heterozygous and 53.5% wild-type plants. This segregation of 1:1:0 clearly suggested a defect in gametophyte transmission of the T-DNA insertion (Johnson-Brousseau and McCormick *et al*., 2004). Backcross to wild-type using mutated pollen as well as mutated ovules, showed that both, the male and the female gametophyte were able to transmit the mutated *oep24.1-1* allele, but in an impaired form. The female gametophyte was able to transmit the mutation only in 16.8% (n= 1037) and the male gametophyte only in 21.4% (n= 1439). To explain the lack of *oep24.1-1* homozygous mutant plants, an additional embryo/seed developmental defect was proposed. A detailed analysis showed that although the pollen grains of the mutant line looked normal under light microscopy and were vital, *in vitro* they were not able to germinate properly. The pollen germination rate in this mutant line was only 52% compared to the wild-type in the T3 generation, and 59% of the wild-type in the T4 generation (A. Timper, K. Philippar, unpublished data).

Due to the fact that SAIL_1225_B03 represented the only T-DNA insertion line available for the physiological study of OEP24.1 at the beginning of my thesis, the aim was to complement this mutant line by introducing a normal copy of *OEP24.1* in the *oep24.1-1* mutant background. Thereby, the phenotype – absence of homozygous progeny for the mutation and impaired pollen germination – should be rescued. In addition, two other mutant lines of OEP24.1 (*oep24.1-2 and oep24.1-3*) that appeared during my work were characterised.

1.1.1 The oep24.1-1 mutant line

Due to the localisation of the T-DNA insertion in the first intron of *OEP24.1* in the line *oep24.1-1* (Figure 3), the absence of homozygous progeny for the T-DNA insertion and previous work that showed an unaltered coding sequence as well as normal amount of *OEP24.1* transcript in mutant pollen (A. Timper, K. Philippar unpublished results), a molecular analysis of the until yet unclear 3’ end of the T-DNA insertion was performed. After amplification with several combinations of specific T-DNA right and left border and *OEP24.1* gene primers, cloning of the different amplification products and subsequent sequencing, it could be demonstrated that the 3’ end of the T-DNA insertion in the *oep24.1-1* line as well as the 5’ end also corresponds to a left border (LB) sequence (Figure 3). Furthermore, the T-DNA insertion caused a deletion of 28 bp of intron 1 from *AtOEP24.1*. After an *in silico* analysis, it was discovered that three potential cis-regulatory elements (MYBILEPR, CORECDC 3 and BOXII, data not shown) are located in this region.

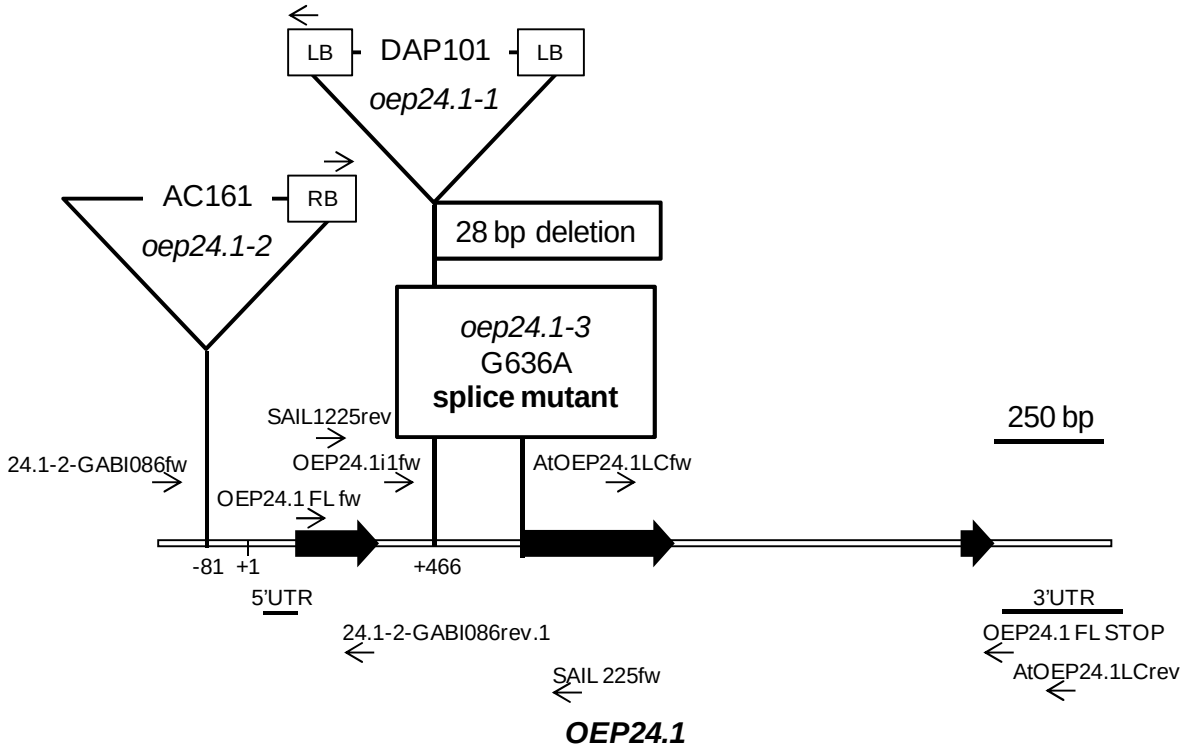

Figure 3: Characterisation of OEP24.1 mutant lines
OEP24.1 from *Arabidopsis thaliana* (At1g45170). Black arrows denote exons, white lines introns. The insertion sites of T-DNAs in lines SAIL_1225_B03 *(oep24.1-1)* and GABI_086_H07 *(oep24.1-2)* are indicated by triangles. The location of the point mutation in the TILLING line *oep24.1-3* is indicated by a square. At this site, a splice junction is affected by the mutation. Binding sites for *OEP24.1* gene specific primers and T-DNA specific left (LB) and right border (RB) primers used for genotyping and for real time RT PCR are depicted.

To complement the *oep24.1-1* line, the entire *OEP24.1* gene (4598 bp), including the promoter region as well as the 3' UTR region, was cloned in the pHGW.0 plasmid (Karimi *et al*., 2002) and afterwards stable transformed into the *Arabidopsis oep24.1-1* heterozygous mutant line. Four different lines (#4, #8, #10 and #11) of the F3 generation of *oep24.1-1* were transformed. The plants of the next generation after the transformation (T1) were selected with the antibiotic hygromycin. In addition, transformation and T-DNA insertion of *oep24.1-1* were confirmed by PCR genotyping. Six different lines (#4.3, #4.4, #10.1, # 10.3, #11.2 and #11.5) that presented a positive transformation with the *OEP24.1* gene and were heterozygous for the T-DNA insertion *oep24.1-1*, were selected for further analysis (Table 7). The T2 generation of the selected candidates was analysed by growing the plants on BASTA containing medium (selection marker for the T-DNA insertion in *oep24.1-1*). Resistant plants were subjected to a PCR to test for the presence of the *OEP24.1* gene introduced by the transformation vector. Afterwards, another PCR with a gene specific reverse primer that hybridised 3' downstream of the transformed *OEP24.1* gene and thus amplified only the endogenous *OEP24.1* and not the transformed construct was performed to distinguish between heterozygous and homozygous *oep24.1-1* T-DNA insertions. In case of a successful

complementation in the T2 generation, I expected to find homozygous plants for the *oep24.1-1* T-DNA harbouring a copy of *OEP24.1* introduced by the transformation and thereby complementing the putative lethality of the *oep24.1-1* homozygous status. Unfortunately, at the end of the screening of the T2 generation (494 plants) it was impossible to find a positive transformed and homozygous line for *oep24.1-1* (Table 7).

Table 7: Complementation of *oep24.1-1*
Four lines of the heterozygous *oep24.1-1* F3 generation were stable transformed with the *OEP24.1* gene. For the T1 generation after transformation, the number of hygromycin resistant plants that harboured the stable transformed *OEP24* (trafo +) and were as well heterozygous for *oep24.1-1* (T-DNA) is shown for each line. For the T2 generation, the numbers of heterozygous BASTA resistant and homozygous BASTA resistant *oep24.1-1* plants, stable transformed with *OEP24.1* are shown.

***oep24.1-1* F3 he T0 transformation**	**T1 trafo+ (hyg, PCR) T-DNA + (PCR)**	**T2 trafo + (PCR) T-DNA + (BASTA)**	
		he	**ho**
Line #4	Line #4.3	84 (77%)	0
	Line #4.4	50 (78%)	0
Line #8	no positives in T1		
Line #10	Line #10.1	73 (99%)	0
	Line #10.3	96 (95%)	0
Line #11	Line #11.2	150 (93%)	0
	Line #11.5	41 (93%)	0
Total	6	494	0

However, in the T2 generation two homozygous *oep24.1-1* plants segregated of line #4.3 that were not transformed by the *OEP24.1* gene construct. The same result appeared in the T3 generation of line #4.3 in which 10 plants were found to be homozygous for *oep4.1-1* but not transformed (data not shown). Surprisingly these represented the first homozygous *oep24.1-1* lines after genotyping of at least 737 plants before and after the complementation experiment. The two homozygous lines found in the T2 generation were further characterised by a full length 5'-3' PCR using cDNA as the template. In comparison to controls, no amplification band was achieved for these lines confirming the knock-out status in *oep24.1-1* (Bachelor thesis Olga Lesina, 2010). However these knock-out lines of *AtOEP24.1* showed no obvious phenotype under normal growth conditions.

1.1.2 Characterisation of the oep24.1-2 line

During the course of my work, an additional T-DNA insertion line in the promoter region of *OEP24.1*, *oep24.1-2* (GABI_086_H07, Figure 3) was acquired and characterised. The initial screening of the F2 and F3 generations showed that this line – in contrast to *oep24.1-1*– segregated in a normal way giving homozygous, heterozygous and wild-type alleles of the T-DNA insertion. As the insertion of the T-DNA is located in the promoter region of the gene (Figure 3), further characterisation was performed to clarify the influence of this insertion on the expression of *OEP24.1*. The 3' end of the T-DNA was amplified, cloned and sequenced

so that the exact site of the insertion could be determined (Figure 3). To verify if the homozygous lines correspond to knock-out mutants, total RNA from 14-days old-seedlings of the F3 generation was prepared, reverse transcribed, and analysed by quantitative real time RT PCR. The results showed that the homozygous line corresponds to an overexpression line with about 200 times the amount of *OEP24.1* transcripts when compared to wild-type plants (Figure 4A). The amount of *OEP24.2* RNA was also tested, showing no significant differences between the different lines (data not shown). The overexpression of AtOEP24.1 could also be verified at the protein level (Figure 4B). This OEP24.1 overexpression line showed no obvious phenotype under normal growth conditions.

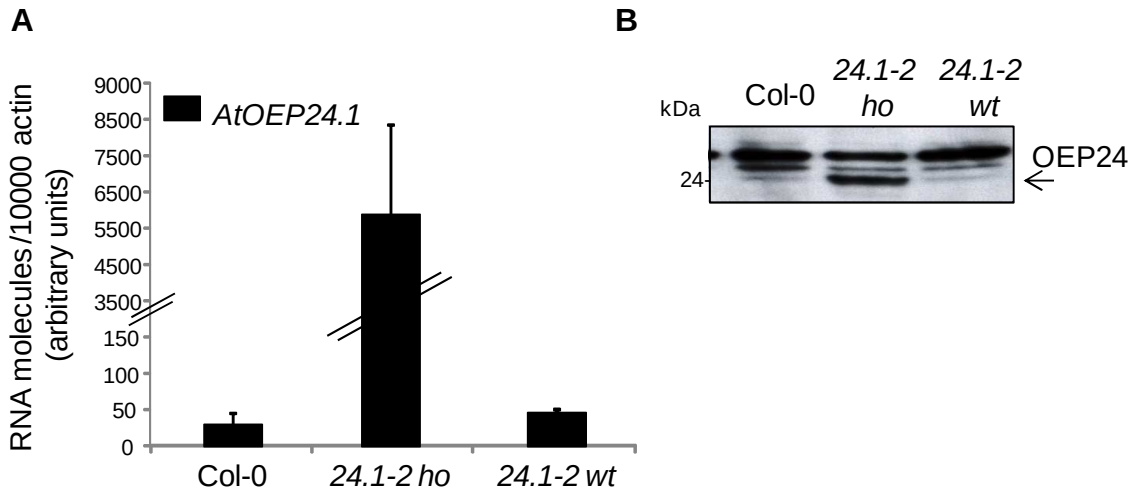

Figure 4: OEP24.1 transcript and protein levels in line *oep24.1-2*
A) Quantification of the *OEP24.1* mRNA level using real time RT PCR. mRNA was prepared from 14-days-old seedlings of Col-0 as well as *oep24.1-2* homozygous and *oep24.1-2* wild-type background plants. The mRNA amount (arbitrary units, n= 3±SD) was normalised to 10000 actin transcripts. **B)** Immunoblot of *Arabidopsis* leaf protein extract (20 µg) using an antiserum raised against AtOEP24.1. OEP24 is shown by an arrow; the other signals correspond to unspecific binding of the antiserum.

1.1.3 Characterisation of the oep24.1-3 line

In addition to the two lines, a third mutant line for OEP24.1, *oep24.1-3* was obtained. This line corresponds to a TILLING line. TILLING (*Targeting Induced Local Lesions in Genomes*) is a general reverse-genetic strategy that provides an allelic series of induced point mutations produced by the mutagen ethyl-methanesulfonate in the gene of interest. *Arabidopsis* TILLING lines for point mutations in *OEP24.1* were subjected to a screening by the Seattle *Arabidopsis* TILLING Project (Till *et al*., 2003). From this screening, the line CS91501 was ordered and named *oep24.1-3*. *oep24.1-3* harbours a point mutation in which the nucleobase guanine of position 636 changes to the nucleobase adenine leading to a possible misspliced OEP24.1 RNA and to a frame shift in the open reading frame (see Figure 3). For the initial screening of the M3 generation, the DNA of 16 plants was isolated as

described in materials and methods. After that, the region comprehending the expected point mutation was amplified with gene specific primers, and the amplified product was sent for sequencing. The results showed a segregation of two wild-types, eight heterozygous and six homozygous plants for the point mutation. As this point mutation is located in a splice junction site, a possible missplice was analysed as well. For this purpose, *OEP24.1* cDNA of a homozygous line for the point mutation was amplified, cloned and sequenced, thereby revealing missplicing of the *OEP24.1* RNA. 82 base pairs belonging to the first intron were not properly spliced out, leading to a frame shift and thus several stop codons within the open reading frame of the protein. This loss of function line did not show an obvious phenotype when grown under standard conditions.

1.2 Characterisation of a mutant line for OEP24.2

For *OEP24.2* there is no T-DNA insertion line available. Instead, a TILLING line was requested from the Seattle Arabidopsis TILLING Project (Till *et al*., 2003) as well. After the PCR-based screening, one line (CS92311: *oep24.2-1*) containing a point mutation at position 1004 in which the nucleobase guanine changes to the nucleobase adenine was identified. This mutation leads to the appearance of a stop codon at amino acid position 177 of the OEP24.2 open reading frame (Figure 5). For screening of the M3 generation a part of the OEP24.2 gene harbouring the point mutation was amplified and sequenced from 11 plants. The segregation of the point mutation resulted in three wild-type lines, five heterozygous and three homozygous lines. Unfortunately it was not possible to perform a detailed analysis of these mutant lines due to the diverse background and TILLING induced phenotype that all the plants (homozygous, heterozygous and wild-type) exhibited under normal growth conditions.

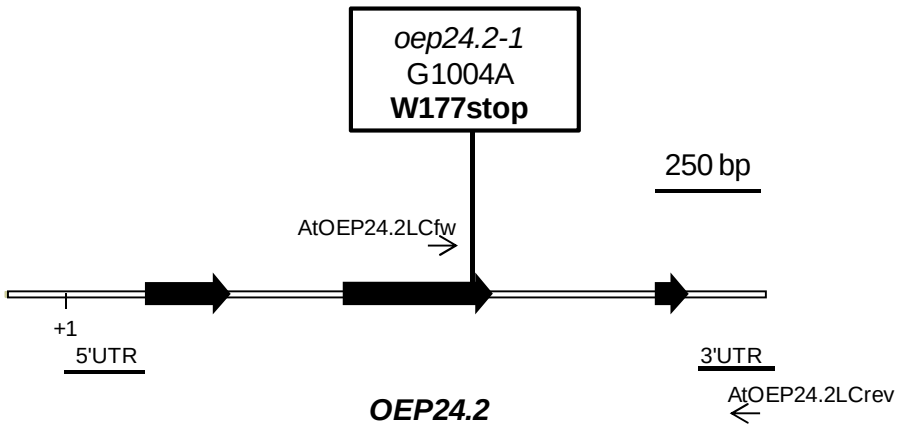

Figure 5: Characterisation of mutation lines of OEP24.2
OEP24.2 from *Arabidopsis thaliana* (At5g42960). Black arrows denote exons, white lines introns. The location of the point mutation in the TILLING line *oep24.2* is indicated by a square. The point mutation leads to a premature stop codon at the position of amino acid 177. Binding sites for *OEP24.2* gene specific primers used for screening and for real time RT PCR are depicted.

2 OEP21 in *Arabidopsis*

OEP21 was first identified and characterised in pea. *In vitro* electrophysiological analysis allowed the speculation that the chloroplast export of primary photosynthesis products is regulated via OEP21 at the level of the outer envelope membrane (Bölter *et al*., 1999; Hemmler *et al*., 2006).

There are two isoforms of OEP21 in *Arabidopsis*: OEP21.1 (At1g76405) and OEP21.2 (At1g20816). Both proteins have an isoelectric point of 9.9 and share an amino acid identity of 78% (167 amino acids), giving a molecular weight of 19.5 kDa for OEP21.1 and 19.8 kDa for OEP21.2. OEP21.1 is also present as a splice variant with 59 amino acids and a molecular weight of 6.6 kDa (TAIR, Lamesch *et al*., 2011). Both OEP21 isoforms show a basal expression in the vegetative rosette of *Arabidopsis* (AtGenExpress Consortium, Schmid *et al*., 2005). Immunoblot analysis of *Arabidopsis* chloroplast sub-fractions showed the localisation of OEP21 in the outer envelope membrane (Figure 6).

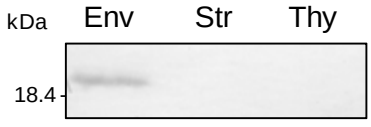

Figure 6: Localisation of OEP21 at the envelope of *Arabidopsis* chloroplast
Immunoblot analysis of the *Arabidopsis* chloroplast sub-fractions envelope (Env), stroma (Str) and thylakoids (Thy) using an antiserum raised against AtOEP21.1. For all sub-fractions 4 µg of protein were loaded.

2.1 Characterisation of OEP21 single mutants in *Arabidopsis*

To clarify the physiological function of OEP21, different mutant lines for OEP21.1 and OEP21.2 were analysed. At the beginning of my thesis, two homozygous T-DNA insertion lines for OEP21.1, *oep21.1-1* (SAIL_548_C05) and *oep21.1-2* (SALK_058578) were available (Figure 7A). In the line *oep21.1-1*, the T-DNA insertion is located in the fourth exon of the gene. Real time RT PCR showed that the transcript is absent in *oep21-1* representing a knock-out line for OEP21.1 (Figure 8).

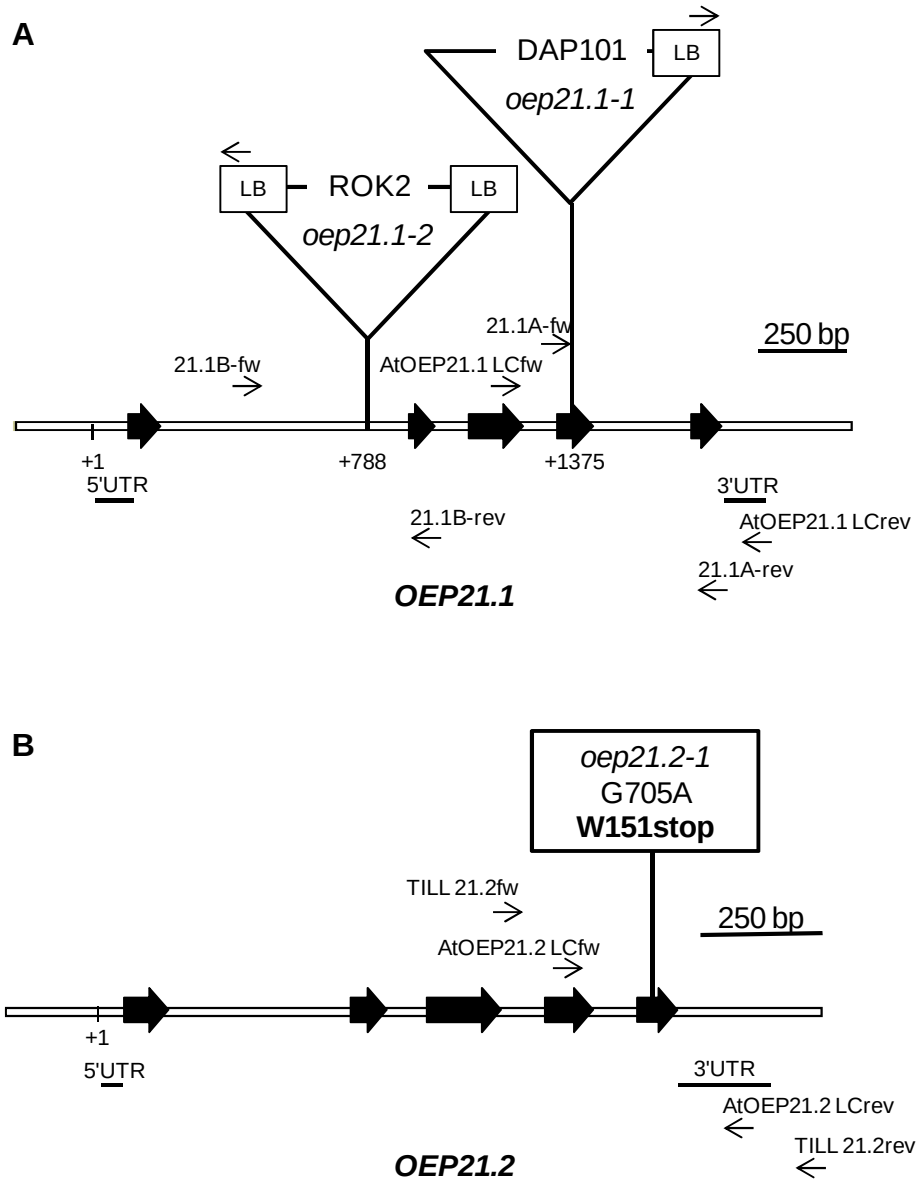

Figure 7: Characterisation of OEP21.1 and OEP21.2 mutant lines
A) *OEP21.1* from *Arabidopsis thaliana* (At1g76405). Black arrows denote exons, white lines introns. The insertion sites of T-DNAs in lines SAIL_548_C05 (*oep21.1-1*) and SALK_058578 (*oep21.1-2*) are indicated by triangles. Binding sites for *OEP21.1* gene specific primers and T-DNA specific left (LB) primers used for genotyping and for real time RT PCR are depicted.
B) *OEP21.2* from *Arabidopsis thaliana* (At1g20816). Black arrows denote exons, white lines introns. The location of the point mutation in the TILLING line *oep21.2* is indicated by a square. The point mutation leads to a premature stop codon at the position of amino acid 151. Binding sites for *OEP21.2* gene specific primers used for screening and for real time RT PCR are depicted.

In *oep21.1-2,* the T-DNA insertion is located in the first intron of the gene (Figure 7A). For this mutant, the 3' end of the T-DNA was analysed and it could be demonstrated that it also corresponds to a left border (LB) (Bachelor thesis Olga Lesina, 2010). Real time RT PCR results showed a reduction of the transcript amount of *OEP21.1* to 40 % when compared to the wild-type Col-0 (Figure 8). Further, PCR amplification and sequencing analysis of the *oep21.1-2* cDNA indicated that there is a case of alternative splicing in the first intron at the

T-DNA insertion site. Part of the cDNA showed a correct splicing of the first intron, leading to a wild-type copy of *OEP21.1*. On the other part of the cDNA the T-DNA was not correctly and completely spliced out, leading to a mutated *OEP21.1*. In summary it can be assumed that *oep21.1-2* corresponds to a knock-down allele.

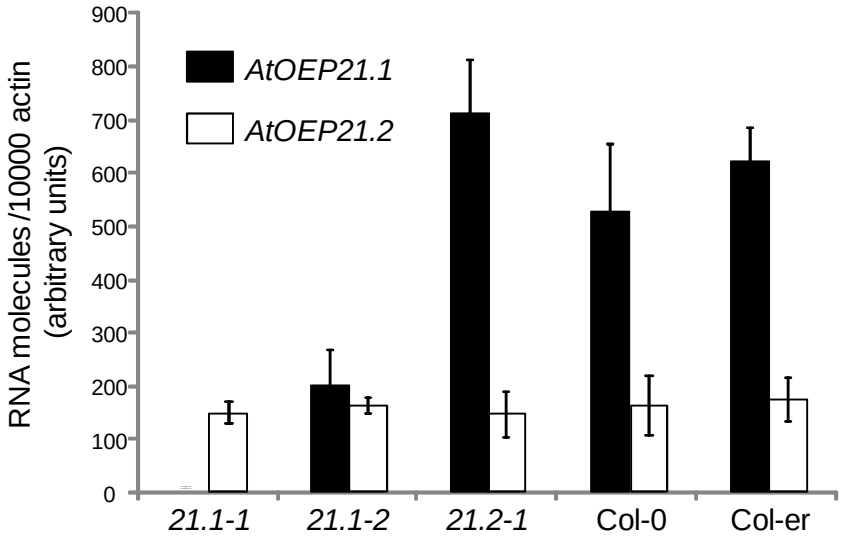

Figure 8: *OEP21.1* and *OEP21.2* transcript levels in the mutant lines
Quantification of the *OEP21.1* and *OEP21.2* mRNA level using real time RT PCR. mRNA was prepared from 15-days-old seedlings. The two T-DNA insertion lines for OEP21.1 (*oep21.1-1*, *oep21.1-2*) and the TILLING line for OEP21.2 (*oep21.2-1*) were tested. Wild-type Col-0, as the background genotype for the T-DNA insertion mutants and wild-type Col-er, as the background genotype for the TILLING line were also tested. The mRNA amount (arbitrary units, n= 3±SD) was normalised to 10000 actin transcripts.

For OEP21.2, one TILLING line: CS86516 (Seattle Arabidopsis TILLING Project, Till *et al*., 2003) was available. In this line, named *oep21.2-1*, a point mutation changes the nucleobase guanine at position 705 to the nucleobase adenine, resulting in a premature stop codon at amino acid position 151 of the OEP21.2 open reading frame (Figure 7B). The line was homozygous for the point mutation. For all three OEP21 mutants the content of *OEP21.2* RNA was tested using quantitative real time RT PCR. No significant differences to wild-type could be detected (Figure 8). In a previous work (A. Timper; R. Thomson, unpublished) all tree homozygous OEP21 mutant lines (*oep21.1-1*, *oep21.1-2* and *oep21.2-1*) were analysed and showed no obvious phenotype under standard growth conditions. During the curse of my thesis, a second mutant line for OEP 21.2, *oep21.2-2* was ordered. It corresponds to the T-DNA insertion line SALK_122968. The T-DNA insertion is located at the promoter region (-47 bp) of *OEP21.2* (not shown). This mutant line contains five times more *OEP21.2* RNA when compared to Col-0) (Bachelor thesis Olga Lesina, 2010). The line did not show any obvious phenotype when grown under standard conditions. Thus, no further analysis of this line was performed.

2.2 OEP21 double mutants

The aim of my work was to cross the homozygous mutant lines *oep21.1-1* and *oep21.1-2* with the homozygous mutant line *oep21.2-1* in order to generate a double mutant to clarify the function of OEP21 *in vivo*.

Homozygous *oep21.1-1* (F4) and *oep21.1-2* (F6) were crossed with the homozygous line *21.2-1* (F4) generation. The next generation – F1 after crossing – was genotyped and heterozygous plants for *oep21.1-1, oep21.1-2* and *oep21.2-1* were selected. In the F2 generation of the cross between *oep21.1-1* and *oep21.2-1*, only one homozygous double mutant line (21dmA#35) was found after genotyping 376 plants. For this line the corresponding background wild-type (21dwtA#38) was also selected. For the cross between *oep21.1-2* and *oep21.2-1* (21dmB) cross, five homozygous double mutant lines were found after genotyping 190 plants. The double mutant 21dmA#35 and two double mutant lines of 21dmB were genotyped again in the F3 generation to verify the homozygous double mutant status.

The double mutant and double wild-type lines for OEP21 were subjected to phenotype analysis. Seedlings grown on 0.5% MS media with and without supplementation of sugar and plantlets germinated on soil were tested under different light conditions (long day, short day, constant light). No obvious phenotype could be detected in any line. For detailed analysis only the double mutant line 21dmA#35 and the corresponding wt-line (21dwtA#38) were selected because they descended from the cross of the knock-out line *21.1-1* and *21.2-1*. The double knock-out status from this line was demonstrated at the protein level (Figure 9A and B).

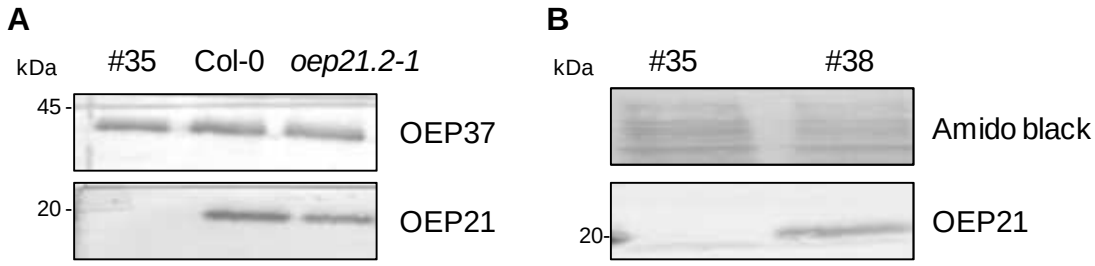

Figure 9: Confirmation of the OEP21 double mutant line at the protein level
Chloroplast envelope (10 ug of protein) of 4-weeks-old *Arabidopsis* plants was separated in a Shägger gel. Immunoblot was performed using antibodies raised against AtOEP21.1. **A)** Signals of OEP37, an outer envelope protein of the chloroplast, are shown as a loading control. #35: double mutant line 21dmA#35, Col-0: wild-type Columbia-0.
B) An amido black stained fraction of the blot is shown as a loading control. #35: double mutant line 21dmA#35, #38: double wild-type line 21dwtA#38.

2.3 Complementation of the OEP21 double mutant

The double mutant line 21dmA#35 was stable transformed with the entire *OEP21.1* gene (4275 bp), including the promoter of the gene as well as 3' UTR region and with the *OEP21.1* cDNA under the control of the 35S promoter. The aim of this experiment was to have a complemented line as a control for further experiments. From this complementation experiment two lines (K4.3 and K2.4) were selected. Real time RT PCR of 14-days-old seedlings, of the line K4.3 (transformed with the *OEP21.1* gene) displayed similar levels of *OEP21.1* RNA, and the K2.4 line (transformed with the *35S::21.1* cDNA) showed 7 times more *OEP21.1* RNA level when compared to the wild-type Col-0 (data not shown). Immunoblot analysis of *Arabidopsis* chloroplast using an antiserum raised against AtOEP21.1 corroborated these results (Figure 10).

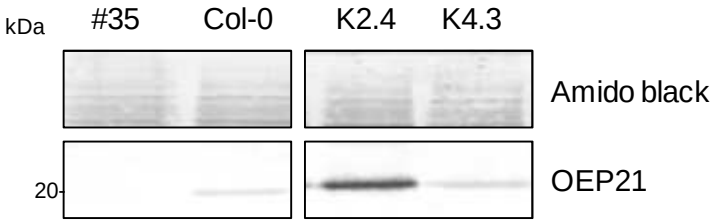

Figure 10: Confirmation of the overexpression and complementation lines of OEP21.1
Immunoblot analysis of *Arabidopsis* isolated chloroplasts (10 ug of proteins) using an antiserum generated against AtOEP21.1. An amido black stained fraction of the blotted membrane is shown as a loading control. #35: double mutant line 21dmA#35, Col-0: wild-type, K2.4: overexpression *OEP21.1* line, K4.3: complemented *OEP21.1* line.

2.4 Stromal proteins of the OEP21 double mutant

As the double mutant line (21dmA#35) did not show any visible phenotype when grown under different light conditions a screen for changes in the proteome of mutant chloroplasts was performed. Stroma samples of the double mutant and the double wild-type was separated in 2D IEF/SDS-PAGE (Figure 11). Protein spots that showed an apparent increase or decrease compared to the corresponding wt-line (21wtA#38) samples were analysed by Peptide Mass Fingerprint (MALDI, Matrix Assisted Laser Desorption/Ionization) at the "Zentrallabor für Proteinanalytik" of the LMU München (Dr. Lars Israel). From this analysis five proteins could unequivocally identified as the plastid intrinsic GAPDH (glyceraldehyde-3-phosphate dehydrogenase), embryo defective 2726 (RNA binding/translation elongation factor), RuBisCo activase, RuBisCo and CpHsc70-1. The change discovered for RuBisCo, RuBisCo activase, and GAPDH could be an indication for an alteration in the carbohydrate metabolism in the mutant line. In order to quantify protein contents immunoblot analysis using antisera raised against GAPDH, cpHsc70-1 and RuBisCo activase were performed. Unfortunately, no significant differences in the amount of the tested proteins could be detected when comparing

stroma and total protein leaf extract from the double mutant and the double wild-type lines (data not shown).

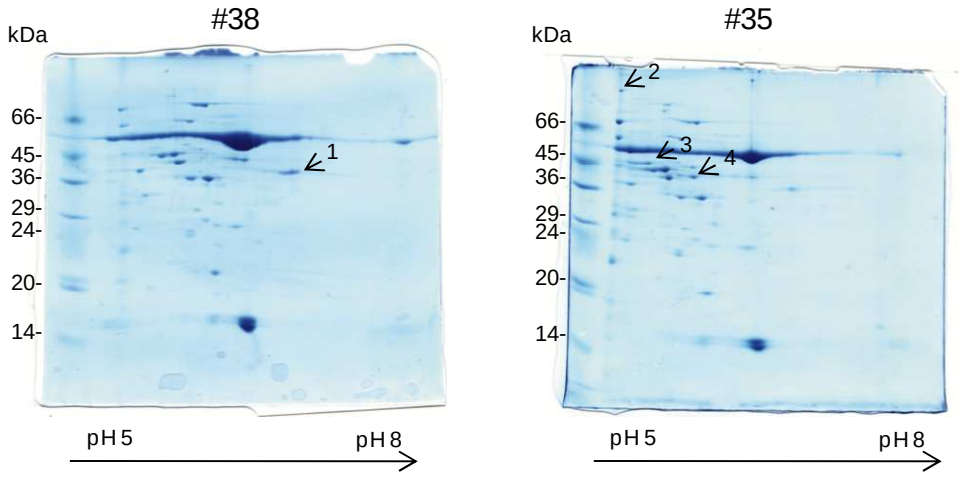

Figure 11: Comparative 2D IEF/SDS-PAGE analysis of 21dmA#35 and 21dwtA#38 chloroplast stroma.
Protein spots with an apparent increase or decrease (arrows) in protein amount relative to the wt sample were cut and identified by mass spectrometry: 1) GAPDH, 2) embryo defective 2726, 3) and 4) RuBisCO activase. 100 µg of proteins were used. The experiment was performed twice. For the second time, where RuBisCo and CpHsc70-1 were detected, 200 µg of protein were loaded (data not shown). #35: double mutant line 21dmA#35, #38: double wild-type line 21dwtA#38.

2.5 Metabolite analysis of the OEP21 double mutant

In order to elucidate if the transport or storage of chloroplast metabolites was impaired in the OEP21 double mutant, contents of glycolysis and citric acid cycle intermediates as well as sugars and amino acids were determined. For that purpose, 4-week-old plants grown in a 12 hours light (9 to 21 h) and 12 hours dark rhythm from the mutant line 21dmA#35 and the wild-type line 21dwtA#38 were compared. In addition, the complemented K4.3 and the overexpression K2.4 lines were analysed as controls. No significant changes in glycolysis and citric acid cycle metabolites could be observed between the tested lines. In contrast, a significant increase of the amino acids serine, threonine, phenylalanine, tryptophan, tyrosine, leucine and isoleucine, at the end of the night could be detected in the K2.4 overexpression line when compared to all other lines (Figure 12A, B). This change was still visible after one hour of light exposure for phenylalanine, leucine and isoleucine (Figure 12B). For the time points 14 h (mid day), 20 h (end of the day) and 22 h (one hour dark) no change could be registered (data not shown).

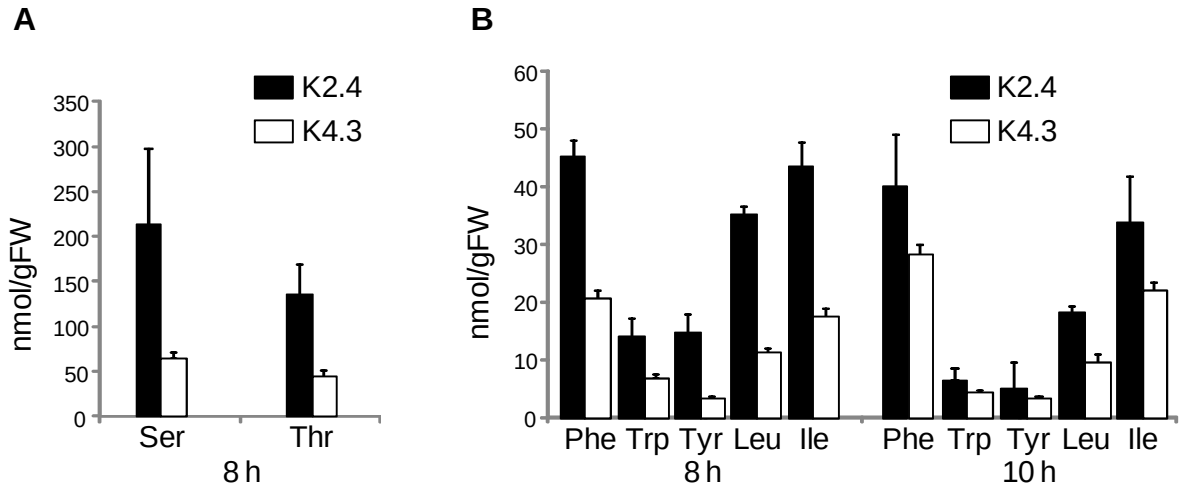

Figure 12: Amino acids are increased in the OEP21.1 overexpression K2.4 line at the end of the night

Amino acids were determined in 4-week-old plants grown at a 12 hours light (9 to 21 h) and 12 hours dark rhythm. Comparison between the overexpression line K2.4 (black bars) and the complemented K4.3 line (white bars) are shown. **A)** Amino acids Ser: serine and Thr: threonine at time point 8 h are shown for both mutants. **B)** Amino acids Phe: phenylalanine, Trp: tryptophan, Tyr: tyrosine, Leu: leucine, Ile: isoleucine at time point 8 h (1 h before light) and 10 h (1h light) are shown.

3 New membrane intrinsic proteins in the chloroplast envelope

The aim of this part of my thesis was to discover new so far unknown chloroplast envelope proteins that are implicated in metabolite transport. For this purpose, purified outer envelope of pea was separated by SDS-PAGE in absence and in presence of urea (previous work Andreas Timper, Figure 13).

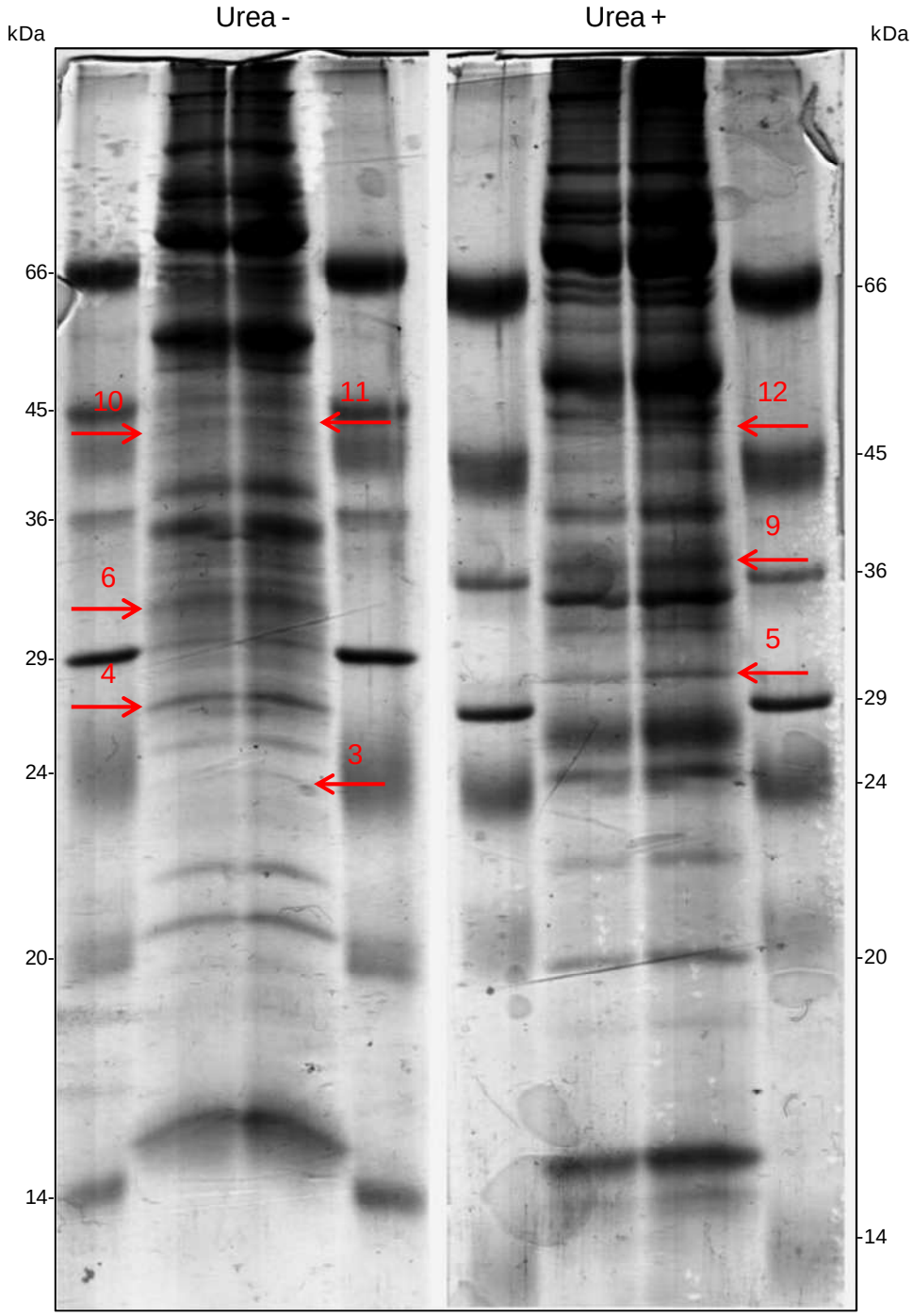

Figure 13: Outer envelope proteins of pea separated by SDS-PAGE
Purified outer envelope of pea was separated by SDS-PAGE in absence and in presence of urea. Protein bands depicted by arrows were selected for protein sequencing. PsNOEP23 was detected in band 3, PsNOEP40 in bands 10 and 12, and PsNIEP57 was detected in band 10, 11 and 12.

Both gels were compared carefully and bands that exhibited a shift in the running behaviour were selected for further analysis. It is known that especially outer envelope membrane proteins displaying a β-barrel structure show a different running behaviour when they are separated in the presence of urea (personal communication Prof. Soll). As usually chloroplast outer envelope membrane proteins built a β-barrel pores (for overview see Duy *et al*., 2007), this feature was selected as the first hint to search for new outer envelope proteins acting as metabolite transporters. Eight bands were excised from the gels (Figure 13) and sent for sequencing at the "Zentrallabor für Proteinanalytik" at the LMU München (Dr. Lars Israel). The samples were sequenced using LC-MS/MS and the resulting peptide masses were compared with a pea EST database (Franssen *et al*., 2011) to identify the respective protein in *Pisum* and the ortholog in *Arabidopsis*. All proteins with a molecular weight consistent with their band size on the gel, a basic isoelectric point (IP), and a putative chloroplast/outer envelope localisation according to Ferro *et al*., (2010) or TAIR-prediction (Lamesch *et al*., 2011), were selected as candidates. As the pea EST database is composed by all possible open reading frames, the pea sequenced peptides for each candidate was tested to be in frame with the presented orthologous protein in *Arabidopsis*. From this analysis, three putative new envelope proteins were selected and named according to the molecular weight of the protein in *Arabidopsis*. At2g17695: NOEP23 (new outer envelope protein of 23 kDa), At3g57990: NOEP40 (new outer envelope protein of 40 kDa) and At5g24690: NIEP57 (most likely representing new inner envelope protein of 57 kDA) (Table 8). The selected candidates were further characterised *in silico* for the presence of α-helical membrane regions using a total of 18 different prediction algorithms and for the presence of a β-barrel structure (five to six prediction algorithms) all available in the ARAMEMNON database (ARAMEMNON plant membrane protein database, Schwacke *et al*., 2003). Only for AtNIEP57, two to four α-helical membrane domains were predicted (Table 8). For AtNOEP40, a probable β-barrel structure was proposed by three of the five algorithm tested. For AtNOEP23 neither α-helical domains nor a β-barrel pore was suggested. To analyse the localisation of the candidates in more detail, an *in silico* prediction by a total of 17 different targeting prediction programs available in the ARAMEMNON database (Schwacke *et al*., 2003) was used (Table 8). From this analysis only AtNIEP57 was annotated as a chloroplast protein, due to the existence of a transit peptide of 41 amino acids (ChloroP, Emanuelsson *et al*., 1999). For AtNOEP23 and AtNOEP40 no classical chloroplast transit peptide was predicted. In addition for AtNOEP23 and AtNIEP57, domains of unknown function were found. The domain in AtNOP23 is fully uncharacterised and the domain in AtNIEP57 that is present in eukaryotes, is typically between 168 to 186

amino acids long, has a conserved RYQ sequence motif and comprises amino acids 239 to 409 of AtNIEP57 (TAIR, Lamesch *et al*., 2011). Interestingly a glycine and aspartic acid rich motif at the soluble N-terminal part of the protein was detected (Figure 14, Figure 23).

Table 8: Putative new chloroplast envelope proteins in *Arabidopsis*
The AGI code for the selected candidates, the molecular weight (MW) in kDA, the isoelectric point (IP), the predicted localisation by the presence of a transit peptide (TP) (ARAMEMNON), the length of transit peptide (ChloroP), presence of α-helical transmembrane domain or β-barrel structure (ARAMEMNON) as well as the potential function and protein domains are shown.

	MW kDa	IP	Predicted localisation (TP)	α-helical	β-barrel	Function	Domains
At2g17695 (AtNOEP23)	23.2	9.6	-----	0	maybe	unknown	unknown function (DUF1990)
At3g57990 (AtNOEP40)	39.8	10	-----	0	yes	unknown	-----
At5g24690 (AtNIEP57)	56.8	9.4	chloroplast 41 aa	2-4	-----	unknown	unknown function (DUF3411)

With the help of the EST pea contigs (Franssen *et al*., 2011) and the already known sequence in *Arabidopsis*, primers for the isolation of the complete cDNA sequences in pea were designed. After PCR amplification using pea cDNA as template, cloning and sequencing, the coding sequences of PsNOEP23, PsNOEP40 and PsNIEP57 were obtained (Table 9); Figure 14). Whereas PsNOEP23 was represented by only one peptide in the proteomic sequencing for PsNOEP40 three different peptides in two sequenced bands and for PsNIEP57 five different peptide bands in three different sequenced bands were found (Table 9, Figure14).

Table 9: Putative new pea chloroplast envelope proteins in pea
The molecular weight (MW) in kDa and the isoelectric point (IP) of the proteins were calculated using Vector NTI, the predicted localisation by the presence of a transit peptide (TP) and its length was analysed using the online programs TargetP and ChloroP. The number of sequenced peptides for each protein after analysing the proteomic results is given.

	MW kDa	IP	Predicted localisation (TP)	No. of sequenced peptides
PsNOEP23	23.6	9	-----	1
PsNOEP40	42.4	9.3	-----	3
PsNIEP57	57.4	9.1	chloroplast 45 aa	5

The amino acid sequences for the new envelope proteins found in pea and in *Arabidopsis* are shown in Figure 14. The identity between AtNOEP23 and PsNOEP23 is 62%, AtNOEP40 and PsNOEP40 share 27%, and AtNOEP57 and PsNOEP57 64% amino acids, respectively.

A


AtNOEP23 : MVFLSWGRPSSEQCQQVINKTGTFNYDNKYRGVSSRSIAKIKEDSEIDKDGFLINHARVLVGSGRESYEKGKKALQNWKH : 80
PsNOEP23 : MVFLSWVRPTTQDQNTGINKSGTFNYDDRYKGATAKSISSLQQDKALSNDGFLLNNARVLIGNGIDTFEKGKTALRTWRH : 80
AtNOEP23 : FGMDWAFVDPATPVETGKKFCICVKEVLPWVMLPLQVVYVDESRKSRKGPAHFGYGSGTLQGHLLAGEEKFSIELDGNGE : 160
PsNOEP23 : FGMNWAFVDPETPIQCGAKFCICVKEFLPWLMMPLQVVYVNETKTTKNRGASFGFGSGTLQGHLLAGEERFSIEIDENNQ : 160
AtNOEP23 : VWYEITSFSKPAHFLSFLGYPYVKLRQKHFARHSSEAVLKHVNAS--- : 205
PsNOEP23 : VWYEILSFSKPAHVLSFVGYPYVMLRQKYFAHESAKVMLKHINSSKS- : 207

B

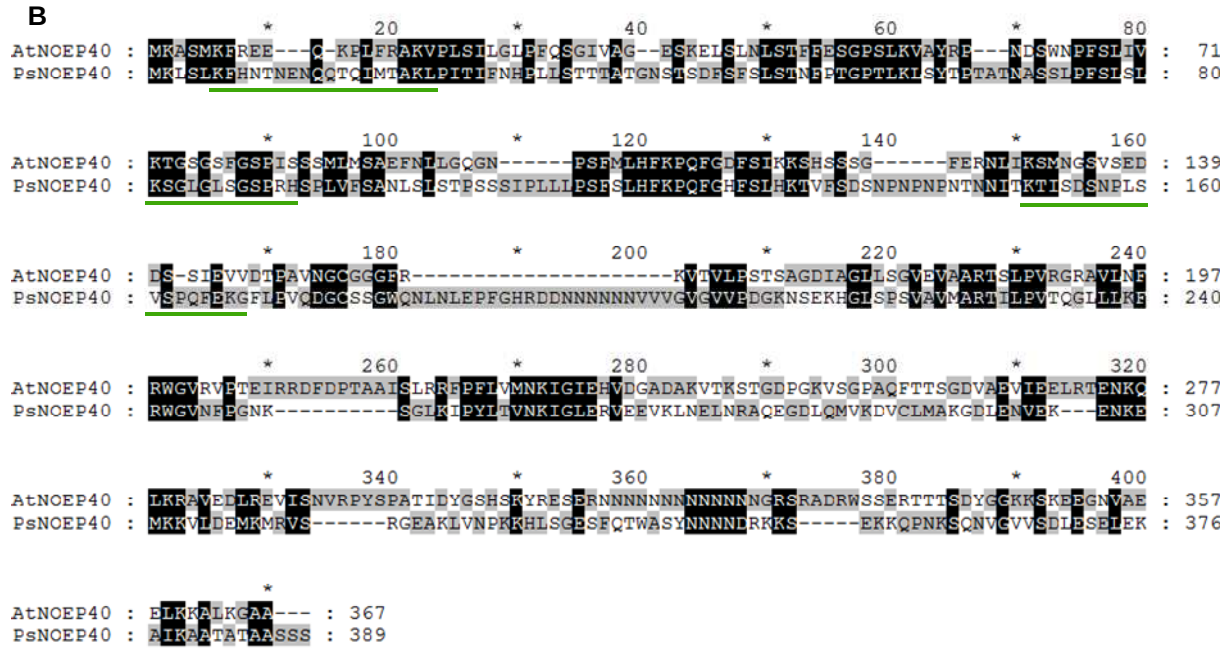
AtNOEP40 : MKASMKFREE---Q-KELFRAKVPLSILGLFFQSGIVAG--ESKELSLNLSTFFESGPSLKVAYRF---NDSWNPFSLIV : 71
PsNOEP40 : MKLSLKFHNTNENQQTQIMTAKLPITIFNHFLLSTTTATGNSTSDFSFSLSTNFPTGPTLKISYTFTATNASSIPFSLSL : 80
AtNOEP40 : KTGSGSFGSFISSSMLMSAEFNLLGQGN------PSFMLHFKPQFGLFSIKKSHSSSG------FERNLIKSMNGSVSED : 139
PsNOEP40 : KSGLGLSGSFRHSPLVFSANLSLSTPSSSIPLLLPSFSLHFKPQFGHFSLHKTVFSDSNPNPNPNTNNITKTISDSNPLS : 160
AtNOEP40 : LS-SIEVVDTEAVNGCGGGFR--------------------KVTVLFSTSAGDIAGLLSGVEVAARTSLPVRGRAVLNF : 197
PsNOEP40 : VSPQFEKGFLFVQDGCSSGWQNLNLEPFGHRDDNNNNNNVVVGVGVVFDGKNSEKHGLSPSVAVMARTILPVTQGLLLKF : 240
AtNOEP40 : RWGVRVPTEIRRDFDPTAAISLRRFPFIVMNKIGIEVDGADAKVTKSTGDPGKVSGPAQFTTSGDVAEVIEELRTENKQ : 277
PsNOEP40 : RWGVNFPGNK----------SGLKIPYITVNKIGLERVEEVKLNELNRAQEGDLQMVKDVCLMAKGDLENVEK---ENKE : 307
AtNOEP40 : LKRAVEDLREVISNVRPYSPATIDYGSHSKYRESPRNNNNNNNNNNNNGRSRADRWSSERTTTSDYGGKKSKEEGNVAE : 357
PsNOEP40 : MKKVLDEMKMRVS------RGEAKLVNPKKHLSGPSFQTWASYNNNNDRKKS-----EKKQPNKSQNVGVVSDIESELEK : 376
AtNOEP40 : ELKKALKGAA--- : 367
PsNOEP40 : AIKAATATAASSS : 389

Figure 14: **Amino acid sequence of the new envelope proteins of *Arabidopsis* and pea**
Identical amino acids are shaded in black, similar amino acids in grey and the sequenced peptides in pea are underlined in green. **A)** AtNOEP23 and PsNOEP23, **B)** AtNOEP40 and PsNOEP40, **C)** AtNIEP57 and PsNIEP57. The predicted α-helical transmembrane domains are depicted in red boxes, and the glycine and aspartic acid rich motif with a blue box.

3.1 Subcellular localisation of the new envelope proteins

3.1.1 In vivo GFP targeting

To determine the subcellular localisation of the selected protein candidates, a transient transformation of mesophyll *Arabidopsis* protoplast using the *Arabidopsis* proteins fused to a C-terminal GFP was performed. A confocal laser scanning microscope was used to analyse the GFP- and autofluorescence of transformed protoplasts. The red autofluorescence that appears when chlorophyll is excited by the laser of the microscope was used as a marker for chloroplasts (Figure 15).

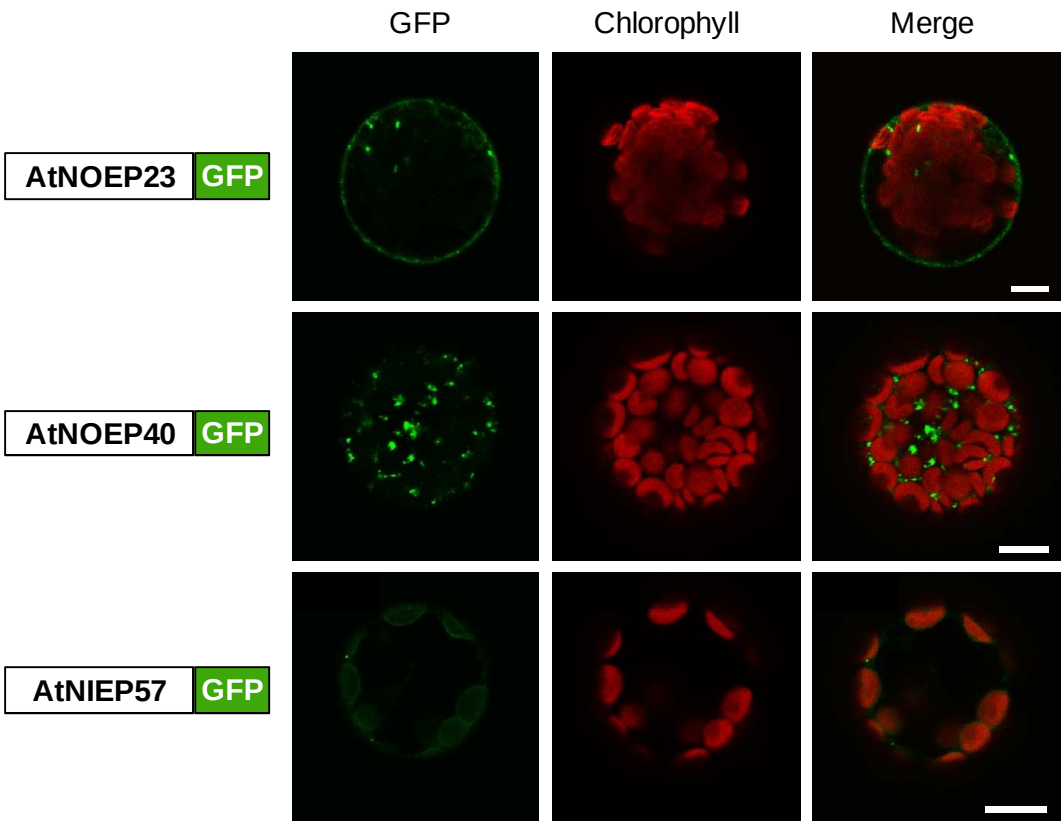

Figure 15: Subcellular localisation of AtNOEP23, AtNOEP40 and AtNOEP57 in *Arabidopsis* protoplasts
Arabidopsis mesophyll protoplasts were transiently transformed with C-terminal GFP fusions to AtNOEP23, AtNOEP40 and AtNIEP57. Signals for GFP fluorescence (GFP), chlorophyll autofluorescence (chlorophyll), and the overlay of both (merge) are shown. Bar, = 10 µm.

For AtNOEP23, possible plasma membrane localisation was detected in protoplasts transformed with the construct. For AtNOEP40, it was not possible to achieve a clear localisation due to the formation of aggregates in the cytoplasm. In contrast, weak but clear chloroplast envelope signals were obtained for AtNOEP57.

3.1.2 Immunoblot analysis

For the subcellular and biochemical characterisation of the new chloroplast envelope proteins in pea, antisera against PsNOEP23, PsNOEP40 and PsNIEP57 were raised. Therefore the full coding sequences of PsNOEP23 and PsNOEP40 were subcloned into the pET21d plasmid vector. In this vector six histidine residues were fused to the C-terminal part of the proteins. The constructs were overexpressed in BL21 *E.coli* cells and subsequently purified from inclusion bodies by affinity chromatography. The purified recombinant proteins (Figure 16) were sent for the generation of antiserum to Pineda Antikörperservice, Berlin. For PsNOEP40 two bands (43.6 and 41.3 kDa) of the overexpressed protein appeared. This is probably due to the existence of a methionine at position 21 of the protein that can act as a second translational start.

The purification of PsNIEP57 for the generation of antiserum was more difficult. The full length mature protein was not able to be overexpressed using different plasmids such as pET21d, pPROEX, pSP65 or pCOLD. For each vector, two different temperatures (12°C and 37°C) and different types of growth media (LB and M9ZB) as well as different *E.coli* strains (BL21, BL21-lys, Rossetta-lys, C43 cells) were tested without success. Two N-terminal constructs of PsNIEP57 (amino acid 44 to 278 and amino acid 44 to 345) were also tried to be overexpressed (pET21d, BL21cells, M9ZB, 37°C, 12°C) without positive result. Only the C-terminal part (amino acid 301-526) of the protein could be successful purified from *E. coli* (vector pET21d, BL21 *E.coli* strain, M9ZB media, 37°C; Figure 16C) and therefore selected for the generation of the antiserum. After overexpression of PsNOEP57, purification of inclusion bodies and purification of the protein using the Ni-NTA column, an additional step of purification was necessary. For that purpose, the recombinant protein was electroeluted from the acrylamid gel and sent for the generation of antiserum (Pineda Antikörperservice, Berlin).

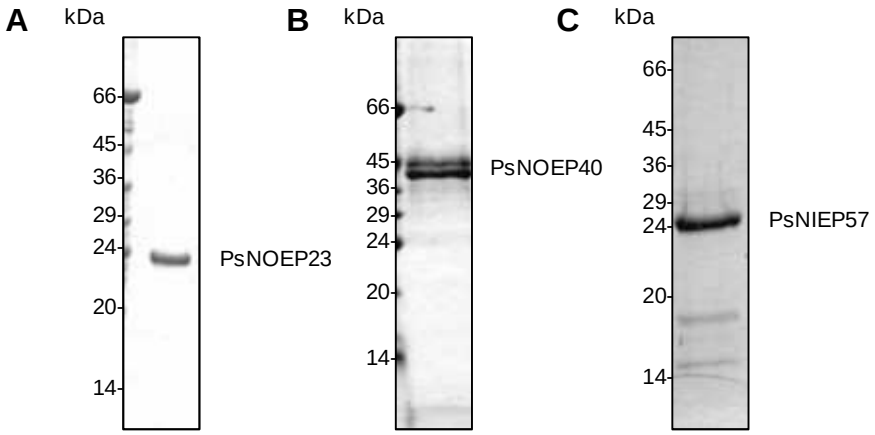

Figure 16: Purification of recombinant PsNOP23, PsNOEP40 and PsNIEP57
A) PsNOEP23 (24.5 kDa) was recovered in the 500 mM and **(B)** 5 µg PsNOEP40 (43.6 and 41.3 kDA depending on the start methionine) in the 50 mM imidazole fraction from the Ni-NTA column.
C) PsNIEP57 (25.8 kDa for the C-terminal part) was recovered in the 500 mM imidazole fraction. 2 µg PsNOEP23, 4 µg PsNOEP40 and 6 µg PsNIEP57 were loaded on the gel and stained.

In the following, antisera generated in rabbit after 240 days for PsNOEP23, 270 days for PsNOEP40 and 270 days for psNIEP57 were used to perform immunoblot analysis of pea chloroplast sub-fractions. For PsNOEP40 it was necessary to perform a purification of the antiserum using recombinant protein coupled to cyanogen-bromide activated sepharose due to the high background. A localisation at the outer envelope of the chloroplast could be detected for PsOEP40 (Figure 17A). PsNIEP57 instead was localised at the inner envelope of the chloroplast in pea as well as in the chloroplast envelope fraction in *Arabidopsis* (Figure 17A, B).

For PsOEP23, although the antiserum did recognize well the overexpressed recombinant protein (Figure 17C), no signal could be detected neither in the pea chloroplast subcellular fractions nor in pea mitochondria or pea microsomal fractions (artificial vesicles formed from the endoplasmic reticulum as well as from the plasma membrane when cells are disrupted (Abas *et al*., 2010, data not shown).

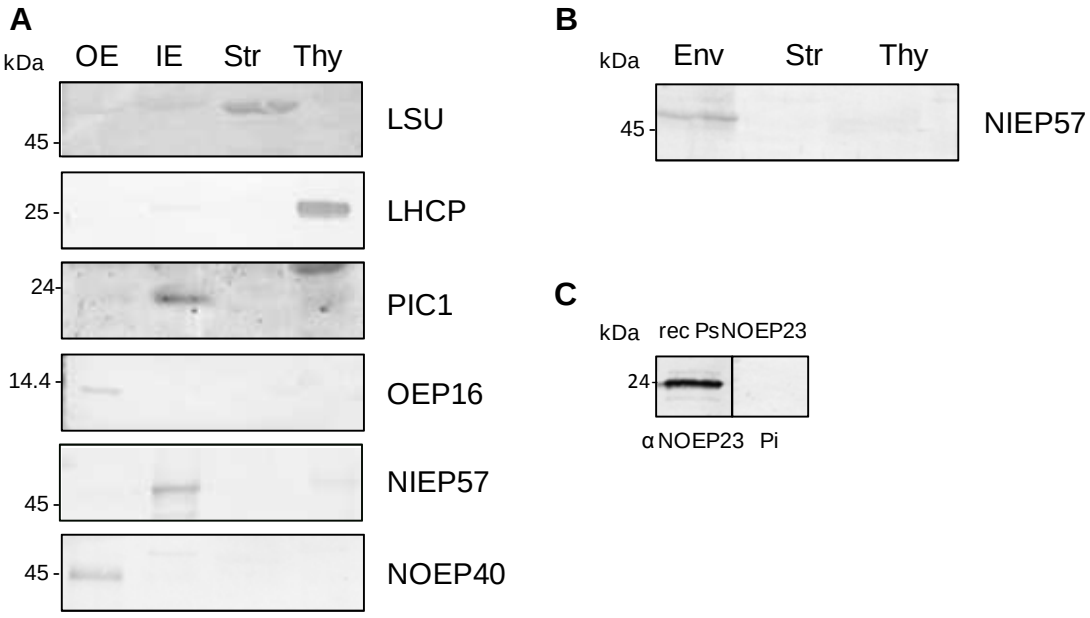

Figure 17: Immunoblot of the new envelope proteins in pea and *Arabidopsis* chloroplast fractions
A) Immunoblot of the *pea* chloroplast sub-fractions OE (outer envelope), IE (inner envelope), stroma (Str) and thylakoids (Thy) using an antiserum raised against PsNOEP40 (5 µg of protein) and PsNIEP57 (2 µg of protein). LSU (large subunit of RuBisCO, 1 µg of protein) appears as a marker of the stroma, LHCP (light-harvesting complex proteins, 0.6 µg of protein) as a marker of the thylakoid fraction, PIC1 (permease in chloroplasts, 10 µg of protein) as a marker protein of the inner envelope of the chloroplast, and OEP 16.1 (1 µg of protein) as a marker of the outer envelope of the chloroplast. **B)** Immunoblot of the *Arabidopsis* chloroplast sub-fractions envelope (Env), stroma (Str) and thylakoids (Thy) using an antiserum raised against PsNIEP57. For all sub-fractions 4 µg of protein were loaded. **C)** Immunoblot of the recombinant (rec) PsNOEP23 (50 ng) using antiserum raised against PsNOEP23 (120 days) as well as the preimmune serum (Pi).

3.2 Molecular characterisation of PsNIEP57

PsNIEP57 was further characterised to determine whether the protein corresponds to an integral membrane protein or is only superficially attached to the inner envelope of the chloroplast. For this purpose inner envelope vesicles of pea chloroplasts were treated with NaCl, Na_2CO_3, urea and triton. Afterwards membrane proteins were pelleted from soluble proteins and analysed by immunoblotting (Figure 18). PsNIEP57 could only be solubilised from membranes by the membrane disrupting detergent triton indicating that PsNIEP57 corresponds to an integral membrane protein.

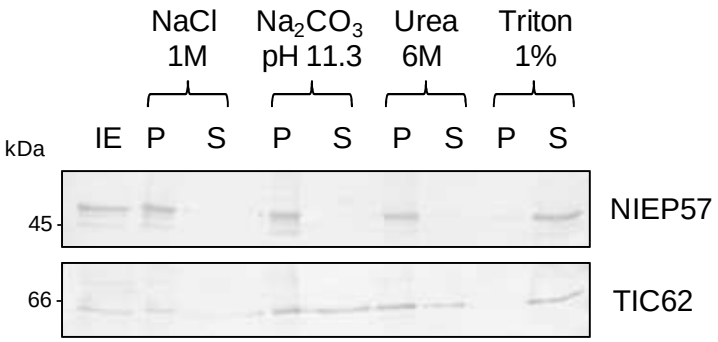

Figure 18: PsNIEP57 is an integral membrane protein of the inner chloroplast envelope
Inner envelope of pea chloroplasts (4 ug of protein) were treated with NaCl (1 M), Na_2CO_3 (0.1 M pH 11.3), urea (6 M) and triton 1%. Afterwards envelopes were ultracentrifuged at 100,000 x g. Pellet (P) and supernatant (S) were loaded separately on the gel and an immunoblot was performed using antibodies raised against PsNIEP57.TIC62, a protein that is only attached to the inner envelope of the chloroplast was used as a control (Stengel *et al*., 2008).

As mentioned before, for AtNIEP57 four α-helical transmembrane domains were predicted. Four transmembrane domains were also predicted for the mature form of psNIEP57 when analysed with the prediction program TopPred 0.01 (Heijne 1992; Claros and Heijne 1994) (Figure 19A). To analyse the topology of PsNIEP57 in more detail, a chemical cysteine modification assay in pea inner envelope membranes was performed. PsNIEP57 contains six cystein residues in the primary sequence which are orientated as follows when four transmembrane domains are proposed: two cysteins facing the stroma, two buried within the envelope membrane, and two facing the intermembrane space (Figure 19B). To test this prediction, inner envelope vesicles were incubated with PEG-maleimide (PEG-Mal). Maleimide is a chemical compound that reacts with the thiol group of cysteines. Due to the five kDa size of the PEG-Mal molecule, covalently PEG-Mal bound to cystein containing proteins will lead to an increased molecular weight that can be visualized by immunoblotting (Figure 19C). As the PEG-Mal reagent is membrane non permeable and the inner envelope vesicles were prepared according to the protocols of Keegstra and Youssif (1986) and Waegemann *et al*. (1992), giving vesicles with a right-side-out orientation (Heins *et al*., 2002; Balsera *et al*., 2009), only the cysteins facing the intermembrane space should be able to react with the reagent. After 30 min of incubation with PEG-Mal, two bands became visible in the assay. This suggests that the four remaining cysteine residues of the protein are not accessible for the reagent. In presence of 1% SDS, where the inner envelope vesicles are solubilised and membranes are disrupted, all protein cysteins are PEGylated, as demonstrated by the presence of five bands on the immunoblot (Figure 19C). The fact that only five instead of six bands are detected can be interpreted by the assumption of one cysteine being faster PEGylated than the others so that no proteins with two PEGylated cysteins can be observed by immunoblot. The change in the molecular weight is bigger than expected for the PEGylation and can be due to a

different running behaviour of the protein in the Bis-Tris/SDS-PAGE used in this approach (Kovács-Bogdán *et al.*, 2011). This experiment corroborates the assumption of four transmembrane domains for psNIEP57, but cannot explain the orientation of NIEP57 due to the equal number of cysteins on both sides of the membrane.

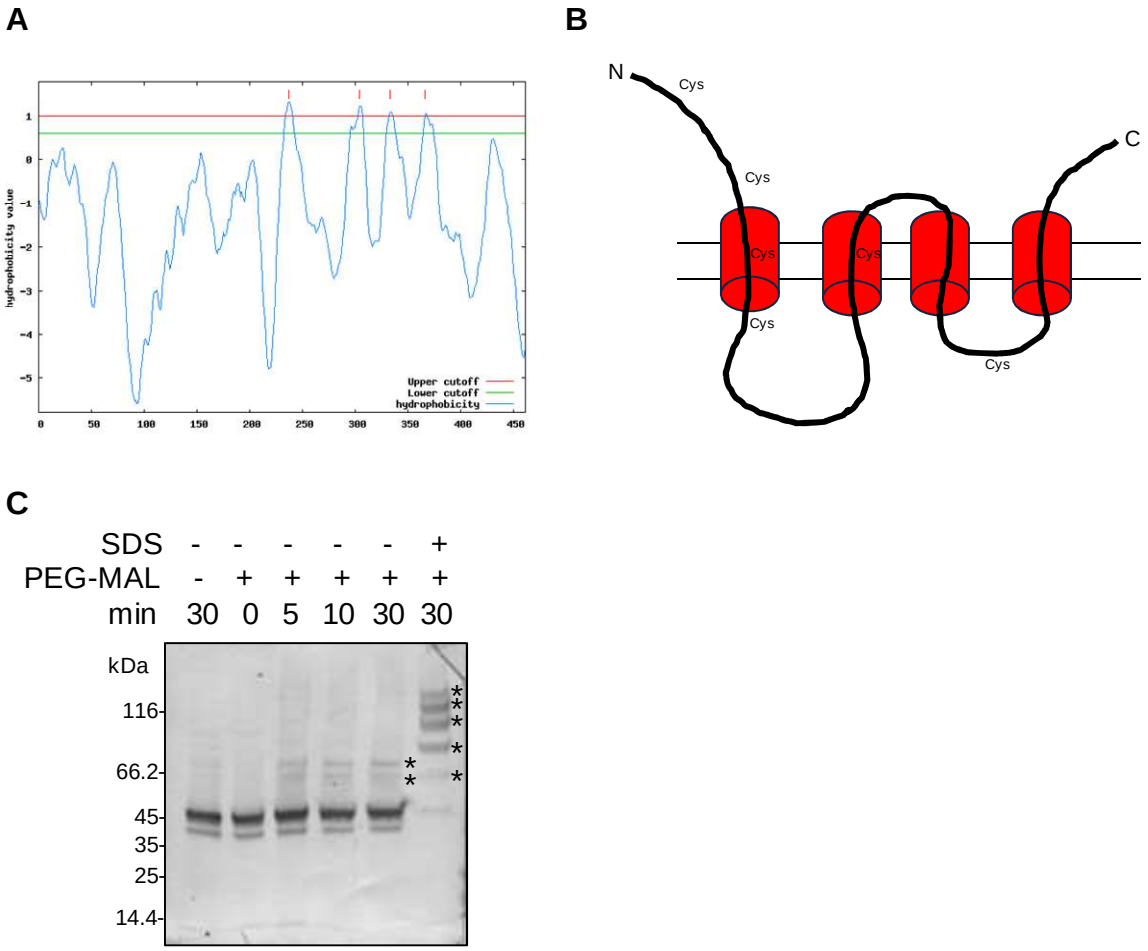

Figure 19: PsNIEP57 is composed of four transmembrane domains
A) Graphical output showing four predicted transmembrane domains for PsNIEP57 using the TopPred program**. B)** Topology model predicted for PsNIEP57. **C)** Verification of the topology prediction by PEGylation of PsNIEP57 in inner envelope membrane vesicles. Inner envelopes (5 µg of protein) of pea chloroplasts were treated for the indicated time points (min) with 7.5 mM of PEG-maleimide in presence (+) or absence (-) of 1% SDS. The reaction was stopped adding 100 mM DTT. The proteins were separated using SDS-PAGE and immunoblot was performed using an antiserum raised against PsNIEP57. Cys: cystein, IMS: intermembrane space, N: N-terminal, C: C-terminal.

To analyse the orientation of PsNIEP57, proteolysis analysis of inner chloroplast envelopes was performed. The vesicles with a right-side-out orientation were treated with proteases in the presence or absence of triton 1%. In the absence of triton, only a certain amount of proteolytic sites depending of the topology of the protein are accessible for the proteases. In contrast, in the presence of triton that disrupts the membrane proteins are fully accessible to proteolysis. The different fragment band pattern with and without triton should allow to clarify the membrane orientation of PsNIEP57. Due to four predicted transmembrane domains

two expected orientations of the protein are possible: one with N- and C-termini orientated towards the intermembrane space, and the other with N- and C-termini orientated towards the stroma (Figure 20A). Figure 20B, shows vesicles treated with thermolysin. Here one band of 45 kDa appears that is completely absent when proteolysis is performed in the presence of detergent. It can be assumed that available N- and C-termini of the protein are digested. This shift of 7 kDa can thus only be explained when N- and C-termini are facing the IMS. In the presence of triton a core of about 35 kDa can be observed, indicating that more sites of the N- and C-part are accessible for proteolysis. When the experiment was performed with trypsin three bands appeared (Figure 20C). The size of the resulted bands (~10, ~15 and ~17 kDa) indicates that trypsin can digest the protein more efficiency than thermolysin, leaving an intact fragment of about 10 kDa in the presence of triton. Unfortunately the band sizes obtained with the trypsin proteolysis cannot exclude the topology of the protein with N- and C-termini orientated toward the stroma. Depending on where the protein is digested, a similar band pattern is expected for both orientations. The N-terminal peptide of about 27 kDa that would be protected from the protease if the N- and C-terminal were orientated toward the stroma cannot be detected because the antibody was not raised against the soluble N-terminal part and first transmembrane domain of the protein. In general, thermolysin as well as trypsin cut very often within PsNIEP57, so no clear expected pattern due to selected cutting sites could be expected as for other proteins. However, an orientation of N- and C-termini of PsNIEP57 towards the intermembrane space (Figure 20A, left) is most likely.

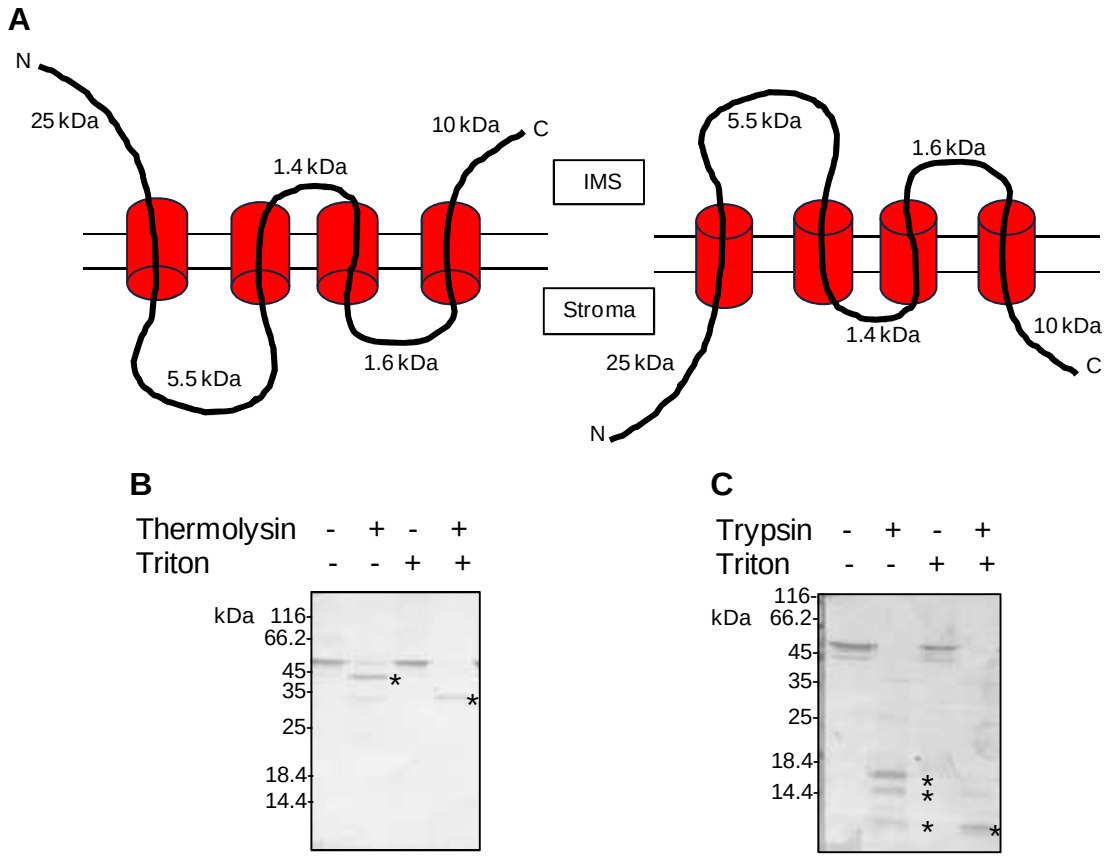

Figure 20: Topology prediction of PsNIEP57
A) Two possible topology predictions for PsNIEP57. The molecular weight in kDa is giving for each hydrophilic part of the protein. The molecular weight for the transmembrane domains is about 2 kDa each. **B)** Proteolysis using thermolysin (5 µg). For each line 5 µg of protein was used. The reaction was incubated 15 min on ice **C)** Digestion using trypsin (0.5 µg). For each line 5 µg protein was used. The digestion was incubated 5 min on ice. 1% triton was used for membrane solubilisation. The proteins were separated using SDS-PAGE and immunoblot was performed using an antiserum raised against PsNIEP57, IMS: intermembrane space, N: N-terminal, C: C- terminal.

3.3 Mutation of NOEP23 and NOEP40 in *Arabidopsis*

In order to describe the physiological role of the new chloroplast envelope proteins, *Arabidopsis* T-DNA insertion lines for AtNOEP23 and AtNOEP40 were analysed.

3.3.1 NOEP23

NOEP23 was found in mono- as in dicotyledonous plants, in *Physcomitrella* and in green algae. Interestingly, NOEP23 is also present in bacteria. Moreover, the unknown domain (DUF 1990) described for NOEP23 is mostly present in the bacteria kingdom and AtNOEP23 is the only protein in *Arabidopsis* harbouring this domain. The expression profile of AtNOEP23 as well as co-expression analysis cannot be analysed due to the absence of the gene in the ATH1 microarray chip.

For AtNOEP23 only one T-DNA insertion line was available: GABI_279G09. For this line the T-DNA was localised at the 3'UTR of the gene (data not shown). Homozygous and

heterozygous plants showed no obvious phenotype when grown under standard conditions (data not shown).

3.3.2 NOEP40

In *Arabidopsis*, NOEP40 corresponds to a single gene family. Orthologs of AtNOEP40 are present in mono- and dicotyledonous plants, in the moss *Physcomitrella patens* and in the spike moss *Selaginella moellendorffii*. No orthologous protein was found in green algae or cyanobacteria. The expression profile showed that AtNOEP40 has its highest expression in cauline leaves, but is expressed ubiquitously throughout plant development (AtGenExpress Consortium, Schmid *et al*., 2005). Co-expression analysis revealed that AtNOEP40 is co-expressed with several unknown chloroplast located proteins, an S-adenosyl-methionine dependent methyltransferase, a chloroplast envelope protein involved in FeS-cluster synthesis, a plastid predicted ABC1-family and kinase-domain containing protein, as well as with the mitochondrial D-lactate dehydrogenase (AtD-LDH) and a putative glyoxalase located in the chloroplast (Atted II database, Obayashi *et al*., 2011 and Bachelor thesis Olga Lesina, 2011).

For NOEP40, the T-DNA insertion line SAIL_266_D10 (*noep40-1*) was analysed. In this line, the insertion is located in the promoter region of the gene at position -25 bp. The F2 generation was genotyped and homozygous, heterozygous as well as the out crossed wild-type background lines were selected (Bachelor thesis Olga Lesina, 2011). To test if the homozygous lines correspond to knock-out mutants, total RNA from 15-days-old seedlings of the T4 generation was prepared, reverse transcribed, and the RNA amount of *NOEP40* was determined using real time RT PCR. The results showed that the homozygous line corresponds to a knock-down line presenting only one third of the transcript level when compared to the wild-type background and the Col-0 wild-type (Figure 21A). The homozygous *noep40-1* knock-down mutants interestingly showed a faster growth and earlier flowering when compared with the wild-type during slow growth at low temperature conditions (10°C) (Figure 21B). To further characterise the importance of AtNOEP40 in the development of the plant, RNAi as well as overexpression lines were generated and an additional T-DNA insertion line: SAIL_759_A01 (that was no available at the beginning of the study) disrupting the single exon of the gene, was ordered.

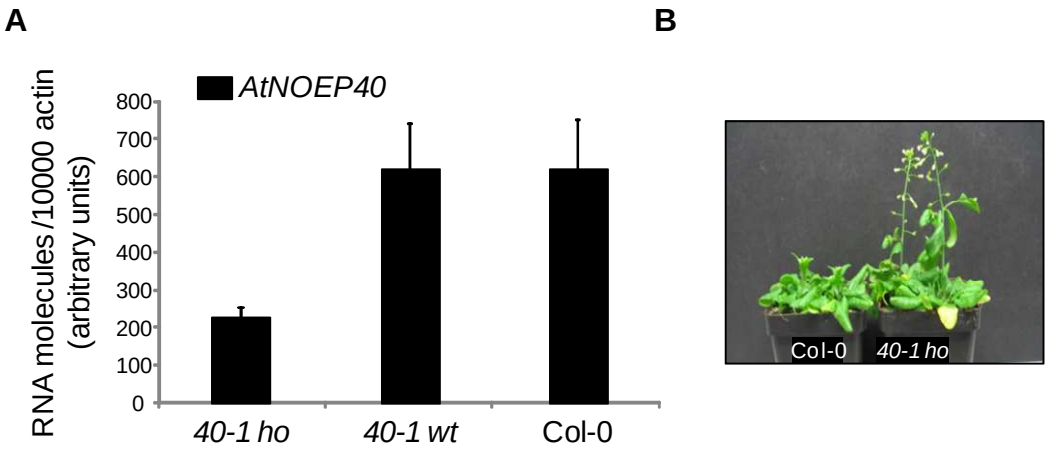

Figure 21: NOEP40 transcript levels and phenotype in line *noep40-1*
A) Quantification of the *NOEP40* mRNA level using real time RT PCR. mRNA was prepared from15-days-old seedlings of Col-0 as well as *noep40-1* wild-type background and homozygous plants. The mRNA amount (arbitrary units, n=3±SD) was normalised to 10000 actin transcripts. **B)** Phenotype of 82-old-days Col-0 and *noep40-1* growth at 10℃ (Bachelor thesis Olga Lesina).

3.4 *In planta* function of NIEP57

3.4.1 Relatives and expression of NIEP57

NIEP57 has been annotated as potential solute transporter with plant-specific but not prokaryotic evolutionary origin (Figure 22A; Tyra *et al*., 2007). AtNIEP57 is present in mono- and dicotyledonous plants as well as in the moss *Physcomitrella patens* and it was also found to be present in green algae, red algae and glaucophytes (Figure 22A). In *Arabidopsis* AtNIEP57 is annotated to be similar to RER1 (*reticulata-related 1*, 20% identical amino acids, Figure 23), a potential chloroplast inner envelope protein of unknown function harbouring three predicted α-helices (ARAMEMNON database, Schwacke *et al*., 2003). Interestingly, after a similarity search of AtNIEP57 against GenBank more than one form or NIEP57 was found for several species indicating the existence of subfamilies (Figure 22B). NIEP57 of subfamily II showed a longer N-terminal part than the forms of subfamily I (Figure 22C).

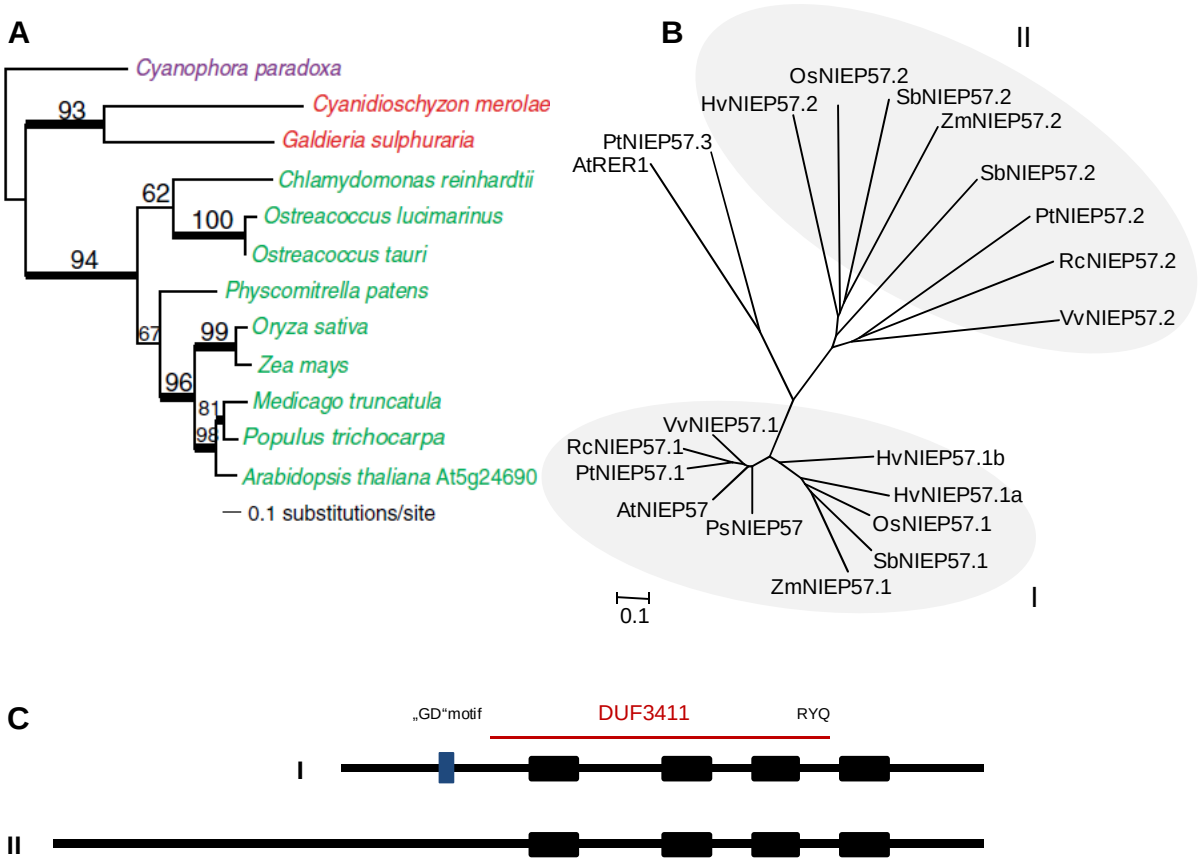

Figure 22: NIEP57 is a plant specific protein.
A) Phylogenetic tree of AtNIEP57 (At5g24690) from Tyra *et al*., (2007), where AtNIEP57 was described as a plant specific transporter. The different algal groups are shown in different colours: red for red algae, green for green algae as well as land plants, and magenta for glaucophytes. **B)** Phylogenetic tree showing the subfamilies present in mono and dicotyledonous plants. **C)** Graphical representation of the alignment between NIEP57 subfamily I and II. Black boxes: predicted transmembrane domains, DUF3411: domain of unknown function, RYQ: conserved motif in DUF3411, GD motif: glycine and aspartic acid rich motif.

The glycine and aspartic acid rich motif was not present in the subfamily II and is partially present in AtRER1 (Figure 23). N- and C-termini of AtRER1 and PtNIEP57.3 are even shorter when compared to the NIEP57 subfamily I (Figure 23).

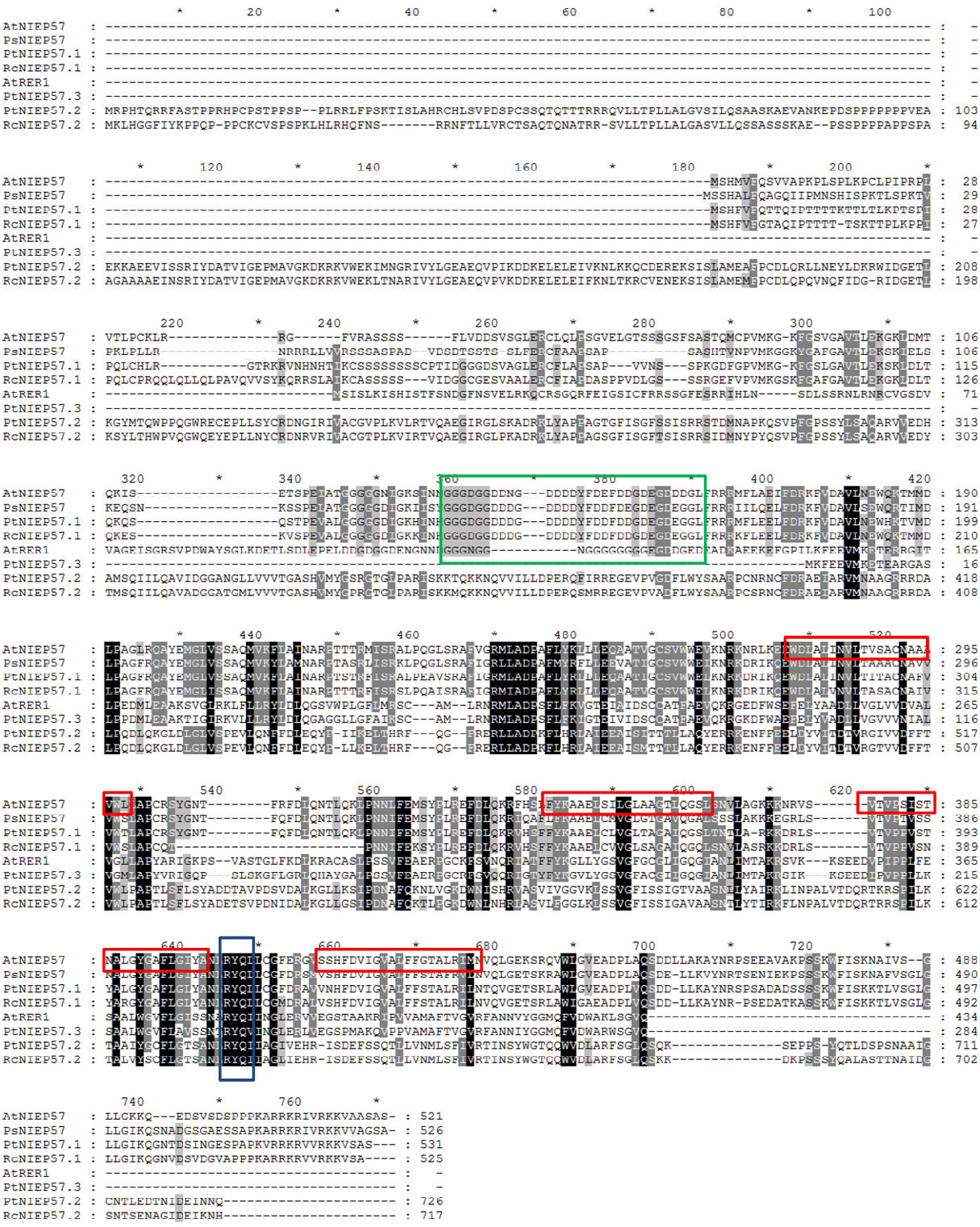

Figure 23: Alignment between NIEP57 of different plant species
Identical amino acids are shaded in black, similar amino acids in grey. NIEP57 of *Arabidopsis* (AtNIEP57), pea (PsNIEP57), AtRER1 (At5g22790), and different forms of NIEP57 present in *Populus trichocarpa* (PtNIEP57) and *Ricinus communis* (RcNIEP57) are shown. The predicted α-helical transmembrane domains are depicted in red boxes, the glycine and aspartic acid rich motif in a green box and the RYQ conserved motif of DUF 3411 in a blue box.

Transcripts of AtNIEP57 in *Arabidopsis* are present throughout plant development and peak in rosette and senescing leaves, (Figure 24A; AtGenExpress Consortium, Schmid *et al*., 2005). A detailed expression analysis of NIEP57 in the different tissues of *Arabidopsis* embryo development (http://seedgenenetwork.net) shows the highest expression at the globular stage in the chalazal seed coat and the peripheral endosperm (Figure 24B).

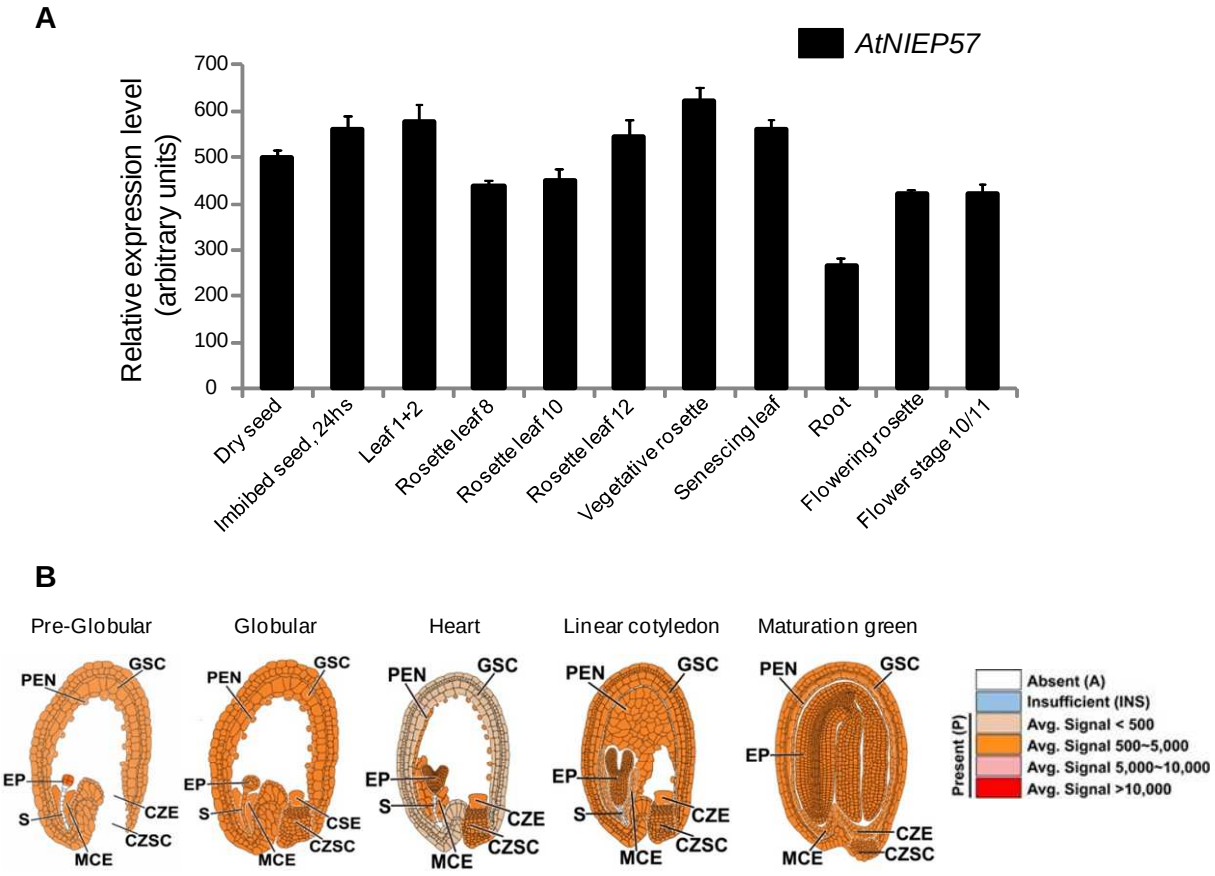

Figure 24: Expression profile of *AtNIEP57* during plant and embryo development
A) Expression of *AtNIEP57* during plant development, AtGenExpress Consortium (Schmid *et al*., 2005). Mean signal intensities (arbitrary units±SD) were averaged from 2–3 replicates. **B)** Tissue-specific expression pattern of *AtNIEP57* in pre-globular, globular, heart, linear cotyledon and maturation green stages (Harada-Goldberg *Arabidopsis* LCM Gene-Chip Data Set). Different tissues are defined as follows: CZE - Chalazal Endosperm; CZSC - Chalazal Seed Coat; EP - Embryo Proper; GSC - General Seed Coat; MCE - Micropylar Endosperm; PEN - Peripheral Endosperm; S - Suspensor; WS - Whole Seed. Seed tissues are coloured according to transcript density for signals that are absent (white), insufficient (blue), <500 (beige), 500–5000 (orange), 5000–10 000 (purple), and >10 000 (dark red). Data available at http://seedgenenetwork.net.

In a large scale protein-protein interaction study, NIEP57 was classified as one of 123 new potential cell-cycle proteins, because NIEP57 interaction was confirmed with a protein, which binds to the E3-ubiquitin ligase of an anaphase-promoting complex (Van Leene *et al*., 2010). Co-expression analysis (Atted II database, Obayashi *et al*., 2011), reveals potential functional links of NIEP57 to (1) plastid thiamine metabolism: co-expression with a) the thiamine monophosphate synthase TH1, and b) a putative hydrolase involved in phylloquinone

synthesis that binds thiamine pyrophosphate); to (2) nucleoside triphosphate/phosphorylation -controlled processes: co-expression with a) GTP-binding potential chloroplast outer membrane protein, b) a GTPase involved in the regulation of the organization of thylakoids c) a putative PP2C-type protein phosphatase (AtPP2C19) from the plasma membrane, and d) with a membrane-bound protein serine/threonine kinase that functions as blue light photoreceptor involved in stomatal opening, chloroplast movement and phototropism); and to (3) metabolite transport activity: co-expression with a) a member of the ATH subfamily (ATH8) involved in chloroplast transport, b) a putative Ca-binding mitochondrial carrier-type protein, and with c) AtBAT2/AtBASS1 a putative chloroplast bile acid: sodium symporter-like transporter). In particular the BAT1 and BAT5 isoforms of the latter transporter family have recently been described to function in Na-dependent plastid pyruvate (BAT1, Furumoto *et al*., 2011) and 2-keto acid transport (BAT5, Gigolashvili *et al*., 2009).

3.4.2 Knock-out mutation of NIEP57 in Arabidopsis

For *AtNIEP57* four T-DNA insertion lines were available: SAIL_64_A05 (*niep57-1*), SAIL_1156_E1 (*niep57-2*), SALK_033007 (*niep57-3*) and SALK_089076 (*niep57-4*). For all lines, the exact insertion site was determined (Figure 25). In *niep57-1*, the T-DNA insertion is located in the 6th exon and the 3’ end of the T-DNA insertion is also a left border. In *niep57-2* the T-DNA is located in the last intron and the 3’ end of the T-DNA insertion could not be determined. In *niep57-3* the insertion is located in the 3th intron and the 3’ end of the T-DNA insertion could be determined. Moreover, it could be seen that the insertion caused a deletion of 16 bp from exon number 4. In *niep57-4* the T-DNA insertion line is also located in intron number 3 (5 bp behind the 3th exon) but the 3’ end of the T-DNA insertion could not be determined (Figure 25).

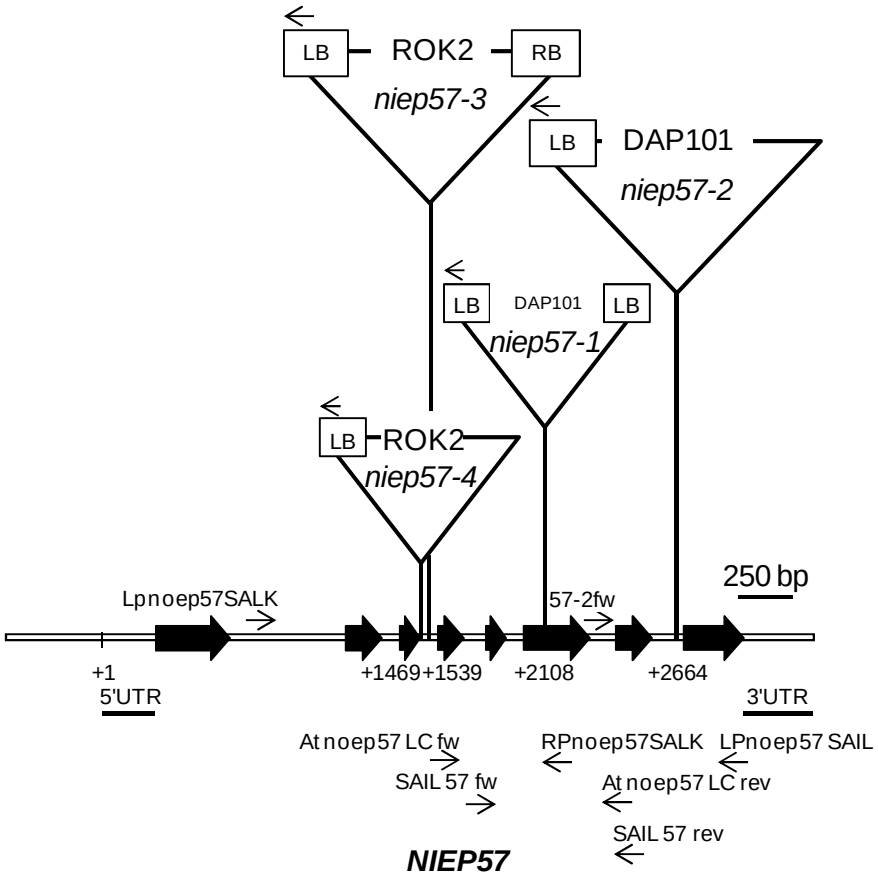

Figure 25: Characterisation of NIEP57 mutant lines
NIEP57 from *Arabidopsis thaliana* (At5g24690). Black arrows denote exons, white lines introns. The insertion sites of T-DNAs in lines SAIL_64_A05 (*niep57-1*), SAIL_1156_E1 (*niep57-2*), SALK_033007 (*niep57-3*), SALK_089076 (*niep57-4*) are indicated by triangles. Binding sites for *NIEP57* gene specific primers and T-DNA specific left (LB) border primers used for genotyping and for real time RT PCR are depicted.

For all four lines it was not possible to find homozygous alleles for the T-DNA insertion (Table 10.)

Table 10: Segregation of the T-DNA insertion in *niep57-1*, *niep57-2*, *niep57-3* and *niep57-4*
Two generations for each line were genotyped. The percentage of wild-type (wt) and heterozygous (he) plants from two generations is depicted as well as the total amount analysed for each line.

niep57-1		***niep57-2***		***niep57-3***		***niep57-4***	
wt	**he**	**wt**	**he**	**wt**	**he**	**wt**	**he**
F2 25%	75%	F2 37.5%	62.5%	F3 73.3%	26.6%	F3 21.4%	78.5%
F3 49.4%	50.5%	F3 44.4%	55.5%	F4 40%	60%	F4 14.8%	85.1%
48.3%	**51.6%**	**41.1%**	**58.8%**	**51.1%**	**48.8%**	**17.03%**	**82.9%**
(n= 196)		**(n= 17)**		**(n= 45)**		**(n= 41)**	

The heterozygous plants did not show an obvious phenotype under standard growth conditions. Due to the absence of homozygous descendants for the T-DNA insertion, a detailed observation of the siliques of heterozygous plants was performed to analyse a

possible embryo lethal phenotype. For this purpose, green siliques from heterozygous, wild-type background and Col-0 plants were harvested and cleared for a few days in 100% ethanol at 4°C. Afterwards the siliques were analysed under the binocular microscope. From this observation a phenotype for lines *niep57-1*, *niep57-2* and *niep57-3* could be detected: approximately 25% of the seeds in each silique looked abnormal (Figure 26A). In young siliques the aborted seeds looked white and empty without an embryo inside. When the silique became older, their seed coat turned brown and dehydrated (Figure 26B and C).

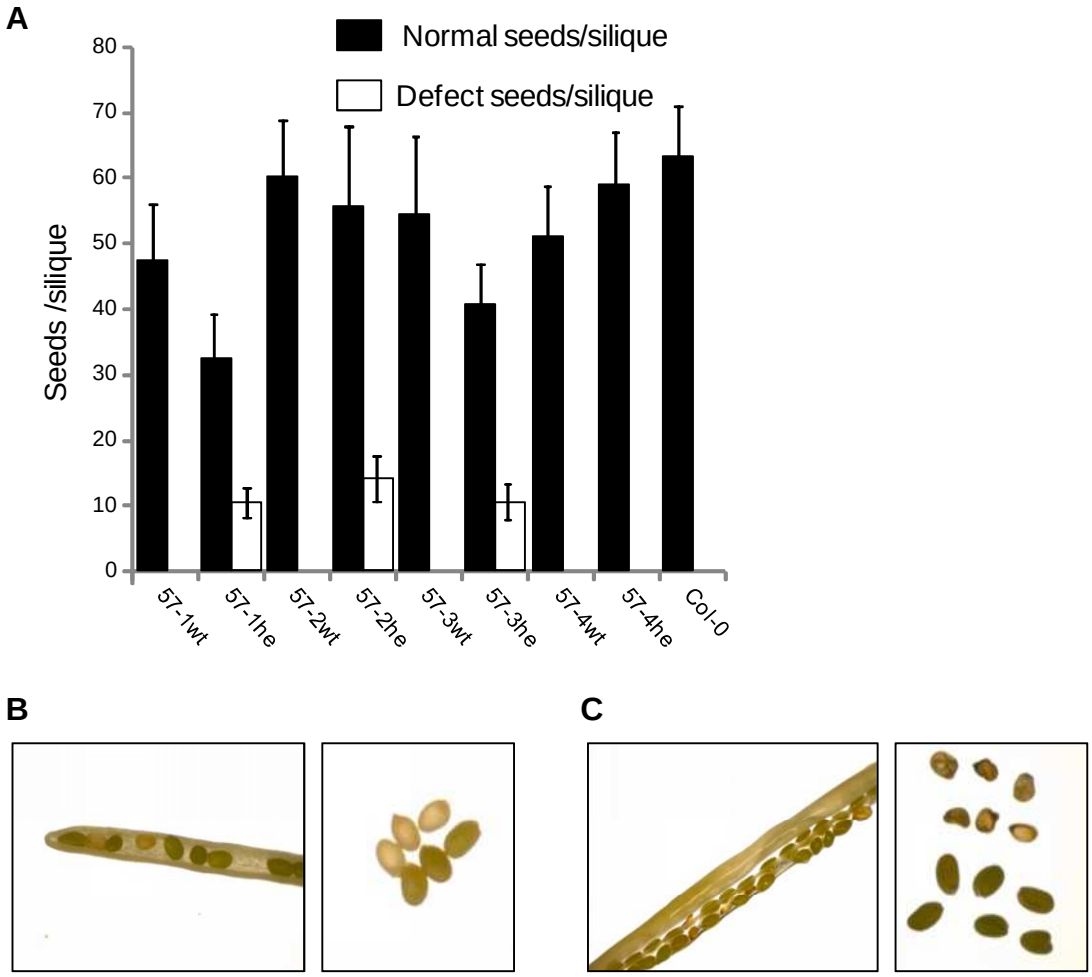

Figure 26: Phenotype of *niep57* mutant seeds
Siliques form heterozygous and wild-type *niep57-1, niep57-2, niep57-3 and niep57-4 and* Col-0 plants were observed under the binocular after clearance in 100% ethanol. **A)** For each line the normal and defect seeds per silique were counted. **B)** Young silique and young seeds of *niep57-1* **C)** Old silique and old seeds of *niep57-1*.

In the abnormal seeds it was impossible to detect the presence of an embryo under the binocular. To analyse the embryo development more detail, siliques of different ages of heterozygous *niep57-1* and *niep57-3* plants – the two lines that clearly disrupt the coding sequence of *NIEP57* – were harvested and cleared using the mounting media Hoyer's solution (Liu and Mainke, 1998) and observed using differential interference contrast microscopy.

In both *niep57* mutant lines it could be observed that in the abnormal seeds indeed there was an embryo inside, but that the normal development was usually arrested at the globular embryo stage (Figure 27). Moreover, an abnormal cell division pattern could also be detected in some cases in the embryo proper as well as in the suspensor part (Figure 27, panel M, N and O). For late developmental stages (Figure 27 panel P) no embryo could be detected at all.

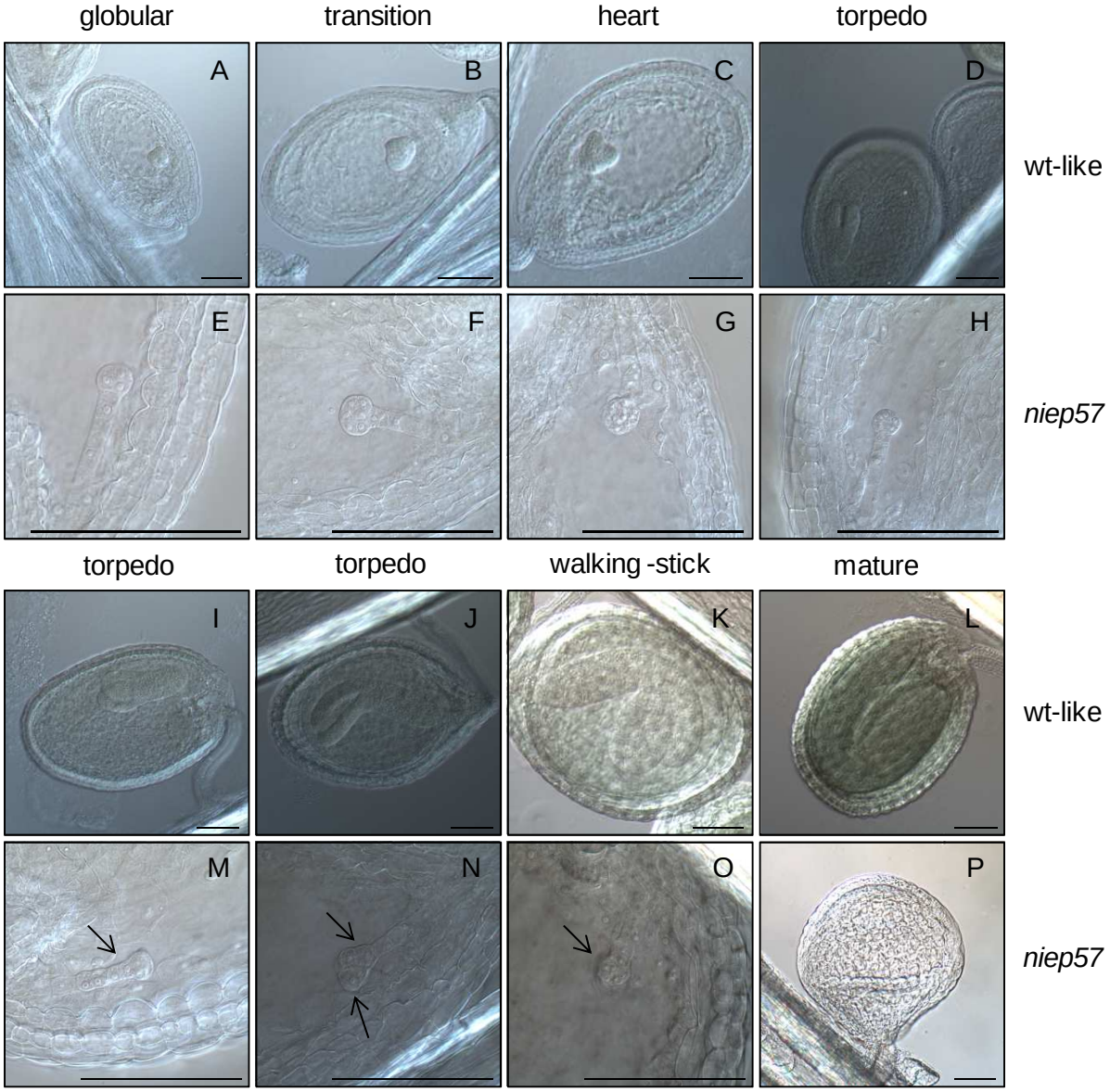

Figure 27: Arrested embryo development in *niep57-1.*
Niep57-1 heterozygous siliques were dissected and seeds were cleared using Hoyer's solution. After incubation of one day in the dark, the embryos were observed using differential interference contrast microscopy. For each developmental stage, pictures of normal wild-type like embryos **(A-D, I-L)** were taken. The corresponding abnormal embryo (coming from the same silique) was also photographed **(E-H, M-P)**. Bar, = 100 µm. Arrows show abnormal cell division pattern.

The conclusion from this observation is that these abnormal and aborted embryos correspond to homozygous alleles for the T-DNA insertion in *NIEP57*, leading to the discovery of a novel inner envelope chloroplast located protein that is required for proper embryo development in

Arabidopsis. Most likely the function of NIEP57 is crucial in the globular stage, where gene expression peaks (Figure 24B) and embryos are arrested (Figure 27).

3.4.3 Overexpression and RNAi lines for AtNIEP57

Due to the embryo lethal phenotype of homozygous T-DNA insertion lines for *AtNIEP57*, another experimental approach was selected in order to clarify the physiological function. For this purpose overexpression and RNAi lines for AtNIEP57 were generated. To generate the overexpression lines, the cDNA of *AtNIEP57* was subcloned into the pH2GW7 plasmid vector under the control of the 35S promoter. For the RNAi lines, the first 380 bp of *AtNIEP57* were cloned in the pH7GWIWG2(II),0 plasmid vector (Karimi *et al*., 2002). Both constructs were stable transformed into Col-0 *Arabidopsis* plants. Positive transformed plants (T1) were selected on MS media supplied with the selection agent hygromycin. Although 14 *Arabidopsis* Col-0 plants were transformed with the RNAi construct and after several attempts of the selection with hygromycin only two positive transformed plants were recovered. These two lines showed no obvious phenotype. In contrast, for the overexpression line, 11 *Arabidopsis* Col-0 plants were transformed and 28 positive transformed plants were recovered. Here apart from the normal growth of positive stable transformed a lot of seedlings exhibited a phenotype already in the T1 generation. These seedlings were albino, very small and grew very slow (Figure 28, panel B, H). After recreation on MS media without selection agent the small albino plants were transferred to soil. Most of these chlorotic plants could however not grow on soil and died after a few days. Besides this first albino phenotype observed for the plants, other phenotypes randomly appeared during the development and further of the plants (Figure 28). The presence of anthocyanins could be detected in albino plants (Figure 28, panel I), others plants had very short roots and an aberrant development (Figure 28, panel J). Some lines could be successfully transferred to soil where they continued to grow with a very slow development producing seeds in some cases. Other plants that were chlorotic at the beginning turned green or presented a variegated phenotype (Figure 28, panel K, G, A, E). In contrast, some plantlets that looked normal at the first developmental stages became spontaneously chlorotic starting from the inner inflorescence of the plant and moving to the leaves. The stem and siliques became also variegated (Figure 28, panel F, C, D and L). One interesting feature was that the plants that exhibited an albino/variegated and small phenotype used to live longer than normal wild-type plants (Figure 28, panel K).

From the lines were it was possible to obtain seeds, the T2 generation was sowed on MS media to analyse if the phenotype was reproducible. Four lines (9.2, 9.5, 9.6 and 11.3 clearly segregated showing the same phenotype: the seedlings presented albino cotyledons and green

true leaves (Figure 28, panels M-P). The cotyledons turned to green after a few days. The lines were also grown on MS media with and without sugar and subjected to different light conditions (constant low light, constant light, long day and short day). No obvious effect on the phenotype was visible due to the different light and media conditions (data not shown).

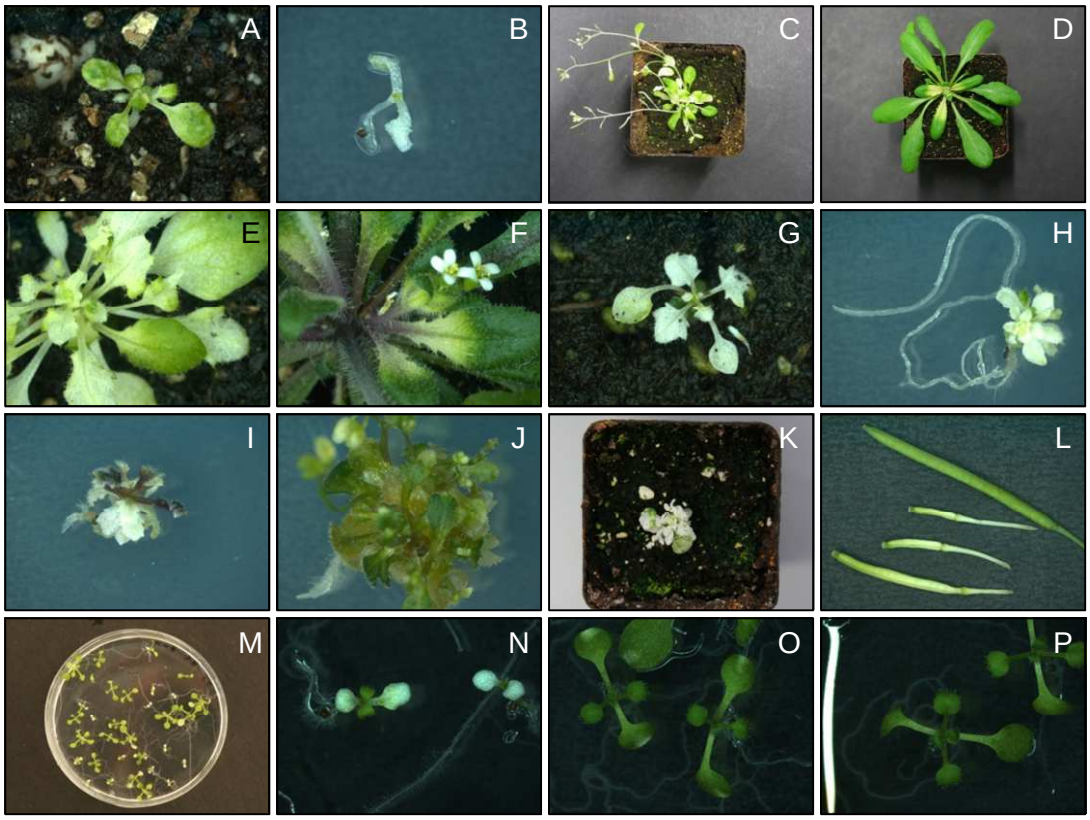

Figure 28: Phenotype of the AtNIEP57 overexpression lines
Panel A to L shows the different phenotypes present in the T1 generation after stable transformation of Col-0 plants with *35S*::*NIEP57.* The age in days in given in brackets A: 8.1, (24 d); B: line 10.3, (27 d); C: 10.7, (43 d); D: 9.3, (47 d); E: 9.2, (50 d); F: 10.3, (50 d), G: 10.6, (50 d); H: 11.4, (52 d); I: 11.6, (52 d), J: 11.5, (52 d); K: 11.6, (106 d); L: siliques of line 10.2. Panel M to P shows the phenotype present in the T2 generation of line 9.5, (12 d). All plants were grown under a 16 h light period. Plants on media: MS supplied with 1% sucrose.

To analyse if the phenotype was caused due to an overexpression of *AtNIEP57,* RNA from green and chlorotic sectors of the same plant was isolated, reverse transcribed, and the RNA amount of *AtNIEP57* was determined using quantitative real time RT PCR (Figure 29). The results showed that the *AtNIEP57* gene is rather silenced than overexpressed in the chlorotic parts of the plant when compared to the green sectors of the plant. The *35S::NIEP57* cDNA thus most likely corresponds a transgene induced gene silencing.

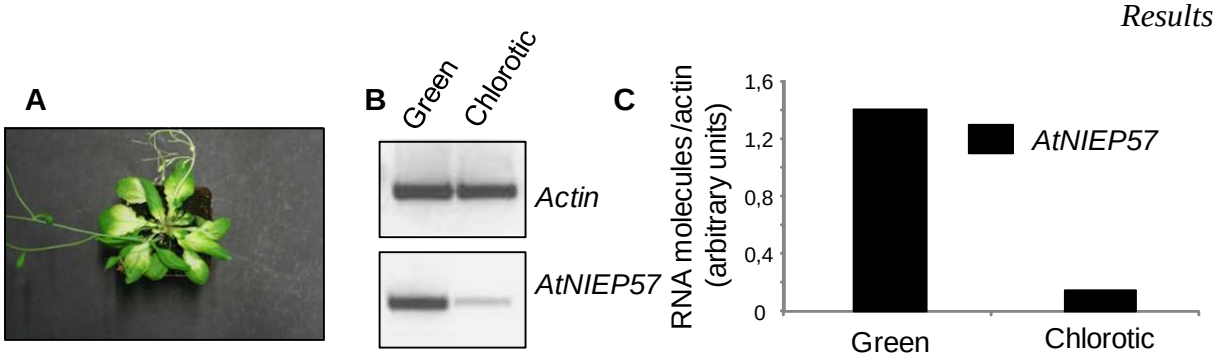

Figure 29: The 35S::*NIEP57* cDNA corresponds to a transgene induced gene silencing
A) Line 10.2 (T1), 47-days-old, grown under 16 h day light period. **B)** mRNA was prepared from the green and chlorotic parts of the plant showed in A) and subjected to real time RT PCR analysis. PCR products of 435 bp (actin) and 455 bp (*AtNIEP57*) are shown. **C)** The level of *AtNIEP57* mRNA was quantified and normalized to actin (n=1).

3.4.4 Inducible overexpression and RNAi lines for AtNIEP57

Due to the embryo lethal phenotype in homozygous T-DNA insertion lines for NIEP57, the almost absent AtNIEP57 RNAi lines obtained after transformation, and the induced gene-silencing effect produced in the overexpression lines, inducible overexpression and RNAi lines were produced in the following. For this purpose, the same constructs used for the stable overexpression and RNAi lines were subcloned into the pOpOn and pOpOffII system (Wielopolska *et al*., 2005) and Col-0 plants were stable transformed. This plasmid vector system allows dexamethasone-inducible RNAi or overexpression of plant genes. Especially the inducibility of an RNAi knock-down from this system may be useful in helping to identify the function of genes, which when constitutively silenced give embryo lethality or pleiotropic phenotypes (Wielopolska *et al*., 2005), and thus are a suitable system to characterise the physiological role of AtNIEP57 in the plant. Transformed plants were selected in the T1 and the T2 generation of the pOpOffII plants (RNAi) and were treated using the inducible agent dexamethasone. On the one hand seeds from the T2 generation sowed directly on MS + dexamethasone media showed the same phenotype as the constitutive overexpression lines (Figure 30). On the other hand, plants were first allowed to grow six days on MS media and then transferred to dexamethasone. For these plants, the chlorotic phenotype appeared in new developing organs, showing a similar effect as the constitutively overexpression lines that were green and then turned chlorotic from the inside to the outside of the plant (not shown). When plants directly grown on soil were treated with dexamethasone the effect was less drastic and a chlorotic effect could only be achieved in the stem (Annette Schock, personal communication). These results confirmed the idea that a reduced level of AtNIEP57 is responsible for the chlorotic phenotype.

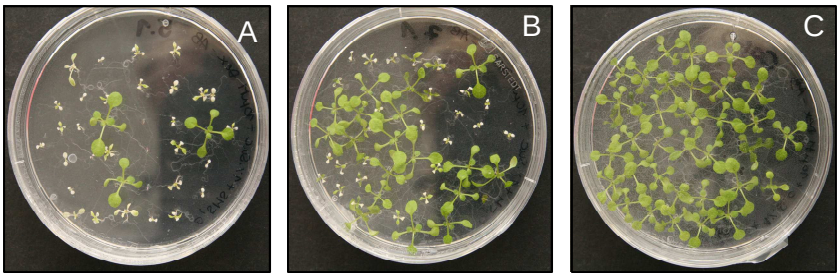

Figure 30: Inducible RNAi of AtNIEP57
12-days-old T2 generation of Col-0 plants transformed with the inducible RNAi system AtNIEP57/pOpOffII grown on MS + 1% sucrose supplied with 10 µM dexamethasone. The plants were grown in a 16 h light period, **A)** line 5.1, **B)** line 7.1, **C)** Col-0.

Due to the fact that AtNIEP57 is co-expressed with genes involved in the thiamine metabolism and that the phenotype of gene-silenced AtNIEP57 is similar to the *35S::IspH* cDNA transgene lines of IspH – an enzyme involved in the non mevalonate pathway in the plastid, in which the biosynthesis of the thiamine precursor 1-deoxy-D-xylulose 5-phosphate is produced (Hsieh *et al*., 2005) – an experiment to rescue the phenotype of the *35S::NIEP57* lines supplying the media with thiamine and thiamine pyrophosphate was performed. For that purpose, two *35S::NIEP57* lines (T2) showing a clear phenotype similar to line 9.5, (please refer to Figure 28, chlorotic cotyledons at the seedling stage) as well as Col-0 were sowed on MS media, supplied with 1% sucrose and thiamine or thiamine pyrophosphate (0, 5, 30, 50, 100, 200 µM). Unfortunately the chlorotic phenotype could not be rescued by this experiment (data not shown).

V. Discussion

1 OEP24

OEP24 was initially discovered and well characterised in pea as a β-barrel outer envelope protein (Pohlmeyer *et al*., 1998) and was proposed to be a high-conductance (slightly cation-selective) solute channel. Moreover, PsOEP24 was able to replace the mitochondrial VDAC in yeast (Röhl *et al*., 1999), suggesting that OEP24 acts more or less as a porin-like type of channel that is principally permeable to small hydrophilic solutes and metabolites. Indeed sugars, glucose 6-phosphate, gluconate, phosphoglyceric acid, dihydroxyacetone, ATP, acetate, malate, α-ketoglutarate, Pi and charged amino acids permeated through recombinant PsOEP24 reconstituted into artificial lipid bilayers (Pohlmeyer *et al*., 1998). The existence of two different isoforms in *Arabidopsis* AtOEP24.1 and AtOEP24.2, with different expression patterns during pollen and embryo development, suggested that OEP24 could be important for solute transport during pollen and/or embryo development. At the beginning of my work this idea was strongly supported by the phenotype present in the only *Arabidopsis* T-DNA insertion mutant available for the study of OEP24: *oep24.1-1*. For this line no homozygous progeny for the T-DNA insertion could be isolated and segregation was of 50% wild-type, 50% heterozygous plants. Further, the heterozygous plants showed about 50% reduced germination rates of pollen grain *in vitro*. Gametophyte defects were reported also previously for mutants of the *Arabidopsis* plastid glucose 6-phophate/phosphate translocator GPT1. GPT1 is a transporter located at the inner envelope of plastids and imports glucose-6-phosphate into plastids of non green tissues (Niewiadomski *et al*., 2005). A linkage between GPT1 at the inner envelope and OEP24 seemed thus be possible with OEP24 being the channel transporting small solutes including glucose-6-phosphate across the outer envelope. To clear the situation of OEP24.1, a complementation assay was performed during my thesis work thereby stable transforming heterozygous *oep24.1-1* mutant plants with AtOEP24.1 gene to see if the gametophyte lethal phenotype in the mutant line could be rescued. As previous attempts using the promoter of *OEP24.1* and the cDNA failed to complement the phenotype, an approach with the *OEP24.1* promoter and the entire gene was tested. Due to the location of the T-DNA in the first intron of the gene (see Figure 3) and the deletion of regulatory elements (MYBILEPR, CORECDC 3 and BOXII) produced by this insertion which perhaps have an important role in the expression regulation of the *OEP24.1* gene, this experiment would be the only suitable to try to complement the line. Unfortunately this approach could not complement the phenotype after genotyping of 494 plants. Moreover, for

the first time, the discovery of two homozygous lines for the *oep24.1-1* T-DNA insertion in the T2 generation that appeared after the complementation experiment but in plants not transformed with the *OEP24* construct was really not expected. The fact that there was indeed no transformed *OEP24.1* construct in these lines was tested by PCR using primers that amplified only the stable transformed *OEP24.1* (*OEP24.1* gene specific primer and attB2 primer that amplified a part of the destination vector used for the transformation), and two more primer sets that amplified two independent regions (promoter region and 3'UTR region were point mutations in the *OEP24.1* complementation product were found). The amplification and subsequent sequencing with these primer sets also proved the absence of a stable transformation with the *OEP24.1* constructs in these lines. Further the plants were not resistance to hygromycin (selection agent carried by the transformation vector). In summary none of the two homozygous plants for the *oep24.1-1* T-DNA insertion prove to be stable transformed with the *OEP24.1* gene construct used for complementation. The idea that the lines indeed could be complemented by the transformed *OEP24.1* by a stable transformation only produced by a part of the *OEP24.1* gene (*e.g*. due to a DNA rearrangement producing the loss of the primer sites and hygromycin resistance but sufficient for the complementation) seems not to be correct, since for all other transformed lines the genotyping approaches could be performed without problems. The only speculation that can be made regarding these results is that the homozygous lines that appeared here after several self pollinations and one transformation treatment lost some unknown regulatory factors linked with the gametophyte lethality produced by the T-DNA insertion in the intron region of OEP24.1. This seems to be the case due to the finding of ten more homozygous lines in the T3 generation. All *oep24.1-1* homozygous lines found in the T2 and T3 generation descended from the same line transformed in T1 (line #4.3). It is well known that the integration pattern of T-DNA fragments not only affects transformation efficiency and stability, but also expression properties of the transgenes. The integration of vector backbone sequences into the plant genome, producing potentially regulatory effects is also common (for overview see Lee and Gelvin, 2008). It is well known that introns display several active regulatory functions as well (Morello and Brevario *et al*., 2008), indicating a possible but unknown gametophyte specific regulation mode of AtOEP24.1 that was lost in the respective line #4.3.

To clarify the situation of OEP24.1, the two other mutant lines were characterised. The homozygous *oep24.1-2* overexpression line showed no obvious phenotype when analysed under standard conditions, although an increased expression for more than 200 times could be shown (see Figure 4A and B) as well as an increase in the protein level. However, after the

characterisation of the TILLING line *oep24.1-3* it can be concluded that the gametophyte phenotype demonstrated in the *oep24.1-1* line is maybe independent of the *OEP24.1* gene due to the presence of homozygous *oep24.1-3* plants that for the point mutation show a clear frame shift in the transcript. Certainly, here the question is open, if the missplicing affects all the transcripts of *OEP24.1* or only a part, giving normal transcripts of *OEP24.1* at all, which are enough to support the OEP24 function in the plant. In this work, two independent amplification and sequencing results of the cDNA of *oep24.1-3* homozygous mutants showed only the misspliced form of the cDNA. An immunodecoration showing the knock-out status of this line at the protein level could not be performed due to the similarity of OEP24.1 and the OEP24.2 isoform, which is still intact in this line. In summary, the physiological role of OEP24.1 in *Arabidopsis* could not be clarified using the mutant lines available.

A further characterisation of OEP24.2 was also not possible due to the high amount of background mutations and phenotypes present in the only TILLING mutant line available for OEP24.2. It is well known that this kind of mutant lines harbour a high mutant background due to the mutagenesis technique, which they are subjected. It was previously estimated, on average, that each M2 TILLING plant carries 720 mutations, whereas for the T-DNA populations only 1.5 insertions per line are found (Till *et al*., 2003; Alonso *et al*., 2003, for overview see Kurowska *et al*., 2011).

In spite of the different expression patterns of both isoforms, the similarity between OEP24.1 and OEP24.2 could also be a reason why the single mutants do not show any visible phenotype. It may be possible that one isoform can replace the absence of the other. It would be therefore reasonable to cross both homozygous TILLING lines from each gene, to analyse if a phenotype linked to the impaired transport capacity of OEP24 in a double mutant could clarify the physiological role of OEP24 during the plant life. Prior to this experiment both TILLING lines however should undergo intensive backcrossing with wild-type due to the possible multiple background mutations present.

2 OEP21

Like OEP24, OEP21 was first discovered and characterised in pea and *in vitro* studies proposed OEP21 as an important transporter of primary photosynthesis products of the outer envelope of the chloroplast (Bölter *et al*., 1999) transporting HPO_4^{2-} and phosphorylated carbohydrates (triosephosphate, 3-phosphoglycerate, Gluc-6-phosphate). *In vitro* a regulation of the recombinant PsOEP21 channel was proposed due to the existence of two ATP-binding sites: one high affinity site and the second harbouring an FX_4K motif (Hemmler *et al*., 2006).

In *Arabidopsis* the OEP21.2 isoform is equipped with the FX_4K motif, while for the second isoforms, OEP21.1, as well as in other plants species, the conserved phenylalanine is changed by to a leucine. It was shown previously that the ATP-binding site of Ca^{2+}ATPases is given by the conserved lysine rest present in both isoforms and that the phenylalanine – in the case of OEP21.1 the leucine – delivers more a stability function (for overview see Kühlbrandt, 2004). However, *in vitro* electrophysiological studies showed that the presence of the phenylalanine in PsOEP21 and AtOEP21.2 has a function in channel rectification (Hemmler *et al*., 2006). In *Arabidopsis* both isoforms are very similar and due to a basal and relative low expression of both isoforms in all plant tissues, it was assumed that both isoforms independently can form a functional channel. That was consistent with the observation of no obvious phenotype of the single mutants for both isoforms under standard conditions. In my work it was clarified that only *oep21.1-1* corresponds to a knock-out of OEP21.1 at the transcriptional level. In contrast, *oep21.1-2* – with the T-DNA insertion in the intron – corresponded to a knock-down line for OEP21.1 (see Figure 8). No alteration in the expression level of OEP21.2 could be seen in both lines excluding the idea of an induction of OEP21.2 to support the absence of OEP21.1. The subsequent analysis of the double mutant was performed only on the descendants from *oep21.1-1* crossed with *oep21.2-1*. Only one homozygous double mutant was found after genotyping 376 plants. The percentage of double mutants lines found for this cross was thus relatively low (0.26%) but could be expected as both genes are located on the same chromosome and it was therefore necessary to have a crossing over event to get the double mutant. The OEP21 double mutant could be well characterised at the protein level (see Figure 9). Due to the fact that the antiserum against AtOEP21.1 recognizes both isoforms of OEP21, the result of the immunodecoration showed that – although *oep21.2-1* is a TILLING mutant harbouring a point mutation in the last exon of the protein, leading to a premature stop in the translation – the truncated OEP21.2 protein is totally degraded in the double mutant giving no OEP21 at all (see Figure 9). The double mutant showed also no obvious phenotype when grown at different light conditions, although a de-regulation of the carbohydrate metabolism of the plant was expected. Therefore, a more detailed characterisation of the mutant proteome and analysis of the metabolites involved in glycolysis and citric acid cycle as well as of sugars and amino acids was performed. Previously, an *Arabidopsis* knock-out mutant for the triose phosphate/phosphate translocator located at the inner chloroplast envelope showed accumulation of starch content and reduction of sucrose and glucose (Schneider *et al*., 2002). 3-phosphoglycerate and triosephosphate were also increased in the mutant line. The lack of triosephosphate export for cytosolic sucrose

biosynthesis was almost fully compensated by accelerated starch turnover and export of neutral sugars from the stroma throughout the day (Schneider *et al.*, 2002). An expected similar phenotype was not detected for the OEP21 double mutant line, instead changes in the amount of amino acids were observed in the OEP21.1 overexpression line when compared to the double mutant, double wild-type and OEP21.1 complemented double mutant. In particular an enhanced amount of aromatic amino acids was detected indicating a possible higher transport carbon for the synthesis of these amino acids that are exclusively produced in plastids. In summary these results indicate at least that OEP21 seems not to play an essential role in the plant model *Arabidopsis*.

The results obtained for OEP24 and OEP21 however, do not exclude the idea of the selectivity in transport capacity of the OEPs. It could be possible that some of them indeed harbour overlapping functions *in vivo*, compensating in this way the absence of the other OEP in *Arabidopsis*. As described previously, OEP24 *in vitro* is also capable to transport hexosephosphates as well as phosphoglyceric acid (Pohlmeyer *et al*., 1998) indicating a possible compensating transport activity for the carbohydrate metabolism. This may be the case for OEP24 and OEP21 but not for the well characterised amino acid-specific OEP16 where a loss of the protein causes a metabolic imbalance, in particular that of aspartate-derived amino acids during seed development and early germination. Thus here it is evident that *in vivo* OEP16 can function in shuttling amino acids across the outer envelope of seed plastids (Pudelski *et al*., 2011). It may also be possible that the C3 model plant *Arabidopsis* is not the most suitable system to study the physiological function of OEP21 and OEP24. In comparative proteomic studies of chloroplast envelope membranes between C3 plants (pea) and mesophyll cell C4 plants (maize) it could be shown that OEP24 as well as OEP37 show a major relative increase in C4 plants (Bräutigam *et al*., 2008a), maybe to compensate the higher metabolite flux between chloroplast and cytosol in C4 plants. In contrast, OEP21 was reduced in relative abundance and OEP16 did not differ in relative spectral abundance between C3 and C4. OEP24 was also found to be present in proplastid envelope proteomic analysis (Bräutigam and Weber, 2009). Proplastids present in the meristems are supplied with reducing power, energy and precursor metabolites from the cytoplasm and provide branched chain and aminoacids, fatty acids and lipid as well as nucleotide precursors to support cell growth. An elevated transport activity and therefore expression of transporters at both membranes of the chloroplast is expected (Bräutigam and Weber, 2009).

3 New chloroplast envelope proteins

At least two new envelope membranes proteins NIEP57 and NOEP40 located at the inner and outer envelope of the chloroplast respectively could be discovered after searching for new envelope membrane proteins of the chloroplast. For this search a different approach as the one used to discover the already known OEPs was performed. The approach I used was not based on the amount of the proteins present in the outer envelope; instead a more fine selection was applied based on some characteristics of the already known OEPs and their related proteins found in Gram-negative bacteria. The most important characteristics included: different running behaviour in urea SDS-page, presence in chloroplast membrane preparations, basic isoelectric point, no transit peptide and β-barrel structure prediction.

3.1 NOEP23

AtNOEP23 was present in a chloroplast proteome database with subplastidial localisation and was afterwards annotated as a putative but still unclear envelope protein (Ferro *et al*., 2010). The idea of NOEP23 being an outer envelope protein of the chloroplast, harbouring a β-barrel structure was strengthened after the structure predictions proposed by the algorithms presented in the ARAMEMNON database (Schwacke *et al*., 2003): absence of classical transit peptide which is common for outer envelope membrane proteins (Schleiff *et al*., 2003) and no α-helical transmembrane domains. NOEP23 thus possess some features of the outer envelope proteins of the chloroplast where relatively little is known about the membrane integration mechanisms (for overview see Walther *et al*., 2009). Unfortunately the localisation for PsNOEP23 could not be verified when testing different pea subcellular fractions by immunoblot (outer and inner envelope, stroma, microsomal fraction) or pea mitochondria. Instead plasma membrane like signals were detected in transient transformation of mesophyll *Arabidopsis* protoplast using AtNOEP23 with a C-terminal GFP (see Figure 15). Regarding the unsuccessful localisation by immunodecoration, it may be possible that the protein is low expressed in the tested outer envelope of the chloroplast of young pea leaves. The proteomic analyses were initially all new candidates were identified was performed on the same type of pea outer envelope preparation. A low expression of the protein in these samples can be deduced due to the representation of PsNOEP23 by only one short peptide in one sequenced band. These results lead also to the question if NOEP23 belongs at all to the chloroplast outer envelope or if the peptide found in the proteomic analyse corresponds to a contamination of the sample. The AtNOEP23 T-DNA insertion mutant located at the 3'UTR so far did not help in the physiological study of the protein during plant development therefore further

characterisation of NOEP23 has to be addressed in future studies. To clarify the subcellular localisation of the protein maybe the generation of a second antiserum would be helpful.

3.2 NOEP40

AtNOEP40 instead was not present in the chloroplast proteome database with subplastidial localisation (Ferro *et al*., 2010), but according to the results of my thesis work is very likely to be a classical outer chloroplast envelope protein. As NOEP23, NOEP40 had no transit peptide or α-helical transmembrane domains predicted. The prediction by ARAMEMNON (Schwacke *et al*., 2003) suggests a β-barrel structure although the predictions for β-barrel forming proteins are complicate due to the short membrane-spanning regions and high variations in properties when compared with α-helical membrane proteins (Yan *et al*., 2011 and references therein). AtNOEP40::GFP failed to yield a chloroplast envelope signal (see Figure 15) which is common for outer envelope β-barrel proteins that for GFP-targeting rather are miss targeted and aggregate in the cytoplasm (personal communication K. Philippar). This phenomenon can be attributed to the structure and insertion mechanism of the OEPs into the outer envelope membrane. The only OEP that gives clear envelope localisation by GFP is the short OEP7 which inserts into the outer envelope membrane of plastids by one α-helix. The immunodecoration in contrast confirmed the localisation of NOEP40 at the chloroplast outer envelope in pea unequivocally (see Figure 17). The fact that NOEP40 is a protein present only in higher plants and not in bacteria is a feature shared with the already known OEPs and is explained by the high mutation rate in amino acid sequence of bacterial porins and channels (in particular in domains facing the external medium) making traditional phylogeny based solely on the primary sequence impossible (for overview see Duy *et al*., 2007). For the observation of the NOEP40 co-expressed proteins it is worth to highlight the mitochondrial lactate dehydrogenase (AtD-LDH) and a chloroplast putative glyoxalase. AtD-LDH is proposed to participate in methylglyoxal detoxification in the mitochondria catalysing the reaction from D-lactate resulting from the cytoplasmic glyoxalase cycle into pyruvate (Engqvist *et al*. 2009). Methylglyoxal corresponds to a cytotoxic product formed spontaneously in plants by nonenzymatic mechanisms under physiological conditions from glycolysis and from photosynthesis intermediates as glyceraldehyde-3-phosphate, and dihydroxyacetone phosphate. It was previously shown that its production in various plants is enhanced under stress conditions and has negative consequences on cellular systems (for overview see Hossain *et al*., 2011). The putative glyoxalase located in the chloroplast is involved in carbohydrate metabolic processes and cold stress (TAIR, Lamesch *et al*., 2011). These observations can be linked to the phenotype observed in the NOEP40 knock-down

mutants grown at low temperature conditions (10°C). Thus, a potential transport function of NOEP40, which has an impact on metabolic signalling in growth and developmental processes as well as during abiotic stress is possible. Further characterisation of the RNAi and overexpression lines and the second T-DNA insertion line as well as electrophysiological studies will help to elucidate the function of NOEP40.

3.3 NIEP57

AtNIEP57 was present in the chloroplast proteome database (Ferro *et al*., 2010). After the *in silico* characterisation classical chloroplast transit peptide, four α-helical membrane domains and GFP-targeting results, the confirmation of the localisation to the inner envelope of the chloroplast by immunodecoration was shown (see Figure 17). Thus is a clear case of contamination of the outer envelope membrane sample that was sent for peptide sequencing, although an additional step of outer envelope purification was performed. In the sequencing data indeed contamination of already known proteins located at the inner envelope of the chloroplast such as components of the TIC complex (TIC110 and TIC55), stroma (large subunit of RuBisCo, RuBisCo activase) and thylakoids (Alb3, LHCA3) were found.

The interesting embryo lethal phenotype of NIEP57 knock-out mutant, however suggests an elemental function of the protein. AtNIEP57 was previously described as a plant specific solute transporter protein (Tyra *et al*., 2007) and the hydrophobicity test (see Figure 18) proved that NIEP57 corresponds to an integral membrane protein as it is expected for a transporter. To be able to transport solutes and metabolites at least four or more transmembrane domains are required (Linka and Weber 2010 and references therein). To analyse the topology of PsNIEP57, several proteolysis experiments as well as a PEGylation assay were performed and a topology of four transmembrane domains with the N- and C-termini orientated towards the intermembrane space was proposed (see Figures 19 and 20). The topology proposed should still be taken with care and more detailed analysis should be performed in order to confirm the prediction. To clarify this situation, peptide antiserum raised against a sequence located at the N-terminal part of the protein was ordered. The long N-terminal part of NOEP57, facing the intermembrane space could possibly be involved in the recognition of metabolites to be transported. In higher plants two to three isoforms for NIEP57 were found for several species, and one subgroup showed a longer N-terminal part suggesting different adaptations of NIEP57. It would be also interesting to analyse in more detail the glycine and aspartic acid rich motif at the soluble N-terminal part of some NIEP57. The C-terminal domain of unknown function (DUF 3411) found for AtNIEP57 is also present in several unknown chloroplast-located *Arabidopsis* proteins and in the related protein

AtRER1. AtRER1 itself is related to two additional unknown proteins, one of them showing a reticulation phenotype in cotyledon and leaves upon mutation (Gonzalez-Bayón *et al*., 2006).

Three of four independent homozygous T-DNA lines showed that AtNIEP57 is an essential embryo protein, causing lethality and aborted embryogenesis in the globular stage when missing (see Figure 27). For the fourth line *niep57-4*, no aborted embryo or other abnormalities as missing seeds could be detected although no homozygous plants were found after genotyping 41 plants and the segregation analysis for this line suggested embryo lethality (see table 10). In the future, germination analysis should be performed for this line to discard any effect of NIEP57 in this process. Unfortunately the 3' end of the T-DNA insertion could not be determined and further characterisation to analyse if the T-DNA is spliced out also failed. Although the other three mutant lines clearly showed aborted embryo development, the segregation ratio of about 50% wild-type:50% heterozygous points to a defect in gametophyte transmission. In order to discard impairment in female or male gametophyte transmission, reciprocal crosses with wild-type should be carried out. The heterozygous *niep57* mutant plants showed no phenotype when compared to the wild-type, indicating that the *niep57* mutation is completely recessive. One copy of the *NIEP57* gene is able to produce sufficient protein for normal plant development.

In the last years many nuclear genes that encode chloroplast proteins required for proper embryo development in *Arabidopsis* were described. Three major types of chloroplast-localised proteins appear to be most frequently associated with embryo lethality in *Arabidopsis* (1) enzymes required for the biosynthesis of amino acids, vitamins, nucleotides, and fatty acids; (2) proteins required for the import, modification, and localisation of essential proteins within the chloroplast; and (3) proteins required for chloroplast translation (Bryant *et al*., 2011). The plastidial glucose-6-phosphate/phosphate antiporter GPT1 described as the major route of entry of carbon into non-photosynthetic plastids was also shown to be essential for morphogenesis in *Arabidopsis* embryos (Andriotis *et al*., 2010). Developmental arrest generally occurs at around the globular stage prior to the formation of embryonic organs, suggesting that some specific plastid functions are essential for embryo development, many of them at the stage of chloroplast differentiation (Andriotis *et al*., 2010 and references therein).

The induced AtNIEP57 silenced plants showed that NIEP57 is not only an essential protein for embryo development but also important in the vegetative life of the plant. The chlorotic phenotype is given by the coordinated silencing of the transgene, arising spontaneously and independently from multiple sites of the plant, and spreading towards younger tissues (see

Figure 28). Interestingly, a very similar phenotype was described previously in *Arabidopsis* transgenic *35S::IspH* (Hsieh *et al*., 2005) with the same silencing effect as *35S::NIEP57*. IspH corresponds to a plastid enzyme involved in the plastid non-mevalonate pathway of isoprenoid biosynthesis. In plants, the mevalonate (MVA) and non-mevalonate pathways are compartmentalized in the cytoplasm and plastid, respectively. The cytosolic pathway proceeds through the intermediate mevalonate and provides precursors for sterols and ubiquinone. The plastidial MVA-independent pathway is used for the synthesis of isoprene, carotenoids, absisic acid, and the side chains of chlorophylls and plastoquinone (Laule *et al*., 2003 and references therein). Although this subcellular compartmentalization allows both pathways to operate independently in plants, there is evidence that they cooperate in the biosynthesis of certain metabolites (Laule *et al*., 2003 and references therein). A linkage between the phenotype in both silencing mutant lines (*IspH* and *niep57*) can suggest that NIEP57 is involved in the transport of metabolites related to the plastid-intrinsic non-MVA pathway. Interestingly the co-expression data relates NIEP57 to the plastid thiamine metabolism and to pyruvate transport, two events connected with the non-MVA pathway as well (Hsieh *et al*., 2005; Laule *et al.*, 2003 and references therein).

VI. Outlook

Electrophysiological characterisation of NOEP40 and NIEP57 is fundamental to clarify if the proteins are transporters. For that purpose first the purification of recombinant NIEP57 protein in heterologous systems has to be optimised. Here other expression systems than *E. coli* (e.g. yeast) and NIEP57 proteins from other organisms than pea should be tested. Topology characterisation of PsNOEP40 by circular dichroism (CD analysis) will hopefully confirm the β-sheet structure and crosslink experiments as well as blue native gel electrophoresis gels will reveal if NOEP40 and NIEP57 form multimers. To elucidate the function of both new envelope proteins metabolite as well as transcriptomic analysis should be performed with the characterised mutant lines. For NIEP57, the inducible RNAi lines created in this work will allow the characterisation of the function of the protein in the vegetative life of the plant. Additionally, for NIEP57 transmission electron microscopy of the chlorotic leaves would be helpful to analyse if and how the chloroplast biogenesis is affected.

VII. Reference List

Abas L and Lusching C (2010) Maximum yields of microsomal-type membranes from small amounts of plant material without requiring ultracentrifugation. *Anal Biochem* 401: 217-227

Alonso JM, Stepanova AN, Leisse TJ, Kim CJ, Chen HM, Shinn P, Stevenson DK, Zimmerman J, Barajas P, Cheuk R, Gadrinab C, Heller C, Jeske A, Koesema E, Meyers CC, Parker H, Prednis L, Ansari Y, Choy N, Deen H, Geralt M, Hazari N, Hom E, Karnes M, Mulholland C, Ndubaku R, Schmidt I, Guzman P, Aguilar-Henonin L, Schmid M, Weigel D, Carter DE, Marchand T, Risseeuw E, Brogden D, Zeko A, Crosby WL, Berry CC, Ecker JR (2003) Genome-wide Insertional mutagenesis of *Arabidopsis thaliana*. *Science* 301: 653-657

Altschul SF, Madden TL, Schaffer AA, Zhang J, Zhang Z, Miller W and Lipman DJ (1997) Gapped BLAST and PSI-BLAST: A new generation of protein database search programs. *Nucleic Acids Res* 25: 3389-3402

Andrès C, Agne B, Kessler F (2010) The TOC complex: preprotein gateway to the chloroplast. *Biochim Biophys Acta* 1803: 715-723

Andriotis VM, Pike MJ, Bunnewell S, Hills MJ, Smith AM (2010) The plastidial glucose-6-phosphate/phosphate antiporter GPT1 is essential for morphogenesis in *Arabidopsis* embryos. *Plant J* 64: 128-139

Aronsson H, Jarvis P (2002) A simple method for isolating import-competent *Arabidopsis* chloroplasts. *FEBS Lett* 529: 215-220

Baginsky S, Siddique A, and Gruissem W (2004) Proteome analysis of tobacco bright yellow-2 (BY-2) cell culture plastids as a model for undifferentiated heterotrophic plastids. *J. Proteome Res* 3: 1128-1137

Balsera M, Goetze TA, Kovacs-Bogdan E, Schürmann P, Wagner R, Buchanan BB, Soll J, Bölter B (2009) Characterization of Tic110, a Channel-forming Protein at the Inner Envelope Membrane of Chloroplasts, Unveils a Response to Ca^{2+} and a Stromal Regulatory Disulfide Bridge. *Journal of Biological Chemistry* 284: 2603-2616

Bechtold N, Ellis J and Pelletier G (1993) *In planta Agrobacterium*-mediated gene transfer by infiltration of adult *Arabidopsis thaliana* plants. *C. R. Acad. Sci. Paris/Life Sci* 316: 1194-1199

Benz JP, Soll J, Bölter B (2009) Protein transport in organelles: The composition, function and regulation of the Tic complex in chloroplast protein import. *FEBS J* 276: 1166-1176

Bölter B, Soll J, Hill K, Hemmler R, and Wagner R (1999) A rectifying ATP-regulated solute channel in the chloroplastic outer envelope from pea. *EMBO* 18: 5505-5516

Bölter B and Soll J (2001) Ion channels in the outer membranes of chloroplasts and mitochondria: open doors or regulated gates? *EMBO* 20: 935-940

Bradford M M (1976) A rapid and sensitive method for the quantitation of microgram quantities of protein utilizing the principle of protein-dye binding. *Anal Biochem* 72: 248-254.

Bräutigam A, Hofmann-Benning S, and Weber APM (2008a) Comparative proteomics of chloroplast envelopes from C-3 and C-4 plants reveals specific adaptations of the plastid envelope to C-4 photosynthesis and candidate proteins required for maintaining C-4 metabolite fluxes. *Plant Physiol* 148: 568-579

Bräutigam A, Shrestha RP, Whitten D, Wilkerson CG, Carr KM, Froehlich JE, and Weber APM (2008b) Low-coverage massively parallel pyrosequencing of cDNAs enables proteomics in non-model species: Comparison of a species-specific database generated by pyrosequencing with databases from related species for proteome analysis of pea chloroplast envelopes. *J Biotech* 136: 44-53

Bräutigam A and Weber APM (2009) Proteomic Analysis of the Proplastid Envelope Membrane Provides Novel Insights into Small Molecule and Protein Transport across Proplastid Membranes. *Molecular Plant* 2: 1247-1261

Bryan J, Vila-Carriles WH, Zhao G, Babenko AP, and Aguilar-Bryan L (2004) Toward Linking Structure With Function in ATP-Sensitive K Channels. *Diabetes* 53: S104-S112

Bryant N, Lloyd J, Sweeney C, Myouga F, Meinke D (2011) Identification of nuclear genes encoding chloroplast-localized proteins required for embryo development in *Arabidopsis*. *Plant Physiol* 155: 1678-1689

Claros MG, von Heijne G (1994) TopPred II: an improved software for membrane protein structure predictions. *Comput Appl Biosci* 10: 685-686

Clausen C, Ilkavets I, Thomson R, Philippar K, Vojta A, Möhlmann T, Neuhaus E, Fulgosi H, Soll J (2004) Intracellular localization of VDAC proteins in plants. *Planta* 220: 30–37

Detlef W and Glazebrook J (2001) *Arabidopsis*: A laboratory Manual. Cold Spring Harbor Laboratory, Cold Spring Harbor Press, New York

Drain P, Li LH, and Wang J (1998) K-ATP channel inhibition by ATP requires distinct functional domains of the cytoplasmic C terminus of the pore-forming subunit. *Proc Natl Acad Sci USA* 95: 13953-13958

Duy D, Soll J, Philippar K (2007) Solute channels of the outer membrane: from bacteria to chloroplasts. *Biol Chem* 388: 879–889

Emanuelsson O, Nielsen H, von Heijne G (1999) ChloroP, a neural network-based method for predicting chloroplast transit peptides and their cleavage sites. *Protein Sci* 8: 978-984

Emanuelsson O, Nielsen H, Brunak S, von Heijne G. (2000) Predicting subcellular localization of proteins based on their N-terminal amino acid sequence. *J Mol Biol* 300: 1005-1016

Engqvist M, Drincovich MF, Flügge UI, Maurino VG (2009) Two D-2-hydroxy-acid dehydrogenases in *Arabidopsis thaliana* with catalytic capacities to participate in the last reactions of the methylglyoxal and beta-oxidation pathways. *J Biol Chem* 284: 25026-25037

Facchinelli F and Weber APM (2011) The metabolite transporters of the plastid envelope: an update. *Frontiers in Plant Science doi:10.3389/fpls.2011.00050*

Ferro M, Brugière S, Salvi D, Seigneurin-Berny D, Court M, Moyet L, Ramus C, Miras S, Mellal M, Le Gall S, Kieffer-Jaquinod S, Bruley C, Garin J, Joyard J, Masselon C, Rolland N (2010) AT_CHLORO, a comprehensive chloroplast proteome database with subplastidial localization and curated information on envelope proteins. *Mol Cell Proteomics* 9: 1063-1084

Franssen SU, Shrestha RP, Bräutigam A, Bornberg-Bauer E, Weber AP (2011) Comprehensive transcriptome analysis of the highly complex *Pisum sativum* genome using next generation sequencing. *BMC Genomics* 12: 227

Froehlich JE, Wilkerson CG, Ray WK, McAndrew RS, Osteryoung KW, Gage DA and Phinney BS (2003) Proteomic study of the *Arabidopsis thaliana* chloroplastic envelope membrane utilizing alternatives to traditional two-dimensional electrophoresis. *J Proteome Res* 2: 413-425

Furumoto T, Yamaguchi T, Ohshima-Ichie Y, Nakamura M, Tsuchida-Iwata Y, Shimamura M, Ohnishi J, Hata S, Gowik U, Westhoff P, Bräutigam A, Weber APM and Izui K (2011) A plastidial sodium-dependent pyruvate transporter. *Nature* 476: 472-475

Gasteiger E, Gattiker A, Hoogland C, Ivanyi I, Appel RD, Bairoch A (2003) ExPASy: the proteomics server for in-depth protein knowledge and analysis. *Nucleic Acids Research* 31: 3784-3788

Gigolashvili T. Yatusevich R, Rollwitz I, Humphry M, Gershenzon J, Flügge UI (2009) The Plastidic Bile Acid Transporter 5 Is Required for the Biosynthesis of Methionine-Derived Glucosinolates in *Arabidopsis thaliana*. *Plant Cell* 21: 1813-1829

González-Bayón R, Kinsman EA, Quesada V, Vera A, Robles P, Ponce MR, Pyke KA, Micol JL (2006) Mutations in the RETICULATA gene dramatically alter internal architecture but have little effect on overall organ shape in *Arabidopsis* leaves. *J Exp Bot* 57: 3019-3031

Götze TA, Philippar K, Ilkavets I, Soll J, Wagner R (2006) OEP37 is a new member of the chloroplast outer membrane ion channels. *J Biol Chem* 281: 17989–17998

Gould SB, Waller RF, and McFadden GI (2008) Plastid Evolution. *Annu Rev Plant Biol* 59: 491-517

Gross J and Bhattacharya D (2009a) Mitochondrial and plastid evolution in eukaryotes: an outsiders' perspective. *Nature Rev Genet* 10: 495-505

Hanahan D (1983) Studies on transformation of *Escherichia coli* with plasmids. *J Mol Biol* 166: 557-580

Heins L, Mehrle A, Hemmler R, Wagner R, Küchler M, Hörmann F, Sveshnikov D, Soll J (2002) The preprotein conducting channel at the inner envelope membrane of plastids. *Embo Journal* 21: 2616-2625

Hemmler R, Becker T, Schleiff E, (2006) Molecular properties of Oep21, an ATP regulated anion-selective solute channel from the outer chloroplast membrane. *J Biol Chem* 281: 12020–12029

Honys D und Twell D (2003) Comparative analysis of the *Arabidopsis* pollen transcriptome. *Plant Physiol* 132: 640-652

Hossain M A, Piyatida P, Teixeira da Silva J A, Fujita M (2011) Molecular Mechanism of Heavy Metal Toxicity and Tolerance in Plants: Central Role of Glutathione in Detoxification of Reactive Oxygen Species and Methylglyoxal and in Heavy Metal Chelation. *Journal of Botany* doi: 10.1155/2012/872875

Hsieh, MH, Goodman, HM, (2005) The *Arabidopsis* IspH homolog is involved in the plastid nonmevalonate pathway of isoprenoid biosynthesis. *Plant Physiol* 138:641-653

Johnson-Brousseau SA, McCormick S (2004) A compendium of methods useful for characterizing *Arabidopsis* pollen mutants and gametophytically-expressed genes. *Plant J* 39: 761-775

Joyard J, Grossman A, Bartlett SG, Douce R, and Chua NH (1982) Characterization of Envelope Membrane Polypeptides from Spinach-Chloroplasts. ***J Biol Chem*** 257**:** 1095-1101

Karimi M, Inzé D, Depicker A. (2002) GATEWAY vectors for *Agrobacterium*-mediated plant transformation. *Trends Plant Sci* 7:193-195

Keegstra K, Youssif AE (1986) Isolation and characterization of chloroplast envelope membranes. *Methods Enzymology* 118: 316-325

Kleffmann T, Russenberger D, von Zychlinski A, Christopher W, Sjolander K, Gruissem W, Baginsky S (2004) The *Arabidopsis thaliana* chloroplast proteome reveals pathway abundance and novel protein functions. *Current Biol* 14: 354–362

Kogel KH, Voll LM, Schäfer P, Jansen C, Wu Y, Langen G, Imani J, Hofmann J, Schmiedl A, Sonnewald S, von Wettstein D, Cook RJ, Sonnewald U (2010)Transcriptome and metabolome profiling of field-grown transgenic barley lack induced differences but show cultivar-specific variances. *Proc Natl Acad Sci U S A* 107: 6198-6203

Koncz C und Schell J (1986) The promoter of TL-DNA gene 5 controls the tissue-specific expression of chimeric genes carried by a novel type of *Agrobacterium* binary vector. *Mol Gen Genet* 204: 383-396

Kovács-Bogdán E, Benz JP, Soll J, Bölter B (2011) Tic20 forms a channel independent of Tic110 in chloroplasts. *BMC Plant Biol* 11:133

Kühlbrandt W (2004) Biology, structure and mechanism of P-type ATPases. *Nature Rev Mol Cell Biol* 5: 282-295

Kurowska M, Daszkowska-Golec A, Gruszka D, Marzec M, Szurman M, Szarejko I, Maluszynski M (2011) TILLING: a shortcut in functional genomics. J Appl Genet 52: 371-390

Kyhse-Anderson J (1984) Electroblotting of multiple gels-a simple apparatus without buffer tank for rapid transfer of proteins from polyacrylamid to nitrocellulose. *J Biochem Biophys Methods* 10: 203-209

Laemmli UK (1970) Cleavage of structural proteins during assembly of head of Bacteriophage- T4. *Nature* 227: 680-685

Lamesch P, Berardini TZ, Li D, Swarbreck D, Wilks C, Sasidharan R, Muller R, Dreher K, Alexander DL, Garcia-Hernandez M, Karthikeyan AS, Lee CH, Nelson WD, Ploetz L, Singh S, Wensel A, Huala E (2011) The *Arabidopsis* Information Resource (TAIR): improved gene annotation and new tools. *Nucleic Acids Res* 40: 1202-1210

Laule O, Fürholz A, Chang HS, Zhu T, Wang X, Heifetz PB, Gruissem W, Lange M (2003) Crosstalk between cytosolic and plastidial pathways of isoprenoid biosynthesis in *Arabidopsis thaliana*. *Proc Natl Acad Sci U S A* 100: 6866-6871

Lee LY, Gelvin SB (2008) T-DNA Binary Vectors and Systems. *Plant Physiol*: 146: 325-332

Lesina O (2010) Untersuchungen zur *in planta* Funktion von Membranproteinen der äußeren Hüllmembran von Plastiden (Bachelor thesis)

Lesina O (2011) Charakterisierung von NOEP40 in der äußeren Hüllmembran von Chloroplasten (Bachelor thesis)

Li HM, Moore T, and Keegstra K (1991) Targeting of Proteins to the Outer Envelope Membrane Uses A Different Pathway Than Transport Into Chloroplasts. *Plant Cell* 3: 709- 717

Li HM and Chen LJ (1996) Protein targeting and integration signal for the chloroplastic outer envelope membrane. *Plant Cell* 8: 2117-2126

Linka N, Weber AP (2010) Intracellular metabolite transporters in plants. *Mol Plant* 3: 21-53

Liu C M and Meinke DW (1998) The titan mutants of *Arabidopsis* are disrupted in mitosis and cell cycle control during seed development. *Plant J*: 16, 21-31

Masatoshi N and Tadashi A (1974) Isolation of membranes containing protease from the cotyledons of germinating pea seeds. *Plant & Cell Physiol* 15: 331-340

McIntosh DB, Woolley DG, Vilsen B, and Andersen JP (1996) Mutagenesis of segment (487) Phe-Ser-Arg-Asp-Arg-Lys(492) of sarcoplasmic reticulum Ca2+-ATPase produces pumps defective in ATP binding. *J Biol Chem* 271: 25778-25789

Morello L, Breviario D (2008) Plant spliceosomal introns: not only cut and paste. *Curr Genomics* 9: 227-238

Murashige T, Skoog F (1962) A revised medium for rapid growth and bio assays with tobacco tissue cultures. *Physiologia Plantarum* 15: 473-497

Murcha MW, Elhafez D, Lister R, Tonti-Filippini J, Baumgartner M, Philippar K, Carrie C, Mokranjac D, Soll J, Whelan J. (2007) Characterisation of the

preprotein and amino acid transporter gene family in *Arabidopsis. Plant Physiology* 134: 199–212

Nicholas KB and Nicholas HB (1997) GeneDoc: a tool for editing and annotating multiple sequence alignments. Distributed by the authors

Niewiadomski P, Knappe S, Geimer S, Fischer K, Schulz B, Unte US, Rosso MG, Ache P, Flügge UI, and Schneider A (2005) The *Arabidopsis* plastidic glucose 6-phosphate/phosphate translocator GPT1 is essential for pollen maturation and embryo sac development. *Plant Cell* 17: 760-775

Obayashi T, Nishida K, Kasahara K, Kinoshita K (2011) ATTED-II updates: condition-specific gene coexpression to extend coexpression analyses and applications to a broad range of flowering plants. *Plant Cell Physiology* 52: 213-219

Perkins DN, Pappin DJ, Creasy DM, Cottrell JS (1999) Probability-based protein identification by searching sequence databases using mass spectrometry data. *Electrophoresis* 20: 3551-3567

Philippar K, Ivashikina N, Ache P, Christian M, Lüthen H, Palme K, Hedrich R (2004) Auxin activates KAT1 and KAT2, two K^+ channel genes expressed in seedlings of *Arabidopsis thaliana*. *Plant J* 37: 815-827

Philippar K and Soll J (2007) Intracellular transport: solute transport in chloroplasts, mitochondria, peroxisomes and vacuoles, and between organelles. In: Yeo AR Flowers TJ (Eds), Plant solute transport. Blackwell Publishing Oxford UK 133–192

Pohlmeyer K, Soll J, Steinkamp T, Hinnah S, Wagner R (1997) Isolation and characterization of an amino acid-selective channel protein present in the chloroplastic outer envelope membrane. *Proc Natl Acad Sci USA* 94: 9504–9509

Pohlmeyer K, Soll J, Grimm R, Hill K, Wagner R (1998) A high-conductance solute channel in the chloroplastic outer envelope from pea. *Plant Cell* 10: 1207–1216

Pudelski B, Kraus S, Soll J, Philippar K (2010) The plant PRAT proteins – preprotein and amino acid transport in mitochondria and chloroplasts. *Plant Biology* 12: 42-55

Pudelski B, Schock A, Hoth S, Radchuk R, Weber H, Hofmann J, Sonnewald U, Soll J and Philippar K (2011) The plastid outer envelope protein OEP16 affects metabolic fluxes during ABA-controlled seed development and germination. *J Ex Bot* 63: 1919-1936

Röhl T, Motzkus M, Soll J (1999) The outer envelope protein OEP24 from pea chloroplasts can functionally replace the mitochondrial VDAC in yeast. *FEBS Letters* 460: 491–494

Rosso MG, Li Y, Strizhov N, Reiss B, Dekker K, Weisshaar B (2003) An *Arabidopsis thaliana* T-DNA mutagenized population (GABI-Kat) for flanking sequence tag-based reverse genetics. Plant Mol Biol 53: 247-259

Saiki RK Gelfand DH, Stoffel S, Scharf SJ, Higuchi R, Horn GT, Mullis KB, Erlich HA (1988) Primer-directed enzymatic amplification of DNA with a thermostable DNA polymerase. *Science* 239: 487-491

Salomon M, Fischer K, Flugge UI, and Soll J (1990) Sequence-Analysis and Protein Import Studies of An Outer Chloroplast Envelope Polypeptide. *Proc Natl Acad Sci USA* 87**:** 5778-5782

Sambrook J, Fritsch EF and Maniatis T (1989) Molecular Cloning. A Laboratory Manual. Cold Spring Harbor Laboratory, Cold Spring Harbor Press, New York

Schleiff E, Eichacker LA, Eckart K, Becker T, Mirus O, Stahl T, and Soll J (2003) Prediction of the plant beta-barrel proteome: a case study of the chloroplast outer envelope. *Protein Science* 12: 748-759

Schmid M, Davison TS, Henz SR, Pape UJ, Demar M, Vingron M, Scholkopf B, Weigel D, Lohmann JU (2005) A gene expression map of *Arabidopsis thaliana* development. *Nature Genetics* 37: 501–506

Schneider A, Häusler RE, Kolukisaoglu U, Kunze R, van der Graaff E, Schwacke R, Catoni E, Desimone M, Flügge UI (2002). An *Arabidopsis thaliana* knock-out mutant of the chloroplast triose phosphate/phosphate translocator is severely compromised only when starch synthesis, but not starch mobilisation is abolished. *Plant J* 32: 685-699

Scholl RL, May ST, Ware DH (2000) Seed and molecular resources for *Arabidopsis*. *Plant Physiol* 124: 1477-1480

Schwacke R, Schneider A, van der Graaff E, Fischer K, Catoni E, Desimone M, Frommer WB, Flügge UI, Kunze R (2003) ARAMEMNON, a novel database for *Arabidopsis* integral membrane proteins. *Plant Physiology* 131: 16–26

Seigneurin-Berny D, Salvi D, Dorne AJ, Joyard J, Rolland N (2008) Percoll-purified and photosynthetically active chloroplasts from *Arabidopsis thaliana* leaves. *Plant Physiology and Biochemistry* 46: 951-955

Seino, S (1999) ATP-sensitive potassium channels: A model of heteromultimeric potassium channel/receptor assemblies. *Annu Rev Physiol* 61**:** 337-362

Schägger H und von Jagow G (1987) Tricine-sodium dodecyl sulfate-polyacrylamide gel electrophoresis for the separation of proteins in the range from 1 to 100 kDa. *Anal Biochem* 166: 368–379

Stengel A, Benz P, Balsera M, Soll J, Bölter B (2008) TIC62 redox-regulated translocon composition and dynamics. *J Biol Chem* 283: 6656-6667

Thompson JD, Gibson TJ, Plewniak F, Jeanmougin F und Higgins DG (1997) The CLUSTAL_X windows interface: flexible strategies for multiple sequence alignment aided by quality analysis tools. *Nucleic Acids Res* 25: 4876-4882.

Till BJ, Reynolds SH, Greene EA, Codomo CA, Enns LC, Johnson JE, Burtner C, Odden AR, Young K, Taylor NE, Henikoff JG, Comai L, Henikoff S (2003) Large-scale discovery of induced point mutations with high-throughput TILLING. *Genome Res* 13: 524-530

Tyra HM, Linka M, Weber APM, Bhattacharya D (2007) Host origin of plastid solute transporters in the first photosynthetic eukaryotes. *Genome Biol* 8: R212

Van Leene J, Hollunder J, Eeckhout D, Persiau G, Van De Slijke E, Stals H, Van Isterdael G, Verkest A, Neirynck S, Buffel Y, De Bodt S, Maere S, Laukens K, Pharazyn A, Ferreira PC, Eloy N, Renne C, Meyer C, Faure JD, Steinbrenner J, Beynon J, Larkin JC, Van de Peer Y, Hilson P, Kuiper M, De Veylder L, Van Onckelen H, Inzé D, Witters E, De Jaeger G (2010). Targeted interactomics reveals a complex core cell cycle machinery in *Arabidopsis thaliana.* M*olecular Systems Biology* 6: 397

von Heijne G (1992) Membrane protein structure prediction. Hydrophobicity analysis and the positive-inside rule. *J Mol Biol* 225: 487-494

von Zychlinski A, Kleffmann T, Krishnamurthy N, Sjolander K, Baginsky S, and Gruissem W (2005) Proteome analysis of the rice etioplast - Metabolic and regulatory networks and novel protein functions. *Mol Cell Proteomics* 4: 1072-1084

Waegemann K, Eichacker S, Soll J (1992) Outer envelope membranes from chloroplasts are isolated as right-side-out vesicles. *Planta* 187: 89-94

Walther DM, Rapaport D, Tommassen J (2009) Biogenesis of beta-barrel membrane proteins in bacteria and eukaryotes: evolutionary conservation and divergence. *Cell Mol Life Sci* 66: 2789-2804

Wielopolska A, Townley H, Moore I, Waterhouse P, Helliwell C (2005) A high-throughput inducible RNAi vector for plants. *Plant Biotechnol J* 3: 583-590

Yan RX, Chen Z, Zhang Z (2011) Outer membrane proteins can be simply identified using secondary structure element alignment. *BMC Bioinformatics* 12:76

Zeth K, Thein M (2010) Porins in prokaryotes and eukaryotes: common themes and variations. *Biochem J* 431: 13-22

Zhou C, Yang YJ and Jong AY (1990) Mini-Prep in 10 minutes. *Biotechniques* 8: 172-173

Zybailov B, Rutschow H, Friso G, Rudella A, Emanuelsson O, Sun, Q, and van Wijk KJ (2008). Sorting Signals, N-Terminal Modifications and Abundance of the Chloroplast Proteome. *PLoS ONE* 3, e1994

Eidesstattliche Erklärung

Ich versichere hiermit an Eides statt, dass die vorgelegte Dissertation von mir selbständig und ohne unerlaubte Hilfe angefertigt ist.

Holzkirchen, den 16.05.2012

Ingrid Karin Jeshen

Erklärung

Hiermit erkläre ich, dass die Dissertation nicht ganz oder in wesentlichen Teilen einer anderen Prüfungskommission vorgelegt worden ist, und dass ich mich anderweitig einer Doktorprüfung ohne Erfolg **nicht** unterzogen habe.

Holzkirchen, den 16.05.2012

Ingrid Karin Jeshen

Danksagung

Als Erstes möchte ich mich herzlichst bei Prof. Dr. Soll bedanken, da er mir die Gelegenheit gegeben hat, diese Doktorarbeit in Deutschland und in seiner Gruppe durchführen zu können. Seine Unterstützung und Herausforderungen all diesen vier Jahren haben einen wichtigen Beitrag für meine weitere berufliche und persönliche Entwicklung gebracht.

Ein besonderes Dankeschön gilt auch meiner Betreuerin Dr. Katrin Philippar. Ihre Hilfe, Freundlichkeit, Rat und Ermutigung waren für mich immer sehr wichtig. Danke für die schnelle und hilfreiche Korrektur dieser Arbeit!

Auch bei Prof. Wanner und seiner Gruppe möchte ich mich für die Einweisung und Benutzung der DIC-Optik bedanken.

Sehr dankbar bin ich auch meinen Kollegen des Labors „003“, wo ich mich sehr wohlgefühlt habe. Ein spezielles Dankeschön gilt an Dani für die Lesekorrektur dieser Arbeit, an Karl für den allgemeinen hilfsreichen experimentellen Tipp und Annette für die „last-minute“ Experimente. Vielen herzlichen Dank an Angela und Julia für die Hilfe mit den ganzen PCR-Screenings. Olga, es war für mich schön mit Dir zusammenzuarbeiten und hoffe Du hast viel bei uns gelernt. Birgitt, Sabrina, Roland, Ceci, Nannan, Lena und Isabell danke ich nicht nur für die täglichen Unterstützungen und Hilfeleistungen, sondern auch für die schönen und lustigen Momente inner- und außerhalb des Labors.

Allen Postdocs der gesamten Arbeitsgruppe spreche ich auch meinen herzlichen Dank aus, besonders bei Elisabeth, Bettina und Serena. Danke, Irene, für Deine Hilfe mit den Mikroskopie Techniken.

Meinen großen Dank natürlich auch an allen Technischen Assistenten, Doktoranden und ehemalige Doktoranden der gesamten Arbeitsgruppe, für ihre Unterstützung und Ratschläge. Ich habe mit ihnen viele schöne Stunden verbracht und kann sagen, dass ich hier nicht nur Kollegen, sondern auch Freunde getroffen habe.

Zu guter Letzt wollte ich mich bei meiner Familie und meinem Mann William bedanken, die mich während meines ganzen Studiums und der Promotion (aus der Ferne) unterstützt haben: *¡Sin ustedes no lo hubiera logrado!*